

PRECLINICAL EFFICACY AND SAFETY EVALUATION OF NOVEL SMALL-  
MOLECULE TARGETED AGENTS FOR THE PREVENTION AND  
TREATMENT OF PROSTATE CANCER

DISSERTATION

Presented in Partial Fulfillment of the Requirements for  
the Degree of Doctor of Philosophy in the Graduate  
School of The Ohio State University

By

Aaron Matthew Sargeant, D.V.M.

\*\*\*\*\*

The Ohio State University  
2009

Dissertation Committee:

Professor Ching-Shih Chen, Advisor

Professor Robert Brueggemeier

Professor Steven Clinton

Professor Thomas Rosol

Approved by

---

Advisor  
Veterinary Biosciences Graduate Program



## ABSTRACT

Prostate cancer is the most commonly diagnosed noncutaneous cancer and the second leading cause of cancer death in men. To combat the assortment of genomic and cellular aberrations that occur with the progression of this disease, we have developed novel classes of histone deacetylase (HDAC) inhibitors, 3-phosphoinositide dependent protein kinase-1 (PDK1)/Akt inhibitors, and indole-3-carbinol analogs using phenylbutyrate, celecoxib, and indole-3-carbinol, respectively, as scaffolds. Here, we assess both the efficacy and safety of the lead compounds of these classes (OSU-HDAC42, OSU-03012, and OSU-A9) administered orally in a series of preclinical studies carried out, in part, in preparation for prevention and regression trials in the transgenic adenocarcinoma of the mouse prostate (TRAMP) model. Following the acquisition of relevant *in vitro* and dose-ranging data, the tumor-suppressive efficacy of selected doses was evaluated in PC-3 xenograft ± TRAMP-C2 syngeneic mouse models. The oral drug formulation found to achieve the most promising benefit-risk ratio was incorporated into a diet and administered to TRAMP mice for the assessment of its morphologic and molecular effects on the development of prostatic intraepithelial neoplasia (PIN) and carcinoma. Toxicity was evaluated by histopathologic, hematologic, and body and organ weight analysis. OSU-HDAC42 achieved the most potent blockade

of prostate tumorigenesis reported in the TRAMP model, suppressing the absolute and relative weights of the urogenital tracts by 86% and 85%, respectively, in association with intraprostatic modulation of biomarkers indicative of HDAC inhibition, increased apoptosis and differentiation, and decreased proliferation. This compound, while sparing body weight, caused reversible testicular degeneration and hematologic alterations. In addition to its prostate chemopreventive effects, OSU-03012 was found to induce the hepatic biotransformation enzymatic system and caused phenotypic changes partially linked to sustained PDK1/Akt inhibition through inactivation of the downstream regulator of glycogen synthesis, glycogen synthase. OSU-A9 was compared vis-à-vis two slightly modified agents, of which the methylated derivative OSU-A9M was selected for continued lead optimization. Collectively, this work suggests therapeutic value in incorporating these novel compounds into the treatment regimen of patients with PIN, and reveals other biological parameters that should be considered for monitoring in the future preclinical and clinical use of these and similarly-targeted agents.

Dedicated to my wife Andrea and daughters Samantha and Alexandra

## ACKNOWLEDGEMENTS

I thank my advisor Dr. Ching-Shih Chen for his advice and encouragement and for making these projects possible, Dr. Samuel Kulp for his constant support and assistance with experimental design and manuscript preparation, and all of the Chen lab members whose hard work and enthusiasm have helped to create a formidable and enjoyable research team. I also appreciate the support of all my committee members.

I thank Alan Flechtner, Kim Partee, Mary Ross, and Anne Saulsbery of the Department of Veterinary Biosciences Histology/Immunohistochemistry Core, and Kimberly Carter for assistance with slide processing and immunohistochemistry, Dr Mamoru Yamaguchi for expertise with electron microscopy, and Robert Rengel for help with TRAMP colony management and necropsy.

I appreciate Dr. Robert Russell and others at WIL Research Laboratories, LLC, for helpful discussion on the drug-induced testicular degeneration (chapter 2), and Dr. Daphne Vasconcelos and Dr. Richard Peterson for advice on investigating certain toxicologic sequelae of drug therapy, and for providing mentorship in the field of toxicologic pathology.

I acknowledge the training support of the American College of Veterinary Pathologists/Society of Toxicologic Pathology Coalition for Veterinary Pathology

Fellows, through which Dr. Mark Cartwright of Schering Plough Research Institute is my industrial mentor.

Finally, I thank my family for their unwavering support and for making this experience an exciting adventure.

## VITA

- July 25, 1978 .....Born – Dayton, Ohio, USA
- 2000 .....Bachelor of Science, Biology  
Ohio Northern University  
Ada, OH
- 2004 .....Doctor of Veterinary Medicine  
The Ohio State University  
Columbus, OH
- 2004-present .....Residency in Veterinary Anatomic  
Pathology  
The Ohio State University  
Columbus, OH
- 2004-present .....Graduate Research Associate  
Department of Veterinary Biosciences  
The Ohio State University  
Columbus, OH
- 2008 .....Diplomate, American College of Veterinary  
Pathologists

## PUBLICATIONS

### Research Publications

1. Sargeant A, Rengel R, Kulp S, Klein R, Clinton S, Wang YC, and Chen CS. OSU-HDAC42, a histone deacetylase inhibitor, blocks prostate tumor progression in the transgenic adenocarcinoma of the mouse prostate model. *Cancer Research* 2008;68(10):3999-4009.

2. Wang YC, Kulp SK, Yang CC, Sargeant A, Yang YT, Yamaguchi M, Kashida Y, Chang GD, and Chen CS. Combination of celecoxib derivative OSU03012 and EGFR inhibitors enhances cell death in gefitinib/erlotinib-resistant lung cancer cells through induction of ER stress-related apoptosis and suppression of Akt signaling. *Cancer Research* 2008;68(8):2820-30.
3. Sargeant A, Kulp S, Lu YS, Cheng AL, and Chen CS. Histone deacetylase inhibitors in cancer therapy. In: *Cancer Epigenetics*. CRC Press LLC; Taylor & Francis Group, Boca Raton, Florida. Tollefsbol, TO (ed.). 2008:383-400.
4. Weng JR, Tsai CH, Kulp S, Wang D, Lin CH, Yang HC, Ma Y, Sargeant A, Chiu CF, Tsai MH, and Chen CS. A potent indole-3-carbinol-derived antitumor agent with pleiotropic effects on multiple signaling pathways in prostate cancer cells. *Cancer Research* 2007;67(16):7815-24.
5. Sargeant A, Klein R, Rengel R, Clinton S, Kulp S, Kashida Y, Yamaguchi M, and Chen CS. Chemopreventive and bioenergetic signaling effects of PDK1/Akt pathway inhibition in a transgenic mouse model of prostate cancer. *Toxicologic Pathology* 2007;35(4):549-61.
6. Muto M, Sargeant A, Tangkawattana P, Nishijima Y, Bonagura J, Hoshijima M, Nakade T, Hosaka Y, Faulkner G, and Yamaguchi M. Intranuclear paracrystals observed in Striated Muscle Specific LIM Protein (MLP<sup>-/-</sup>) mouse cardiomyocytes. *Microscopy Research and Technique* 2007;70(1):50-54.

## FIELDS OF STUDY

Major Field: Veterinary Biosciences

## TABLE OF CONTENTS

	Page
Abstract.....	ii
Dedication.....	iv
Acknowledgements.....	v
Vita.....	vii
List of Tables.....	xi
List of Figures.....	xii
Chapters:	
1. Histone Deacetylase Inhibitors in Cancer Therapy.....	1
Abstract.....	1
Introduction.....	2
Pharmacophore Model of HDACI.....	4
Anticancer Mechanisms of HDACI.....	7
Effects of HDACI on Non-Histone Proteins.....	10
Clinical Development of HDACI.....	16
HDACI in Combination with Other Agents.....	19
Summary and Perspectives.....	22
List of References.....	23
2. OSU-HDAC42, a Histone Deacetylase Inhibitor, Blocks Prostate Tumor Progression in the Transgenic Adenocarcinoma of the Mouse Prostate Model.....	41
Abstract.....	41
Introduction.....	42
Materials and Methods.....	44
Results.....	47
Discussion.....	56
List of References.....	61
3. Chemopreventive and Bioenergetic Signaling Effects of PDK1/Akt Pathway	

Inhibition in a Transgenic Mouse Model of Prostate Cancer.....	80
Abstract.....	80
Introduction.....	81
Materials and Methods.....	84
Results.....	88
Discussion.....	93
List of References.....	100
4. Preclinical Investigation of Novel Indole-3-Carbinol Analogs for the Prevention and Treatment of Prostate Cancer.....	118
Abstract.....	118
Introduction.....	119
Materials and Methods.....	121
Results.....	124
Discussion.....	129
List of References.....	132
Bibliography.....	145

## LIST OF TABLES

Table	Page
1.1	Representative non-histone substrates of HDACs .....39
1.2	Combination strategies of HDACi and other anticancer agents .....40
2.1	Relative urogenital tract weight and incidence of prostate lesions in TRAMP mice treated from 6 to 10 or 24 weeks of age .....77
2.2	Hematology and serum chemistry values of TRAMP mice treated from 6 to 10 or 24 weeks of age .....78
2.3	Absolute and relative organ weight values of wild type mice treated from 6 to 10 or 24 weeks of age .....79
3.1	Serum chemistry values of TRAMP mice after 8 weeks of treatment .....116
3.2	Hematology values of TRAMP mice after 8 weeks of treatment .....117
4.1	Absolute and relative organ weight values of C57BL/6 mice treated for 14 days with OSU-A9 by once daily gavage .....143
4.2	Hematology and serum chemistry values of nontransgenic male littermates of TRAMP mice fed an AIN-76A rodent diet with or without 450 ppm OSU-A9M from 18 to 24 weeks of age .....144

## LIST OF FIGURES

Figure	Page
1.1 Modeled docking of TSA (left) and ( <i>S</i> )-HDAC42 (right) into the active site of histone deacetylase-like protein (HDLP) .....	37
1.2 Modeled docking of TSA and ( <i>S</i> )-HDAC42 into the active site of histone deacetylase-like protein (HDLP) .....	38
2.1 Pilot studies done in preparation for a chemoprevention trial in the TRAMP model .....	67
2.2 OSU-HDAC42 suppressed the development of prostate lesions in 10-week-old TRAMP mice .....	68
2.3 Characterization of lesions in the prostates of 6-week-old TRAMP mice shows that hyperplasia and PIN are present at this age .....	69
2.4 OSU-HDAC42 prevented the progression of prostate lesions to poorly differentiated carcinoma in 24-week-old TRAMP mice .....	70
2.5 Histology and immunochemical analysis of biomarkers in the prostates of TRAMP mice fed an AIN-76A rodent diet with or without 208 ppm OSU-HDAC42 from 6 to 10 or 24 weeks of age .....	72
2.6 Effect of withdrawal of OSU-HDAC42 on lesion progression in the TRAMP model .....	73
2.7 Effects of OSU-HDAC42 on lymphoid organs .....	74
2.8 Characterization of OSU-HDAC42-associated testicular degeneration .....	76
3.1 OSU03012 decreased prostate lobe weights and the severity of epithelial proliferation .....	107
3.2 OSU03012 decreased prostate epithelial lesion development and inhibited the	

	phosphorylation of Akt and the downstream effector GSK3 $\beta$ .....	109
3.3	OSU03012 decreased body fat and prevented body weight gain independent of food intake .....	110
3.4	OSU03012 caused hepatic lesions that can be linked in part to target pathway inhibition .....	112
3.5	Toluidine blue staining and transmission electron microscopy of hypertrophic zone 3 hepatocytes .....	113
3.6	Multifocal, multiphasic necrosis of Type II skeletal myofibers was observed in drug-treated TRAMP mice, and GS was inactivated in skeletal muscle .....	114
3.7	Signaling pathway of PDK1/Akt $\rightarrow$ GS, and proposed protein activity induced by OSU03012 treatment .....	115
4.1	A dose-ranging study shows that OSU-A9 does not compromise body weight when administered up to 200 mg/kg for 14 days by once daily gavage .....	134
4.2	OSU-A9 does not affect liver weight or morphology after repeat oral dosing ...	135
4.3	OSU-A9 administered by gavage at 25, 50, and 100 mg/kg/day achieved statistically significant suppressions of PC-3 tumor growth compared to vehicle alone .....	136
4.4	OSU-A9 prolongs the tumor-defined lifespan of a syngeneic mouse model of prostate cancer (C57BL/6 mice bearing subcutaneous TRAMP-C2 tumors) ...	137
4.5	The suppression of PC-3 and TRAMP-C2 tumor growth by OSU-A9 was associated with decreased proliferation and increased apoptosis indicated by Ki67 and cleaved caspase-3 immunostaining of the tumors .....	138
4.6	Dose and time-course effects of OSU-A9, OSU-A9F, and OSU-A9M vs. indole-3-carbinol on the viability of human PC-3 and murine TRAMP-C2 prostate cancer cells .....	139
4.7	Fluorinated OSU-A9 (OSU-A9F) suppresses the growth of PC-3 xenograft tumors and prolongs the tumor-defined lifespan of the TRAMP-C2 syngeneic model .....	140

4.8	Methylated OSU-A9 (OSU-A9M) suppresses the growth of PC-3 xenograft tumors and prolongs the tumor-defined lifespan of the TRAMP-C2 syngeneic model .....	141
4.9	OSU-A9M administered at 450 ppm in the diet is well tolerated by the TRAMP model .....	142

## **CHAPTER 1**

### **HISTONE DEACTYLASE INHIBITORS IN CANCER THERAPY**

#### **ABSTRACT**

Aberrant activity of histone deacetylases (HDACs) occurs in many disease processes including cancer. Neoplastic cells often exhibit increased HDAC activity associated with altered gene expression, cellular differentiation and proliferation, and increased cell survival. Growing evidence shows that the acetylation-governed epigenetic control of transcription is also associated with the molecular pathogenesis of malignant transformation. In light of the link between irregular epigenetic states and neoplasia, the targeting of HDACs by small molecules is an active focus in the field of anticancer drug discovery. Inhibitors of HDAC (HDACi) represent structurally diverse natural product-derived and synthetic compounds that convey a broad and manifold arsenal of anticancer activities not only through the histone-mediated expression of growth-arrest genes, but also by potent modulation of non-histone proteins, including transcription factors and signal transduction mediators, in cancer cells, the tumor vasculature, and host immune system. Although the vast majority of HDACi exhibit broad-spectrum activity against class I and II HDACs, a few compounds demonstrate isozyme-specific properties and

facilitate the biological characterization of HDACs themselves. A single HDACi, vorinostat, has been granted regulatory approval and many others are in clinical development for use against an assortment of solid and hematopoietic malignancies, either as monotherapies or in combination with other anticancer stimuli. While the literature is inundated with preclinical successes of HDACi used to treat molecularly diverse malignancies, an improved understanding of important mechanistic, pharmacodynamic, and pharmacokinetic properties is needed to extend the usefulness of these agents in the clinic and broaden their future scope in the treatment of cancer.

## **INTRODUCTION**

The transcriptional capacity of genes is intricately controlled in part by the opposing actions of histone acetyltransferases (HATs) and histone deacetylases (HDACs), which contribute to the structural remodeling of chromatin by adding or removing, respectively, acetyl groups from the amino-terminal lysine residues of histones. Acetylation is one of many posttranslational histone modifications and promotes transcription by locally expanding chromatin to permit the access of regulatory proteins to DNA, whereas removal of acetyl groups leads to transcriptional repression via chromatin condensation. These modifications of histones by acetylation are among the epigenetic mechanisms controlling gene expression that are suggested to contribute to malignant transformation.<sup>1-4</sup> HDACs have been implicated in the actions of well-known cellular oncogenes and tumor suppressor genes,<sup>5-8</sup> and a tumor suppressor role for HATs has been described.<sup>9,10</sup> Moreover, associations have been reported between the

expression levels of HDAC enzymes and various features of human malignancies, such as steroid hormone receptor status and clinical outcome in breast cancer,<sup>11-13</sup> prognosis in lung cancer,<sup>14</sup> and response to therapy in acute myeloblastic leukemia.<sup>15</sup> Collectively, these studies suggest a role for histone acetylation in the development and progression of cancer.

Epigenetic regulators of gene transcription such as HDACs are attractive anticancer targets in light of the influence of chromatin structure on cancer development, and considering the reversible nature of epigenetic aberrations. Accordingly, the synthesis of small-molecule inhibitors of HDACs (HDACi) has been an active focus in the field of anticancer drug discovery in recent years. To this end, vorinostat has been approved by the Food and Drug Administration (FDA) for the treatment of refractory cutaneous T-cell lymphoma,<sup>16</sup> and many others follow in various stages of preclinical and clinical development in pursuit of regulatory sanction for use against an array of solid and hematopoietic malignancies.<sup>17-19</sup>

A noteworthy feature of HDACi is the selectivity of their antiproliferative effects for malignant versus normal cells.<sup>20</sup> Proposed mechanisms for this selective toxicity include the differential upregulation of thioredoxin, a protective anti-oxidant protein, in normal cells in response to HDACi treatment.<sup>21</sup> The activation of cell cycle checkpoints in nonmalignant cells that are dysfunctional in tumor cells has also been proposed as a mechanism for the selectivity of HDACi. Targeting of these checkpoints, which include the HDACi-sensitive G2-phase checkpoint and the drug-dependent bypass of the mitotic spindle checkpoint, have been shown to confer the selective cytotoxicity against tumor

cells that is a desirable feature of effective anticancer agents.<sup>22,23</sup>

The re-expression of genes inducing cell death, cell cycle arrest, or differentiation by HDACi underscores the applicability of these agents to the field of cancer therapy and is the conventional rationale for their development.<sup>24</sup> Importantly however, in addition to histone-mediated remodeling of chromatin, HDACs cause a plethora of histone-independent biological effects by modifying the acetylation state of a diverse set of protein substrates including transcription factors that influence gene expression, and mediators of signal transduction that induce apoptosis independent of gene expression.<sup>17,18,25</sup> HDACi consequently convey a broad and manifold arsenal of anticancer activities via these non-histone mechanisms not only in cancer cells but also in the tumor vasculature and host immune system.<sup>26-28</sup> These histone-independent anticancer activities of HDACi reveal molecular targets more diverse than perhaps originally predicted and are a focus of this chapter.

## **PHARMACOPHORE MODEL OF HDACI**

Natural product-derived and synthetic deacetylase inhibitors are classified into structurally distinct categories including short-chain fatty acids, hydroxamic acids, benzamide derivatives, cyclic peptides, and epoxyketones<sup>17,18</sup> (Fig. 1.1B). Most of these compounds demonstrate equal activity against class I, II, and IV HDACs, and all function by binding to various portions of the enzyme catalytic domains. The propensity of HDACi to bind zinc cations within the active catalytic sites of HDACs directly correlates with their inhibitory activity. Many are synthesized on the basis of a three-component

working model consisting of a cap-group, linker, and zinc-chelating motif,<sup>20</sup> as demonstrated for trichostatin A (TSA) in Fig. 1.1A. Specifically, the zinc-binding domain is separated by a linker domain from a surface domain which makes contact with the rim of the HDAC.<sup>18</sup> This mode of protein-ligand interaction serves as a framework for the design and synthesis of HDACi, including the production of trithiocarbonate analogs<sup>29</sup> and our own development of a novel class of phenylbutyrate-derived HDACi, the latter of which is summarized below.<sup>30-32</sup>

#### **Case in Point: Preclinical Development of Phenylbutyrate-Based HDACi:**

Based on the pharmacophore model of HDAC inhibition, a series of phenylbutyrate analogues were tethered to a zinc-chelating motif through a hydrophobic linker resulting in the synthesis of hydroxamate-tethered phenylbutyrate (HTPB), which exhibited an  $IC_{50}$  against *in vitro* HDAC activity of 44 nM compared to 0.4 mM for the parent phenylbutyrate molecule. These studies suggest that the active-site pocket of HDAC accommodates cap groups of diverse stereoelectronic properties, considering the variability in cap group structures among HTPB, TSA, vorinostat, and MS-275.<sup>30</sup> Lead optimization strategies with HTPB culminated in the synthesis of OSU-HDAC42 (Fig. 1.2), previously designated as (*S*)-HDAC-42, which inhibited HDAC with even greater potency ( $IC_{50}$  16 nM versus 44 nM for HTPB).<sup>31</sup>

As described in the following sections on the anticancer mechanisms of these agents, HDACi typically exhibit pleiotropic antitumor activities that encompass histone acetylation-dependent and -independent mechanisms. We have demonstrated this wide

range of activity, for instance, with OSU-HDAC42 in models of human cancers *in vitro* and *in vivo*. This broad spectrum of activity includes not only the potent inhibition of HDAC, as indicated by hallmark features of HDAC inhibition such as histone hyperacetylation and upregulated p21 expression, but also of targets regulating multiple aspects of cancer cell survival including Akt signaling, mitochondrial integrity and caspase activity. Our evaluation of the antitumor efficacy of OSU-HDAC42 in *in vitro* and *in vivo* models of prostate cancer<sup>33,34</sup> and hepatocellular carcinoma (HCC)<sup>35</sup> reveal noteworthy features of OSU-HDAC42 that suggest its potential clinical value. First, the assessment of drug effects in nonmalignant cells, specifically prostate epithelial cells and normal hepatocytes, showed them to be approximately 8- to 12-fold less sensitive to the antiproliferative effects of OSU-HDAC42 than panels of prostate cancer and HCC cells.<sup>33,35</sup> Second, in addition to expected effects on HDAC-related biomarkers (p21 expression, histone acetylation), OSU-HDAC42 induced significant reductions in the levels of phospho-Akt, Bcl-xL and the inhibitor of apoptosis protein (IAP) family members, survivin, cIAP-1 and cIAP-2.<sup>33</sup> Third, the oral administration of OSU-HDAC significantly suppressed the growth of subcutaneous (prostate cancer and HCC) and orthotopic (HCC) tumor xenografts in association with intratumoral changes in the biomarkers of drug activity described above; i.e. phospho-Akt, Bcl-xL, and IAPs; and in the absence of limiting toxicity.<sup>33,35</sup> This broad spectrum of activity exhibited by OSU-HDAC42 is common to many HDACi in preclinical and clinical development, and suggests their viability as part of therapeutic strategies for various human cancers.

## ANTICANCER MECHANISMS OF HDACI

The conventional paradigm for the use of HDACi in the treatment of cancer is the activation of growth-arrest genes secondary to histone acetylation.<sup>17,36</sup> Accordingly, although insufficient to molecularly characterize an observed clinical effect, histone acetylation assays are routinely used to assess the activity and bioavailability of HDACi. This measurement may be accomplished on tumor tissue itself or more commonly on peripheral white blood cells which are easily accessible.<sup>16,17</sup> Genes and gene products that negatively impact cancer cell survival and growth that have been upregulated subsequent to treatment with HDACi include the tumor suppressor genes p53, gelsolin, and mpsin, and other regulators such as p21<sup>WAF1/Cip1</sup>, Bcl2, Fas/Fas ligand, and caspase 3 among others.<sup>17,33,37-43</sup>

Given the roles of HDACs in chromatin remodeling and transcriptional regulation, as well as in the modification of diverse transcription factors, hypothetically HDAC inhibition might be expected to have a profound global genomic effect. While the percentage of all genes transcriptionally affected by HDAC inhibition is not precisely known, genetic profiling studies estimate that only a small fraction of genes is regulated.<sup>18,24,44</sup> In fact, Glaser *et al.* evaluated the effects of three HDACi on gene expression in human urinary bladder and breast cancer cells and showed that <10% of 6800 genes evaluated were up- or down-regulated from which a core set of thirteen genes regulated by the three HDACi in three different cell lines was identified. Moreover, the number of genes upregulated secondary to HDACi treatment was reported to be approximately equal to that downregulated.<sup>18,24</sup> The suppression of gene expression by HDACi

treatment may result, in part, from the increased transcription of genes whose products have negative effects on gene expression. Additionally, the acetylation-dependent alteration of transcription factor function may also contribute to down-regulated gene expression. For example, acetylation of Stat1 by HDACi treatment results in its interaction with NFκB and subsequent suppression of NFκB nuclear localization and of target gene expression.<sup>45</sup>

While some HDAC inhibitors exhibit isoform-specific properties,<sup>46,47</sup> the majority of these structurally diverse molecules are comparably nonselective with respect to inhibition of class I and II enzymes. The jury is still out regarding the clinical significance of improving HDAC isoform selectivity.<sup>16,25</sup> In support of developing discriminative HDACi, growing evidence indicates that individual HDACs play different physiological roles,<sup>48</sup> and even that some enzymes show strong correlation with disease. Enzyme knockdown via siRNA for example supports the relationship of class I enzymes with cancer<sup>49</sup> and suggests that inhibitors of these HDACs are more likely to achieve desirable clinical outcomes.<sup>25,50</sup> Moreover, antagonizing certain HDACs within class I such as HDAC1 and HDAC3 may be more desirable in cancer therapy than targeting the entire class,<sup>25</sup> and considering that inhibiting HDAC2 activity may be detrimental in patients with chronic obstructive pulmonary disease.<sup>51</sup> In contrast, similar experiments with class II HDACs failed to significantly impact cancer cells.<sup>49,50</sup> However, it should be noted that, while expression data for certain HDACs in primary tumor tissues have been reported,<sup>52,53</sup> much of the data implicating different roles of class I and class II enzymes, and therefore their validity as anticancer targets, was generated by using

siRNA-mediated knockdown of expression which requires careful interpretation of its clinical relevance. Until the biological functions of individual HDACs are more fully characterized, the potential value of broad-spectrum versus narrow-spectrum HDACi in the context of cancer therapy will remain unclear. While adverse reactions may be theoretically circumvented by streamlining activity to cancer-relevant HDACs,<sup>25</sup> broad-spectrum HDACi may provide advantages by targeting multiple signaling pathways associated with cancer cell survival and proliferation, which could be envisioned to induce more efficient cell death or delay/prevent the acquisition of resistance.<sup>54</sup>

Although a variety of HDACi have demonstrated tumor-specific anticancer selectivity and success in preclinical and clinical studies, there are no reliable methods to predict the sensitivity of a certain tumor to any class of HDAC inhibitor, and the molecular groundwork for this activity remains largely unknown.<sup>17</sup> Continued mechanistic research is needed considering that the use of HDACi actually pre-dated the characterization of HDACs themselves, and that HDACi have been our most valuable means of defining the roles of these enzymes in normal and neoplastic biology.<sup>18</sup> Recent advances in proteomics illustrate one discipline by which acetylation events may be more thoroughly defined. These methodologies have permitted the characterization of specific acetylation patterns of histones in response to HDACi treatment,<sup>55,56</sup> which may help to account for differences in effects induced by these agents. For example, the specific posttranslational modification sites on histone H3 and H4 have been determined by mass spectrometry following separation by acetic acid urea-polyacrylamide gel electrophoresis (AU-PAGE). Peptide mass mapping of histone H4 using this technique revealed an

identical order of acetylation in mouse lymphosarcoma cells treated with TSA and depsipeptide.<sup>55</sup> These and other strategies such as genetic profiling of HDACi-treated cells and tumors will further our understanding of this complex group of molecules and perhaps extend their usefulness in preclinical and clinical settings.

## **EFFECTS OF HDACI ON NON-HISTONE PROTEINS**

Although histones are by bulk mass the most abundant HDAC substrate, the list of other identified key substrates (Table 1.1) is ever-growing, as is an appreciation for their potentially immense influence on the anticancer activities of HDACi. The role of these enzymes as *protein* deacetylases should not be underestimated.<sup>57</sup> Since some HDACs at least partially reside in extranuclear cytoplasmic compartments<sup>58,59</sup> and considering their extensive phylogenetic characterization in prokaryotes as well as eukaryotes, it is believed that HDACs evolved in the absence of histone proteins.<sup>18,60</sup> It is not surprising then that alteration of the histone code alone is insufficient to account for the antitumor success of these agents.<sup>20</sup> The following subsections summarize some of the non-histone anticancer mechanisms of HDACi.

### **HDACI-Mediated Acetylation of Ku70 Induces Caspase-Dependent**

**Apoptosis:** The acetylation-dependent, Bax-binding activity of Ku70 represents another non-histone target of HDACi that may be exploited for anticancer use. Ku70 is commonly upregulated in neoplastic cells where it prevents cell death by binding to and sequestering the pro-apoptotic protein Bax.<sup>61</sup> By inhibiting Bax function, Ku70 acquires

an anti-apoptotic character and even increases the resistance of tumors to chemotherapy. The Bax binding ability of Ku70 has recently been characterized as acetylation-dependent, at least in neuroblastoma cells, and its acetylation status is tightly controlled by multiple HDACs.<sup>61,62</sup> When acetylated Ku70 can no longer bind to Bax, allowing Bax to translocate to the mitochondria where it causes cytochrome C release and caspase 9-mediated apoptosis. Treatment of neuroblastoma cells with TSA caused hyperacetylation of Ku70 and subsequent cell death. This study by Subramanian et al. demonstrates the *in vitro* success of single agent treatment with HDACi and suggests that Ku70 can serve as a target for proapoptotic regulation by HDACi.<sup>62</sup>

In addition to sequestration of Bax, Ku70 mediates a second cytoprotective function through its critical role in the repair of DNA double-strand breaks (DSB). We have shown that TSA, OSU-HDAC42, and MS-275, but not vorinostat, potently induced Ku70 acetylation leading to reductions in the binding affinity of Ku70 to broken DNA ends. Moreover, this inhibitory effect on Ku70's DNA DSB repair activity could be exploited to sensitize prostate cancer cells to cell killing by agents that produce DNA DSB, such as bleomycin, doxorubicin and VP-19.<sup>34</sup>

**HDACI Stabilizes p53 and Causes Cell Cycle Arrest and Apoptosis:** The dysregulation of the p53 tumor suppressor gene in cancer is well established.<sup>63</sup> Evidence shows that posttranslational modifications including acetylation play an important role in its regulation.<sup>64-66</sup> The HAT p300/CBP commonly acetylates p53 in response to p53-activating agents,<sup>67</sup> and degradation of p53 is dependent on HDAC1-associated

deacetylation.<sup>68</sup> Interestingly, Tip60-dependent acetylation of p53 at K120 is crucial for its apoptotic, but not growth arrest, activity.<sup>66</sup>

Treatment of prostate cancer cells with HDACi demonstrated profound effects of post-translational modification on p53 function.<sup>69-73</sup> CG-1521, an HDACi with structural similarity to vorinostat, was shown to modify p53 acetylation in a site-specific manner in LNCaP cells. Specifically, treatment with CG-1521 stabilized the acetylation of p53 at Lys373, which induced cell cycle arrest by increasing p21 expression, and caused apoptosis via translocation of Bax. TSA, in comparison, stabilized acetylation of p53 at Lys382 but failed to change steady state levels of p21 mRNA and had no apoptotic effect.<sup>73</sup> Hyperacetylation of H3 and H4 occurred in the cells much earlier than morphologic evidence of apoptosis or cell cycle arrest, suggesting that these traditional targets may have contributed to cell death by re-expression of anti-proliferative genes.<sup>72</sup> However, the effect on chromatin remodeling by CG-1521 may be secondary to changes in cell function induced by other, non-histone targets and is likely not the key anticancer mediator. Importantly, other studies have shown that p53 expression appears to not be requisite for the antitumor activity of HDACi.<sup>74-76</sup>

### **Hsp90 Loses Chaperone Function Subsequent to HDACI-Induced**

**Acetylation:** In addition to the well known stress-induced effects of heat shock proteins (Hsp), Hsp90 is an important modulator of normal and neoplastic cell signaling and is a potential target in cancer therapy.<sup>77,78</sup> Hsp90 is a molecular chaperone that, with assistance from cochaperones, facilitates the assembly and maturation of client proteins

including glucocorticoid receptor (GR).<sup>79,80</sup> Its activity is acetylation-dependent, with deacetylation mediated specifically by HDAC6.<sup>80</sup> Kovacs et al. demonstrated that siRNA-mediated repression of HDAC6 caused hyperacetylation of Hsp90 and loss of its chaperone activity by dissociation from p23, an essential cochaperone, and subsequent degradation of GR.<sup>80</sup> Similar degradation of Hsp90 client proteins including Akt, Her2/neu, BCR-ABL, ERBB1, and ERBB2 has been observed upon pharmacological inhibition of HDAC, presumably HDAC6.<sup>81-86</sup> The HDACi depsipeptide likewise diminished the level of many oncoproteins normally stabilized by Hsp90 in non-small-cell lung cancer cells.<sup>87</sup> While the isozyme-specific regulation of Hsp90 predicts a positive antitumor response to pharmacological inhibition of HDAC6, the necessity of HDAC6 inhibition for the induction of cell death by HDACi is not certain since several HDACi with potent antitumor properties are not capable of inhibiting this enzyme.<sup>19</sup>

### **STAT3 Acetylation Mediates Its Nuclear Translocation for Transcriptional**

**Regulation:** Upon activation, signal transducers and activators of transcription (Stat) proteins dimerize and translocate to the nucleus to regulate transcription.<sup>88</sup> Recent studies demonstrate that Stat3 can be modified by acetylation both *in vitro* and *in vivo* which stimulates its sequence-specific DNA binding ability.<sup>89-91</sup> Its coactivator p300/CREB-binding protein, a member of an important class of HATs, is responsible for its acetylation and capable of regulating many cellular processes. Treatment of cells with TSA mimicked intensified activity of this protein through increased Stat3 nuclear localization owing to its hyperacetylation.<sup>90</sup> This study defined a novel, alternative

mechanism for Stat3 activation by acetylation, the functional consequences of which are yet to be determined. The activity of another Stat protein has been shown to be governed by acetylation.<sup>45</sup> Kramer *et al.* showed that HDACi-induced acetylation of Stat1 promotes its interaction with NFκB. The nuclear localization of NFκB, and associated expression of anti-apoptotic target genes, are suppressed subsequent to this interaction.<sup>45</sup>

#### **α-Tubulin Acetylation by HDAC6 Inhibition Abates Cell Motility:**

Hypoacetylation of microtubules by HDACs including TSA led to the discovery of “tubacin”, a small-molecule agent designed to inhibit the deacetylation of α-tubulin in mammalian cells.<sup>47</sup> Tubacin specifically inhibits HDAC6, the enzyme responsible for removing acetyl groups from tubulin. The specificity of this novel compound negates other cellular effects such as cell cycle arrest and apoptosis induced by pleiotropic HDACi such as TSA. This specificity was determined by the comparison of genome-wide transcriptional profiles of mouse embryonic stem cells treated with either TSA or tubacin. Whereas 232 genes were increased above a 1.3-fold threshold value after TSA treatment, gene expression in cells treated with tubacin was relatively unaltered and similar to DMSO-treated control cells.<sup>47</sup> Altering the acetylation status of tubulin affects microtubules regulating cell motility and has important potential therapeutic applications in modulating cell movement necessary for metastasis and angiogenesis.<sup>92,93</sup>

**Other Non-Histone Effects of HDACi:** The phosphorylated, active form of Akt is overexpressed in many cancer types where it promotes cell survival and exerts anti-

apoptotic effects.<sup>94</sup> Some HDACs (HDAC1, 6, and 10) form complexes containing protein serine/threonine phosphatases in the cytosol, and inactivation of HDAC6 by mutagenesis or HDACi has been shown to disrupt the HDAC6/protein phosphatase 1 (PP1) complex.<sup>95</sup> Chen et al. demonstrated that the reshuffling of PP1 complexes is one mechanism by which HDACi inactivate Akt.<sup>32</sup> In this study, the HDACi TSA and OSU-HDAC42 caused dose-dependent inactivation of Akt in PTEN-null glioblastoma (U87MG) and prostate (PC3) cancer cells exhibiting constitutively active Akt. Co-immunoprecipitation experiments showed that HDAC1 and 6 form complexes with PP1. Upon treatment with HDACi, PP1 dissociates from HDAC and ‘reshuffles’ to phospho-Akt leading to its inactivating dephosphorylation, and ultimately caspase 9-mediated apoptosis.<sup>32</sup> Similar results obtained by repressing HDAC1 and 6 with isozyme-specific siRNA validate the role of these HDACs in decreasing Akt phosphorylation and activity.<sup>20,32</sup>

Numerous other HDAC effects have been described with less mechanistic certainty. For example, through an unknown mechanism, HDACi can inhibit DNA repair responses in certain cell lines, potentially increasing the sensitivity of these cells to chemo- and radiotherapy. The DNA-binding affinity of the transcription factor nuclear factor  $\kappa$ B (NF- $\kappa$ B) and subsequent transcriptional activation is regulated by acetylation, as is the activity of  $\kappa$ B-  $\alpha$  (I $\kappa$ B $\alpha$ ), the regulator of NF- $\kappa$ B.<sup>96</sup> NF- $\kappa$ B activity is additionally regulated by the acetylation of Stat1.<sup>45</sup> Also, acetylation of transcription factors of several members of the death receptor pathway is thought to promote apoptosis; these members include Fas ligand, death receptor 5 (DR5), and TRAIL

(tumor-necrosis factor-related apoptosis-inducing ligand), the ligand of DR5.<sup>18</sup>

## **CLINICAL DEVELOPMENT OF HDACI**

Nearly a dozen small-molecule HDAC inhibitors are currently in clinical phases of testing in pursuit of regulatory approval, all of which have exhibited some degree of antitumor activity to warrant continued development. These are structurally diverse molecules used as monotherapies or in combination with other agents to treat leukemias, lymphomas, lung cancer, cervical cancer, and other advanced or refractory solid tumors.<sup>18,19</sup> In cell culture and *in vivo*, these inhibitors are consistently found to induce differentiation, cell cycle arrest, or apoptosis,<sup>17</sup> with the latter being the most typical mode of cell death and therefore the most thoroughly investigated.<sup>19</sup> Of note, most of the HDACi used in these studies degrade quickly following administration and are associated with a rapid rise and fall of histone hyperacetylation in tumor cells.<sup>17</sup>

The efficiency of enzyme activity inhibition and clinical effectiveness vary greatly among these structurally heterogeneous compounds.<sup>19</sup> Short-chain fatty acids including butyrate and valproic acid are effective only at high therapeutic doses (IC<sub>50</sub> in low mM range) and, while seemingly well-tolerated in patients in clinical trials, have very short plasma half-lives. Hydroxamic acids have lower IC<sub>50</sub> values (high nM) against class I and II enzymes. Of these, TSA, a natural product, has high potency against cancer cells but adverse toxic effects preclude its use in the clinic.<sup>20</sup> Synthetic suberoylanilide hydroxamic acid (SAHA) or vorinostat (marketed as Zolinza; Merck & Co. Inc., NJ, USA) is a pleiotropic hydroxamate-derived compound that was recently approved by the

FDA for use in refractory cutaneous T-cell lymphoma, and demonstrates potent antitumor activity in a variety of solid and hematopoietic tumors.<sup>16</sup>

PXD101 (belinostat) and LBH589 are two other hydroxamate-based HDACi that have shown promising preclinical results, with the latter exhibiting effective pharmacodynamic modulation in a Phase I trial in patients with hematopoietic neoplasms.<sup>97</sup> LBH589 increases apoptosis of multiple myeloma cells, including those resistant to conventional chemotherapy<sup>98</sup>, and targets angiogenesis *in vitro*.<sup>26</sup> PXD101 exerts anti-tumor effects in preclinical studies of ovarian cancer in the absence of limiting toxicity<sup>99,100</sup> Numerous clinical trials with these agents are currently recruiting patients for their evaluation in solid and hematopoietic tumors ([www.clinicaltrials.gov](http://www.clinicaltrials.gov)).

Benzamides including MS-275 and CI-994 (acetyldinaline) are in Phase I, II, and/or III clinical trials and inhibit HDAC activity at  $\mu\text{M}$  concentrations.<sup>19</sup> MS-275 may be regarded as the most advanced selective class I inhibitor<sup>25</sup> and targets HDAC 1 and 3 more potently than HDAC8 ( $\text{IC}_{50}$  0.3, 8, and  $>100\mu\text{M}$ , respectively).<sup>46</sup> Cyclic peptides are structurally complex inhibitors with  $\text{IC}_{50}$ 's in the nM range. Of these, trapoxin A, apicidin, and CHAPs inhibit class I HDACs with some degree of specificity, but have no or limited use in the clinic.<sup>101-103</sup> Depsipeptide, a cyclic peptolide, is generally classified as a broad-spectrum inhibitor,<sup>25</sup> but has been shown to inhibit class I enzymes with greater potency than class II enzymes.<sup>104</sup> This compound acts as a prodrug with a reduced sulfhydryl group liberated only intracellularly.<sup>104</sup>

Several phase I/II trials have been completed with acceptable toxicity profiles; however, only limited conclusions can be drawn from these preliminary studies.<sup>18</sup> A

common adverse event is the rapid lowering of white blood cell and thrombocyte counts in the blood.<sup>105,106</sup> Interestingly, the time course of this neutropenia and thrombocytopenia in HDACi-treated patients is distinct and different from the myelosuppression that occurs with conventional chemotherapeutic drugs. It is likely that HDACi affect mature myeloid cells, rather than early myeloid precursors, since the occurrence of neutropenia and thrombocytopenia is rapid (nadirs at 5 and 10 days, respectively) and transient (return to pre-treatment levels within 10 days).<sup>106</sup> The hydroxamate vorinostat and cyclic peptide depsipeptide share similar toxicities including neutropenia, thrombocytopenia, fatigue, and dehydration, all of which appear to be reversible following withdrawal of the drug<sup>105-108</sup>

More serious adverse events have been reported for some agents such as depsipeptide, trichostatin A, and valproic acid derivatives, and include cardiotoxicity and teratogenicity.<sup>109-111</sup> While a phase II clinical trial with depsipeptide was terminated prematurely due to potentially serious adverse cardiac events,<sup>20,109</sup> other clinical studies with depsipeptide have shown no association with myocardial damage or impaired cardiac function,<sup>112,113</sup> and fourteen clinical studies are listed as recruiting patients at the time of this review (see [www.clinicaltrials.gov](http://www.clinicaltrials.gov)). In many instances toxicity may be attributed to non-specific, HDACi-independent side effects since some of these compounds are only efficacious at high concentrations, especially the short-chain fatty acids.<sup>20</sup> The relationship between HDACi pharmacodynamic and kinetic properties and toxicity is yet to be determined.<sup>18,20</sup>

Importantly, the *key* targets for HDACi in the context of cancer therapy are

unknown as is the prediction of which patients will respond to treatment. Much work in this area, such as gene profiling of tumor samples from responders compared to non-responders, is critical for optimization of HDACi therapy. And since acetylation is a reversible process, pharmacokinetic considerations are critical because HDACi effects may be diminished soon after treatment and vary significantly between enteral and parenteral administration.<sup>18,107,108</sup> The clinical development of vorinostat, for example, switched from intravenous to oral formulation in early phases of clinical testing due to differences in pharmacokinetic profiles and toxicity.<sup>114</sup>

Indeed the limited pharmacokinetic data available for these agents to date suggest a need for continuous drug exposure to achieve significant *in vivo* antitumor activity.<sup>17</sup> Accordingly, it is logical to predict that continuous inhibition of HDAC activity will lead to a more positive long-term response.<sup>18</sup> To this end, a recent review article discusses the chemopreventive potential of HDACi in the diet.<sup>115</sup> Dashwood et al. propose that continued, subtle regulation of gene expression by dietary weak ligand HDACi may prevent cancer by affecting cell growth and apoptosis. Examples of dietary HDAC inhibitors with weak ligand properties include butyrate, diallyl sulfide, and sulforaphane.<sup>115</sup>

## **HDACI IN COMBINATION WITH OTHER AGENTS**

Additive or synergistic activity, with or without a preconceived molecular basis, has been observed with HDACi in combination with a variety of functionally diverse chemical compounds<sup>19</sup> (Table 1.2). The described broad-spectrum anticancer activity

and relative safety in normal cells make HDACi an attractive choice for combinatorial use. This promising activity, which may be the greatest therapeutic potential of HDACi, has been demonstrated in preclinical and clinical studies in combinations with standard chemotherapeutics, signal transduction inhibitors, demethylating agents, nuclear receptor ligands, HSP90 antagonists, and proteasome inhibitors.<sup>17,82,116-118</sup> While enhanced apoptosis is the most common synergistic effect, HDACi have also been shown to overcome resistance to specific targeted therapy.<sup>98,119-122</sup>

Given that epigenetic control of gene expression involves more than acetylation, potent targeting of transcription in neoplasia may require a combination of chromatin-modifying agents including inhibitors of histone methylase, DNA methyltransferase (DNMT), and HDAC, and specific activators of transcription factors.<sup>123</sup> Since hypomethylation of DNA induces the re-activation of methylation-silenced tumor suppressor genes, there is currently much interest in the therapeutic strategy of combining DNMT inhibitors with HDACi.<sup>124</sup> The demethylating agent 5-aza-2'-deoxycytidine (5-aza-CdR) used in combination with TSA, for example, profoundly induced the re-expression of genes silenced by hypermethylated promoters, including MLH1, TIMP3 (TIMP3), CDKN2B (INK4B, p15) and CDKN2A (INK4, p16).<sup>125</sup> Synergistic effects on the induction of apoptosis, differentiation, and cell growth arrest have also been observed in human breast, thoracic, lung, leukemia, and colon cancer cell lines treated with combinations of HDACi and inhibitors of DNMT.<sup>124</sup> In its limited use in the clinic to date, this combination strategy has shown promising results in the treatment of solid and hematopoietic tumors.<sup>126,127</sup>

HDACi in combination with standard chemotherapeutics have demonstrated enhanced anticancer activity. CI-994 in combination with the antimetabolite gemcitabine or the antimicrotubule agent docetaxel caused synergistic effects on cell cycle arrest and apoptosis of non-small-cell lung cancer cell lines.<sup>128</sup> While limited conclusions on antitumor activity could be drawn from a phase I study of CI-994 and gemcitabine in patients with advanced cancer,<sup>129</sup> a phase II trial with pancreatic cancer showed that CI-994 confers no advantage over gemcitabine alone.<sup>130</sup> Clinical trials of gemcitabine and CI-994 in lung cancer are in progress (see [www.clinicaltrials.gov](http://www.clinicaltrials.gov)).<sup>19</sup> Gemcitabine and docetaxel have also demonstrated enhanced killing of breast cancer cell lines in combination with either of the hydroxamates LAQ824 or SAHA.<sup>85</sup> A clinical trial of the HDACi magnesium valproate added to neoadjuvant doxorubicin and cyclophosphamide in locally advanced breast cancer caused HDAC inhibition and gene reactivation in primary tumors;<sup>131</sup> a randomized phase III study involving this combination strategy is ongoing.

Synergistic effects have been observed with many other combination strategies using HDACi with or without a strong molecular basis. As discussed above, HDACi combined with DNA-damaging agents appears to be a promising therapeutic strategy for prostate and other cancers.<sup>34,132</sup> Death-receptor signaling is enhanced by the HDACi-mediated hypersensitization of malignant cells to apoptosis. This potentiated apoptotic effect has been reported with different HDACi combined with activators of the TRAIL and Fas pathways, and TRAIL-resistant tumor cells have been sensitized to TRAIL-mediated apoptosis by low doses of HDACi.<sup>119,133,134</sup> HDACi also are capable of

potentiating the effects of kinase inhibitors<sup>121,122,135-138</sup> and radiation<sup>139-141</sup> on cancer cell death, and synergistic activity from these combinations are commonly reported.

## **SUMMARY AND PERSPECTIVES**

In summary, acetylation is an important posttranslational modification that regulates gene expression through pleiotropic effects on chromatin structure, protein stability, protein-protein interactions, protein localization, and DNA binding.<sup>142,143</sup> The balance of histone acetylation is regulated by the cooperation of HDACs and HATs. Beyond chromatin remodeling, the HDAC enzyme complex has been linked with numerous regulatory pathways for cellular growth and differentiation.<sup>72</sup> Given the array of non-histone substrates, additional targets such as polyamines and metabolic intermediates should be expected.<sup>60</sup> The growing characterization of non-transcriptional mechanisms suggests that HDACi be considered as *partially* epigenetic therapy<sup>18</sup> and their targets be extended to *protein* deacetylases. Although the selectivity of most deacetylase inhibitors is poor, the development of tubacin<sup>47</sup> exemplifies the feasibility of developing HDACi-specific agents. With growing enthusiasm and resources devoted to the discovery, preclinical, and clinical evaluation of this class of compounds, HDACi will undoubtedly remain an important consideration in the development of novel cancer therapeutic strategies. The present intense interest in these compounds by the scientific community predicts an improved understanding of important mechanistic, pharmacodynamic, and pharmacokinetic properties that will extend the usefulness of HDACi in the clinic and broaden their future scope in the treatment of cancer.

## LIST OF REFERENCES

- <sup>1</sup> Stephen, J. K., Vaught, L. E., Chen, K. M. et al., Epigenetic events underlie the pathogenesis of sinonasal papillomas, *Mod Pathol* 20 (10), 1019-27, 2007.
- <sup>2</sup> Farwell, D. G., Shera, K. A., Koop, J. I. et al., Genetic and epigenetic changes in human epithelial cells immortalized by telomerase, *Am J Pathol* 156 (5), 1537-47, 2000.
- <sup>3</sup> Esteller, M. and Herman, J. G., Cancer as an epigenetic disease: DNA methylation and chromatin alterations in human tumours, *J Pathol* 196 (1), 1-7, 2002.
- <sup>4</sup> Deng, G., Bell, I., Crawley, S. et al., Braf mutation is frequently present in sporadic colorectal cancer with methylated hmlh1, but not in hereditary nonpolyposis colorectal cancer, *Clin Cancer Res* 10 (1 Pt 1), 191-5, 2004.
- <sup>5</sup> Feng, W., Lu, Z., Luo, R. Z. et al., Multiple histone deacetylases repress tumor suppressor gene arhi in breast cancer, *Int J Cancer* 120 (8), 1664-8, 2007.
- <sup>6</sup> Yu, J., Angelin-Duclos, C., Greenwood, J. et al., Transcriptional repression by blimp-1 (prdi-bf1) involves recruitment of histone deacetylase, *Mol Cell Biol* 20 (7), 2592-603, 2000.
- <sup>7</sup> Brehm, A., Miska, E. A., McCance, D. J. et al., Retinoblastoma protein recruits histone deacetylase to repress transcription, *Nature* 391 (6667), 597-601, 1998.
- <sup>8</sup> Magnaghi-Jaulin, L., Groisman, R., Naguibneva, I. et al., Retinoblastoma protein represses transcription by recruiting a histone deacetylase, *Nature* 391 (6667), 601-5, 1998.
- <sup>9</sup> Gayther, S. A., Batley, S. J., Linger, L. et al., Mutations truncating the ep300 acetylase in human cancers, *Nat Genet* 24 (3), 300-3, 2000.
- <sup>10</sup> Giles, R. H., Peters, D. J., and Breuning, M. H., Conjunction dysfunction: Cbp/p300 in human disease, *Trends Genet* 14 (5), 178-83, 1998.
- <sup>11</sup> Zhang, Z., Yamashita, H., Toyama, T. et al., Quantitation of hdac1 mrna expression in invasive carcinoma of the breast\*, *Breast Cancer Res Treat* 94 (1), 11-6, 2005.
- <sup>12</sup> Krusche, C. A., Wulfing, P., Kersting, C. et al., Histone deacetylase-1 and -3 protein expression in human breast cancer: A tissue microarray analysis, *Breast Cancer Res Treat* 90 (1), 15-23, 2005.

13. Saji, S., Kawakami, M., Hayashi, S. et al., Significance of hdac6 regulation via estrogen signaling for cell motility and prognosis in estrogen receptor-positive breast cancer, *Oncogene* 24 (28), 4531-9, 2005.
14. Osada, H., Tatematsu, Y., Saito, H. et al., Reduced expression of class ii histone deacetylase genes is associated with poor prognosis in lung cancer patients, *Int J Cancer* 112 (1), 26-32, 2004.
15. Bradbury, C. A., Khanim, F. L., Hayden, R. et al., Histone deacetylases in acute myeloid leukaemia show a distinctive pattern of expression that changes selectively in response to deacetylase inhibitors, *Leukemia* 19 (10), 1751-9, 2005.
16. Marks, P. A. and Breslow, R., Dimethyl sulfoxide to vorinostat: Development of this histone deacetylase inhibitor as an anticancer drug, *Nat Biotechnol* 25 (1), 84-90, 2007.
17. Drummond, D. C., Noble, C. O., Kirpotin, D. B. et al., Clinical development of histone deacetylase inhibitors as anticancer agents, *Annu Rev Pharmacol Toxicol* 45, 495-528, 2005.
18. Minucci, S. and Pelicci, P. G., Histone deacetylase inhibitors and the promise of epigenetic (and more) treatments for cancer, *Nat Rev Cancer* 6 (1), 38-51, 2006.
19. Bolden, J. E., Peart, M. J., and Johnstone, R. W., Anticancer activities of histone deacetylase inhibitors, *Nat Rev Drug Discov* 5 (9), 769-84, 2006.
20. Lin, H. Y., Chen, C. S., Lin, S. P. et al., Targeting histone deacetylase in cancer therapy, *Med Res Rev* 26 (4), 397-413, 2006.
21. Ungerstedt, J. S., Sowa, Y., Xu, W. S. et al., Role of thioredoxin in the response of normal and transformed cells to histone deacetylase inhibitors, *Proc Natl Acad Sci U S A* 102 (3), 673-8, 2005.
22. Qiu, L., Burgess, A., Fairlie, D. P. et al., Histone deacetylase inhibitors trigger a g2 checkpoint in normal cells that is defective in tumor cells, *Mol Biol Cell* 11 (6), 2069-83, 2000.
23. Warrenner, R., Beamish, H., Burgess, A. et al., Tumor cell-selective cytotoxicity by targeting cell cycle checkpoints, *Faseb J* 17 (11), 1550-2, 2003.
24. Glaser, K. B., Staver, M. J., Waring, J. F. et al., Gene expression profiling of multiple histone deacetylase (hdac) inhibitors: Defining a common gene set produced by hdac inhibition in t24 and mda carcinoma cell lines, *Mol Cancer Ther* 2 (2), 151-63, 2003.
25. Karagiannis, T. C. and El-Osta, A., Will broad-spectrum histone deacetylase inhibitors

be superseded by more specific compounds?, *Leukemia* 21 (1), 61-5, 2007.

26. Qian, D. Z., Kato, Y., Shabbeer, S. et al., Targeting tumor angiogenesis with histone deacetylase inhibitors: The hydroxamic acid derivative lbh589, *Clin Cancer Res* 12 (2), 634-42, 2006.
27. Bonaldi, T., Talamo, F., Scaffidi, P. et al., Monocytic cells hyperacetylate chromatin protein hmgb1 to redirect it towards secretion, *Embo J* 22 (20), 5551-60, 2003.
28. Wang, X. Q., Alfaro, M. L., Evans, G. F. et al., Histone deacetylase inhibition results in decreased macrophage cd9 expression, *Biochem Biophys Res Commun* 294 (3), 660-6, 2002.
29. Dehmel, F., Ciossek, T., Maier, T. et al., Trithiocarbonates-exploration of a new head group for hdac inhibitors, *Bioorg Med Chem Lett* 17 (17), 4746-52, 2007.
30. Lu, Q., Yang, Y. T., Chen, C. S. et al., Zn<sup>2+</sup>-chelating motif-tethered short-chain fatty acids as a novel class of histone deacetylase inhibitors, *J Med Chem* 47 (2), 467-74, 2004.
31. Lu, Q., Wang, D. S., Chen, C. S. et al., Structure-based optimization of phenylbutyrate-derived histone deacetylase inhibitors, *J Med Chem* 48 (17), 5530-5, 2005.
32. Chen, C. S., Weng, S. C., Tseng, P. H. et al., Histone acetylation-independent effect of histone deacetylase inhibitors on akt through the reshuffling of protein phosphatase 1 complexes, *J Biol Chem* 280 (46), 38879-87, 2005.
33. Kulp, S. K., Chen, C. S., Wang, D. S. et al., Antitumor effects of a novel phenylbutyrate-based histone deacetylase inhibitor, (s)-hdac-42, in prostate cancer, *Clin Cancer Res* 12 (17), 5199-206, 2006.
34. Chen, C. S., Wang, Y. C., Yang, H. C. et al., Histone deacetylase inhibitors sensitize prostate cancer cells to agents that produce DNA double-strand breaks by targeting ku70 acetylation, *Cancer Res* 67 (11), 5318-27, 2007.
35. Lu, Y. S., Kashida, Y., Kulp, S. K. et al., Efficacy of a novel histone deacetylase inhibitor in murine models of hepatocellular carcinoma, *Hepatology*, 2007.
36. Rosato, R. R., Almenara, J. A., Yu, C. et al., Evidence of a functional role for p21waf1/cip1 down-regulation in synergistic antileukemic interactions between the histone deacetylase inhibitor sodium butyrate and flavopiridol, *Mol Pharmacol* 65 (3), 571-81, 2004.
37. Hoshikawa, Y., Kwon, H. J., Yoshida, M. et al., Trichostatin a induces morphological

changes and gelsolin expression by inhibiting histone deacetylase in human carcinoma cell lines, *Exp Cell Res* 214 (1), 189-97, 1994.

<sup>38</sup> Kim, J. S., Lee, S., Lee, T. et al., Transcriptional activation of p21(waf1/cip1) by apicidin, a novel histone deacetylase inhibitor, *Biochem Biophys Res Commun* 281 (4), 866-71, 2001.

<sup>39</sup> Kim, M. S., Kwon, H. J., Lee, Y. M. et al., Histone deacetylases induce angiogenesis by negative regulation of tumor suppressor genes, *Nat Med* 7 (4), 437-43, 2001.

<sup>40</sup> Kwon, S. H., Ahn, S. H., Kim, Y. K. et al., Apicidin, a histone deacetylase inhibitor, induces apoptosis and fas/fas ligand expression in human acute promyelocytic leukemia cells, *J Biol Chem* 277 (3), 2073-80, 2002.

<sup>41</sup> Han, J. W., Ahn, S. H., Park, S. H. et al., Apicidin, a histone deacetylase inhibitor, inhibits proliferation of tumor cells via induction of p21waf1/cip1 and gelsolin, *Cancer Res* 60 (21), 6068-74, 2000.

<sup>42</sup> Almenara, J., Rosato, R., and Grant, S., Synergistic induction of mitochondrial damage and apoptosis in human leukemia cells by flavopiridol and the histone deacetylase inhibitor suberoylanilide hydroxamic acid (saha), *Leukemia* 16 (7), 1331-43, 2002.

<sup>43</sup> Sasakawa, Y., Naoe, Y., Inoue, T. et al., Effects of fk228, a novel histone deacetylase inhibitor, on tumor growth and expression of p21 and c-myc genes in vivo, *Cancer Lett* 195 (2), 161-8, 2003.

<sup>44</sup> Van Lint, C., Emiliani, S., and Verdin, E., The expression of a small fraction of cellular genes is changed in response to histone hyperacetylation, *Gene Expr* 5 (4-5), 245-53, 1996.

<sup>45</sup> Kramer, O. H., Baus, D., Knauer, S. K. et al., Acetylation of stat1 modulates nf-kappab activity, *Genes Dev* 20 (4), 473-85, 2006.

<sup>46</sup> Hu, E., Dul, E., Sung, C. M. et al., Identification of novel isoform-selective inhibitors within class i histone deacetylases, *J Pharmacol Exp Ther* 307 (2), 720-8, 2003.

<sup>47</sup> Haggarty, S. J., Koeller, K. M., Wong, J. C. et al., Domain-selective small-molecule inhibitor of histone deacetylase 6 (hdac6)-mediated tubulin deacetylation, *Proc Natl Acad Sci U S A* 100 (8), 4389-94, 2003.

<sup>48</sup> Cho, H. H., Park, H. T., Kim, Y. J. et al., Induction of osteogenic differentiation of human mesenchymal stem cells by histone deacetylase inhibitors, *J Cell Biochem* 96 (3), 533-42, 2005.

- <sup>49</sup> Glaser, K. B., Li, J., Staver, M. J. et al., Role of class i and class ii histone deacetylases in carcinoma cells using sirna, *Biochem Biophys Res Commun* 310 (2), 529-36, 2003.
- <sup>50</sup> Inoue, S., Mai, A., Dyer, M. J. et al., Inhibition of histone deacetylase class i but not class ii is critical for the sensitization of leukemic cells to tumor necrosis factor-related apoptosis-inducing ligand-induced apoptosis, *Cancer Res* 66 (13), 6785-92, 2006.
- <sup>51</sup> Barnes, P. J., Reduced histone deacetylase in copd: Clinical implications, *Chest* 129 (1), 151-5, 2006.
- <sup>52</sup> Wilson, A. J., Byun, D. S., Popova, N. et al., Histone deacetylase 3 (hdac3) and other class i hdacs regulate colon cell maturation and p21 expression and are deregulated in human colon cancer, *J Biol Chem* 281 (19), 13548-58, 2006.
- <sup>53</sup> Zhu, P., Martin, E., Mengwasser, J. et al., Induction of hdac2 expression upon loss of apc in colorectal tumorigenesis, *Cancer Cell* 5 (5), 455-63, 2004.
- <sup>54</sup> Peart, M. J., Smyth, G. K., van Laar, R. K. et al., Identification and functional significance of genes regulated by structurally different histone deacetylase inhibitors, *Proc Natl Acad Sci U S A* 102 (10), 3697-702, 2005.
- <sup>55</sup> Ren, C., Zhang, L., Freitas, M. A. et al., Peptide mass mapping of acetylated isoforms of histone h4 from mouse lymphosarcoma cells treated with histone deacetylase (hdacs) inhibitors, *J Am Soc Mass Spectrom* 16 (10), 1641-53, 2005.
- <sup>56</sup> Zhang, L., Su, X., Liu, S. et al., Histone h4 n-terminal acetylation in kasumi-1 cells treated with depsipeptide determined by acetic acid-urea polyacrylamide gel electrophoresis, amino acid coded mass tagging, and mass spectrometry, *J Proteome Res* 6 (1), 81-8, 2007.
- <sup>57</sup> Yoshida, M., Matsuyama, A., Komatsu, Y. et al., From discovery to the coming generation of histone deacetylase inhibitors, *Curr Med Chem* 10 (22), 2351-8, 2003.
- <sup>58</sup> Hubbert, C., Guardiola, A., Shao, R. et al., Hdac6 is a microtubule-associated deacetylase, *Nature* 417 (6887), 455-8, 2002.
- <sup>59</sup> Fischle, W., Dequiedt, F., Fillion, M. et al., Human hdac7 histone deacetylase activity is associated with hdac3 in vivo, *J Biol Chem* 276 (38), 35826-35, 2001.
- <sup>60</sup> Gregoret, I. V., Lee, Y. M., and Goodson, H. V., Molecular evolution of the histone deacetylase family: Functional implications of phylogenetic analysis, *J Mol Biol* 338 (1), 17-31, 2004.
- <sup>61</sup> Subramanian, C., Opipari, A. W., Jr., Castle, V. P. et al., Histone deacetylase inhibition

induces apoptosis in neuroblastoma, *Cell Cycle* 4 (12), 1741-3, 2005.

<sup>62.</sup> Subramanian, C., Opipari, A. W., Jr., Bian, X. et al., Ku70 acetylation mediates neuroblastoma cell death induced by histone deacetylase inhibitors, *Proc Natl Acad Sci U S A* 102 (13), 4842-7, 2005.

<sup>63.</sup> Levine, A. J., P53, the cellular gatekeeper for growth and division, *Cell* 88 (3), 323-31, 1997.

<sup>64.</sup> Gu, W. and Roeder, R. G., Activation of p53 sequence-specific DNA binding by acetylation of the p53 c-terminal domain, *Cell* 90 (4), 595-606, 1997.

<sup>65.</sup> Vogelstein, B., Lane, D., and Levine, A. J., Surfing the p53 network, *Nature* 408 (6810), 307-10, 2000.

<sup>66.</sup> Tang, Y., Luo, J., Zhang, W. et al., Tip60-dependent acetylation of p53 modulates the decision between cell-cycle arrest and apoptosis, *Mol Cell* 24 (6), 827-39, 2006.

<sup>67.</sup> Ito A, Lai CH, Zhao X et al., P300/cbp-mediated p53 acetylation is commonly induced by p53-activating agents and is inhibited by mdm2, *Embo J* 20, 1331-1340, 2001.

<sup>68.</sup> Ito, A., Kawaguchi, Y., CH, L. et al., Mdm2-hdac1-mediated deacetylation of p53 is required for its degradation., *Embo J* 21, 6236-6245, 2002.

<sup>69.</sup> Juan, L. J., Shia, W. J., Chen, M. H. et al., Histone deacetylases specifically down-regulate p53-dependent gene activation, *J Biol Chem* 275 (27), 20436-43, 2000.

<sup>70.</sup> Luo, J., Su, F., Chen, D. et al., Deacetylation of p53 modulates its effect on cell growth and apoptosis, *Nature* 408 (6810), 377-81, 2000.

<sup>71.</sup> Gu, W., Luo, J., Brooks, C. L. et al., Dynamics of the p53 acetylation pathway, *Novartis Found Symp* 259, 197-205; discussion 205-7, 223-5, 2004.

<sup>72.</sup> Roy, S., Packman, K., Jeffrey, R. et al., Histone deacetylase inhibitors differentially stabilize acetylated p53 and induce cell cycle arrest or apoptosis in prostate cancer cells, *Cell Death Differ* 12 (5), 482-91, 2005.

<sup>73.</sup> Roy, S. and Tenniswood, M., Site-specific acetylation of p53 directs selective transcription complex assembly, *J Biol Chem* 282 (7), 4765-71, 2007.

<sup>74.</sup> Greenberg, V. L., Williams, J. M., Cogswell, J. P. et al., Histone deacetylase inhibitors promote apoptosis and differential cell cycle arrest in anaplastic thyroid cancer cells, *Thyroid* 11 (4), 315-25, 2001.

- <sup>75</sup>. Hague, A., Manning, A. M., Hanlon, K. A. et al., Sodium butyrate induces apoptosis in human colonic tumour cell lines in a p53-independent pathway: Implications for the possible role of dietary fibre in the prevention of large-bowel cancer, *Int J Cancer* 55 (3), 498-505, 1993.
- <sup>76</sup>. Yamamoto, H., Fujimoto, J., Okamoto, E. et al., Suppression of growth of hepatocellular carcinoma by sodium butyrate in vitro and in vivo, *Int J Cancer* 76 (6), 897-902, 1998.
- <sup>77</sup>. Drysdale, M. J., Brough, P. A., Massey, A. et al., Targeting hsp90 for the treatment of cancer, *Curr Opin Drug Discov Devel* 9 (4), 483-95, 2006.
- <sup>78</sup>. Whitesell, L. and Lindquist, S. L., Hsp90 and the chaperoning of cancer, *Nat Rev Cancer* 5 (10), 761-72, 2005.
- <sup>79</sup>. Kovacs, J. J., Cohen, T. J., and Yao, T. P., Chaperoning steroid hormone signaling via reversible acetylation, *Nucl Recept Signal* 3, e004, 2005.
- <sup>80</sup>. Kovacs, J. J., Murphy, P. J., Gaillard, S. et al., Hdac6 regulates hsp90 acetylation and chaperone-dependent activation of glucocorticoid receptor, *Mol Cell* 18 (5), 601-7, 2005.
- <sup>81</sup>. Rahmani, M., Reese, E., Dai, Y. et al., Coadministration of histone deacetylase inhibitors and perifosine synergistically induces apoptosis in human leukemia cells through akt and erk1/2 inactivation and the generation of ceramide and reactive oxygen species, *Cancer Res* 65 (6), 2422-32, 2005.
- <sup>82</sup>. George, P., Bali, P., Annavarapu, S. et al., Combination of the histone deacetylase inhibitor lbh589 and the hsp90 inhibitor 17-aag is highly active against human cml-bc cells and aml cells with activating mutation of flt-3, *Blood* 105 (4), 1768-76, 2005.
- <sup>83</sup>. Bali, P., Pranpat, M., Swaby, R. et al., Activity of suberoylanilide hydroxamic acid against human breast cancer cells with amplification of her-2, *Clin Cancer Res* 11 (17), 6382-9, 2005.
- <sup>84</sup>. Chen, L., Meng, S., Wang, H. et al., Chemical ablation of androgen receptor in prostate cancer cells by the histone deacetylase inhibitor laq824, *Mol Cancer Ther* 4 (9), 1311-9, 2005.
- <sup>85</sup>. Fuino, L., Bali, P., Wittmann, S. et al., Histone deacetylase inhibitor laq824 down-regulates her-2 and sensitizes human breast cancer cells to trastuzumab, taxotere, gemcitabine, and epothilone b, *Mol Cancer Ther* 2 (10), 971-84, 2003.
- <sup>86</sup>. Nimmanapalli, R., Fuino, L., Bali, P. et al., Histone deacetylase inhibitor laq824 both lowers expression and promotes proteasomal degradation of bcr-abl and induces

apoptosis of imatinib mesylate-sensitive or -refractory chronic myelogenous leukemia-blast crisis cells, *Cancer Res* 63 (16), 5126-35, 2003.

<sup>87</sup>. Yu, X., Guo, Z. S., Marcu, M. G. et al., Modulation of p53, erbb1, erbb2, and raf-1 expression in lung cancer cells by depsipeptide fr901228, *J Natl Cancer Inst* 94 (7), 504-13, 2002.

<sup>88</sup>. Darnell, J. E., Jr., Stats and gene regulation, *Science* 277 (5332), 1630-5, 1997.

<sup>89</sup>. O'Shea, J. J., Kanno, Y., Chen, X. et al., Cell signaling. Stat acetylation--a key facet of cytokine signaling?, *Science* 307 (5707), 217-8, 2005.

<sup>90</sup>. Wang, R., Cherukuri, P., and Luo, J., Activation of stat3 sequence-specific DNA binding and transcription by p300/creb-binding protein-mediated acetylation, *J Biol Chem* 280 (12), 11528-34, 2005.

<sup>91</sup>. Yuan, Z. L., Guan, Y. J., Chatterjee, D. et al., Stat3 dimerization regulated by reversible acetylation of a single lysine residue, *Science* 307 (5707), 269-73, 2005.

<sup>92</sup>. Palazzo, A., Ackerman, B., and Gundersen, G. G., Cell biology: Tubulin acetylation and cell motility, *Nature* 421 (6920), 230, 2003.

<sup>93</sup>. Tran, A. D., Marmo, T. P., Salam, A. A. et al., Hdac6 deacetylation of tubulin modulates dynamics of cellular adhesions, *J Cell Sci* 120 (Pt 8), 1469-79, 2007.

<sup>94</sup>. Hennessy, B. T., Smith, D. L., Ram, P. T. et al., Exploiting the pi3k/akt pathway for cancer drug discovery, *Nat Rev Drug Discov* 4 (12), 988-1004, 2005.

<sup>95</sup>. Brush, M. H., Guardiola, A., Connor, J. H. et al., Deactylase inhibitors disrupt cellular complexes containing protein phosphatases and deacetylases, *J Biol Chem* 279 (9), 7685-91, 2004.

<sup>96</sup>. Chen, L. F. and Greene, W. C., Shaping the nuclear action of nf-kappab, *Nat Rev Mol Cell Biol* 5 (5), 392-401, 2004.

<sup>97</sup>. Giles, F., Fischer, T., Cortes, J. et al., A phase i study of intravenous lbh589, a novel cinnamic hydroxamic acid analogue histone deacetylase inhibitor, in patients with refractory hematologic malignancies, *Clin Cancer Res* 12 (15), 4628-35, 2006.

<sup>98</sup>. Maiso, P., Carvajal-Vergara, X., Ocio, E. M. et al., The histone deacetylase inhibitor lbh589 is a potent antimyeloma agent that overcomes drug resistance, *Cancer Res* 66 (11), 5781-9, 2006.

<sup>99</sup>. Plumb, J. A., Finn, P. W., Williams, R. J. et al., Pharmacodynamic response and

inhibition of growth of human tumor xenografts by the novel histone deacetylase inhibitor pxd101, *Mol Cancer Ther* 2 (8), 721-8, 2003.

<sup>100</sup>. Qian, X., LaRochelle, W. J., Ara, G. et al., Activity of pxd101, a histone deacetylase inhibitor, in preclinical ovarian cancer studies, *Mol Cancer Ther* 5 (8), 2086-95, 2006.

<sup>101</sup>. Bhalla, K. N., Epigenetic and chromatin modifiers as targeted therapy of hematologic malignancies, *J Clin Oncol* 23 (17), 3971-93, 2005.

<sup>102</sup>. Vannini, A., Volpari, C., Filocamo, G. et al., Crystal structure of a eukaryotic zinc-dependent histone deacetylase, human hdac8, complexed with a hydroxamic acid inhibitor, *Proc Natl Acad Sci U S A* 101 (42), 15064-9, 2004.

<sup>103</sup>. Furumai, R., Komatsu, Y., Nishino, N. et al., Potent histone deacetylase inhibitors built from trichostatin a and cyclic tetrapeptide antibiotics including trapoxin, *Proc Natl Acad Sci U S A* 98 (1), 87-92, 2001.

<sup>104</sup>. Furumai, R., Matsuyama, A., Kobashi, N. et al., Fk228 (depsipeptide) as a natural produg that inhibits class i histone deacetylases, *Cancer Res* 62 (17), 4916-21, 2002.

<sup>105</sup>. Rubin, E. H., Agrawal, N. G., Friedman, E. J. et al., A study to determine the effects of food and multiple dosing on the pharmacokinetics of vorinostat given orally to patients with advanced cancer, *Clin Cancer Res* 12 (23), 7039-45, 2006.

<sup>106</sup>. Sandor, V., Bakke, S., Robey, R. W. et al., Phase i trial of the histone deacetylase inhibitor, depsipeptide (fr901228, nsc 630176), in patients with refractory neoplasms, *Clin Cancer Res* 8 (3), 718-28, 2002.

<sup>107</sup>. Kelly, W. K., O'Connor, O. A., Krug, L. M. et al., Phase i study of an oral histone deacetylase inhibitor, suberoylanilide hydroxamic acid, in patients with advanced cancer, *J Clin Oncol* 23 (17), 3923-31, 2005.

<sup>108</sup>. Kelly, W. K., Richon, V. M., O'Connor, O. et al., Phase i clinical trial of histone deacetylase inhibitor: Suberoylanilide hydroxamic acid administered intravenously, *Clin Cancer Res* 9 (10 Pt 1), 3578-88, 2003.

<sup>109</sup>. Shah, M. H., Binkley, P., Chan, K. et al., Cardiotoxicity of histone deacetylase inhibitor depsipeptide in patients with metastatic neuroendocrine tumors, *Clin Cancer Res* 12 (13), 3997-4003, 2006.

<sup>110</sup>. Menegola, E., Di Renzo, F., Broccia, M. L. et al., Inhibition of histone deacetylase activity on specific embryonic tissues as a new mechanism for teratogenicity, *Birth Defects Res B Dev Reprod Toxicol* 74 (5), 392-8, 2005.

- <sup>111</sup> Eikel, D., Hoffmann, K., Zoll, K. et al., S-2-pentyl-4-pentynoic hydroxamic acid and its metabolite s-2-pentyl-4-pentynoic acid in the nmri-exencephaly-mouse model: Pharmacokinetic profiles, teratogenic effects, and histone deacetylase inhibition abilities of further valproic acid hydroxamates and amides, *Drug Metab Dispos* 34 (4), 612-20, 2006.
- <sup>112</sup> Piekarz, R. L., Frye, A. R., Wright, J. J. et al., Cardiac studies in patients treated with depsipeptide, fk228, in a phase ii trial for t-cell lymphoma, *Clin Cancer Res* 12 (12), 3762-73, 2006.
- <sup>113</sup> Molife, R., Fong, P., Scurr, M. et al., Hdac inhibitors and cardiac safety, *Clin Cancer Res* 13 (3), 1068; author reply 1068-9, 2007.
- <sup>114</sup> O'Connor, O. A., Heaney, M. L., Schwartz, L. et al., Clinical experience with intravenous and oral formulations of the novel histone deacetylase inhibitor suberoylanilide hydroxamic acid in patients with advanced hematologic malignancies, *J Clin Oncol* 24 (1), 166-73, 2006.
- <sup>115</sup> Dashwood, R. H., Myzak, M. C., and Ho, E., Dietary hdac inhibitors: Time to rethink weak ligands in cancer chemoprevention?, *Carcinogenesis* 27 (2), 344-9, 2006.
- <sup>116</sup> Catley, L., Weisberg, E., Kiziltepe, T. et al., Aggresome induction by proteasome inhibitor bortezomib and alpha-tubulin hyperacetylation by tubulin deacetylase (tdac) inhibitor lbh589 are synergistic in myeloma cells, *Blood* 108 (10), 3441-9, 2006.
- <sup>117</sup> Duan, J., Friedman, J., Nottingham, L. et al., Nuclear factor-kappab p65 small interfering rna or proteasome inhibitor bortezomib sensitizes head and neck squamous cell carcinomas to classic histone deacetylase inhibitors and novel histone deacetylase inhibitor pxd101, *Mol Cancer Ther* 6 (1), 37-50, 2007.
- <sup>118</sup> Rahmani, M., Yu, C., Dai, Y. et al., Coadministration of the heat shock protein 90 antagonist 17-allylamino-17-demethoxygeldanamycin with suberoylanilide hydroxamic acid or sodium butyrate synergistically induces apoptosis in human leukemia cells, *Cancer Res* 63 (23), 8420-7, 2003.
- <sup>119</sup> Rosato, R. R., Almenara, J. A., Dai, Y. et al., Simultaneous activation of the intrinsic and extrinsic pathways by histone deacetylase (hdac) inhibitors and tumor necrosis factor-related apoptosis-inducing ligand (trail) synergistically induces mitochondrial damage and apoptosis in human leukemia cells, *Mol Cancer Ther* 2 (12), 1273-84, 2003.
- <sup>120</sup> Kim, M. S., Baek, J. H., Chakravarty, D. et al., Sensitization to uv-induced apoptosis by the histone deacetylase inhibitor trichostatin a (tsa), *Exp Cell Res* 306 (1), 94-102, 2005.

- <sup>121</sup>. Yu, C., Rahmani, M., Almenara, J. et al., Histone deacetylase inhibitors promote sti571-mediated apoptosis in sti571-sensitive and -resistant bcr/abl+ human myeloid leukemia cells, *Cancer Res* 63 (9), 2118-26, 2003.
- <sup>122</sup>. Nimmanapalli, R., Fuino, L., Stobaugh, C. et al., Cotreatment with the histone deacetylase inhibitor suberoylanilide hydroxamic acid (saha) enhances imatinib-induced apoptosis of bcr-abl-positive human acute leukemia cells, *Blood* 101 (8), 3236-9, 2003.
- <sup>123</sup>. Johnstone, R. W. and Licht, J. D., Histone deacetylase inhibitors in cancer therapy: Is transcription the primary target?, *Cancer Cell* 4 (1), 13-8, 2003.
- <sup>124</sup>. Zhu, W. G. and Otterson, G. A., The interaction of histone deacetylase inhibitors and DNA methyltransferase inhibitors in the treatment of human cancer cells, *Curr Med Chem Anticancer Agents* 3 (3), 187-99, 2003.
- <sup>125</sup>. Cameron, E. E., Bachman, K. E., Myohanen, S. et al., Synergy of demethylation and histone deacetylase inhibition in the re-expression of genes silenced in cancer, *Nat Genet* 21 (1), 103-7, 1999.
- <sup>126</sup>. Gore, S. D., Baylin, S., Sugar, E. et al., Combined DNA methyltransferase and histone deacetylase inhibition in the treatment of myeloid neoplasms, *Cancer Res* 66 (12), 6361-9, 2006.
- <sup>127</sup>. Garcia-Manero, G., Kantarjian, H. M., Sanchez-Gonzalez, B. et al., Phase 1/2 study of the combination of 5-aza-2'-deoxycytidine with valproic acid in patients with leukemia, *Blood* 108 (10), 3271-9, 2006.
- <sup>128</sup>. Loprevite, M., Tiseo, M., Grossi, F. et al., In vitro study of ci-994, a histone deacetylase inhibitor, in non-small cell lung cancer cell lines, *Oncol Res* 15 (1), 39-48, 2005.
- <sup>129</sup>. Nemunaitis, J. J., Orr, D., Eager, R. et al., Phase i study of oral ci-994 in combination with gemcitabine in treatment of patients with advanced cancer, *Cancer J* 9 (1), 58-66, 2003.
- <sup>130</sup>. Richards, D. A., Boehm, K. A., Waterhouse, D. M. et al., Gemcitabine plus ci-994 offers no advantage over gemcitabine alone in the treatment of patients with advanced pancreatic cancer: Results of a phase ii randomized, double-blind, placebo-controlled, multicenter study, *Ann Oncol* 17 (7), 1096-102, 2006.
- <sup>131</sup>. Arce, C., Perez-Plasencia, C., Gonzalez-Fierro, A. et al., A proof-of-principle study of epigenetic therapy added to neoadjuvant doxorubicin cyclophosphamide for locally advanced breast cancer, *PLoS ONE* 1, e98, 2006.

- <sup>132</sup>. Kim, M. S., Blake, M., Baek, J. H. et al., Inhibition of histone deacetylase increases cytotoxicity to anticancer drugs targeting DNA, *Cancer Res* 63 (21), 7291-300, 2003.
- <sup>133</sup>. Guo, F., Sigua, C., Tao, J. et al., Cotreatment with histone deacetylase inhibitor laq824 enhances apo-2l/tumor necrosis factor-related apoptosis inducing ligand-induced death inducing signaling complex activity and apoptosis of human acute leukemia cells, *Cancer Res* 64 (7), 2580-9, 2004.
- <sup>134</sup>. Kim, E. H., Kim, H. S., Kim, S. U. et al., Sodium butyrate sensitizes human glioma cells to trail-mediated apoptosis through inhibition of cdc2 and the subsequent downregulation of survivin and xiap, *Oncogene* 24 (46), 6877-89, 2005.
- <sup>135</sup>. Rahmani, M., Yu, C., Reese, E. et al., Inhibition of pi-3 kinase sensitizes human leukemic cells to histone deacetylase inhibitor-mediated apoptosis through p44/42 map kinase inactivation and abrogation of p21(cip1/waf1) induction rather than akt inhibition, *Oncogene* 22 (40), 6231-42, 2003.
- <sup>136</sup>. Yu, C., Dasmahapatra, G., Dent, P. et al., Synergistic interactions between mek1/2 and histone deacetylase inhibitors in bcr/abl+ human leukemia cells, *Leukemia* 19 (9), 1579-89, 2005.
- <sup>137</sup>. Kim, J. S., Jeung, H. K., Cheong, J. W. et al., Apicidin potentiates the imatinib-induced apoptosis of bcr-abl-positive human leukaemia cells by enhancing the activation of mitochondria-dependent caspase cascades, *Br J Haematol* 124 (2), 166-78, 2004.
- <sup>138</sup>. Kawano, T., Horiguchi-Yamada, J., Iwase, S. et al., Depsipeptide enhances imatinib mesylate-induced apoptosis of bcr-abl-positive cells and ectopic expression of cyclin d1, c-myc or active mek abrogates this effect, *Anticancer Res* 24 (5A), 2705-12, 2004.
- <sup>139</sup>. Zhang, Y., Jung, M., and Dritschilo, A., Enhancement of radiation sensitivity of human squamous carcinoma cells by histone deacetylase inhibitors, *Radiat Res* 161 (6), 667-74, 2004.
- <sup>140</sup>. Nome, R. V., Bratland, A., Harman, G. et al., Cell cycle checkpoint signaling involved in histone deacetylase inhibition and radiation-induced cell death, *Mol Cancer Ther* 4 (8), 1231-8, 2005.
- <sup>141</sup>. Camphausen, K., Scott, T., Sproull, M. et al., Enhancement of xenograft tumor radiosensitivity by the histone deacetylase inhibitor ms-275 and correlation with histone hyperacetylation, *Clin Cancer Res* 10 (18 Pt 1), 6066-71, 2004.
- <sup>142</sup>. Yang, W. M., Tsai, S. C., Wen, Y. D. et al., Functional domains of histone deacetylase-3, *J Biol Chem* 277 (11), 9447-54, 2002.

- <sup>143</sup>. Kouzarides, T., Acetylation: A regulatory modification to rival phosphorylation?, *Embo J* 19 (6), 1176-9, 2000.
- <sup>144</sup>. Cohen, H. Y., Lavu, S., Bitterman, K. J. et al., Acetylation of the c terminus of ku70 by cbp and pcaf controls bax-mediated apoptosis, *Mol Cell* 13 (5), 627-38, 2004.
- <sup>145</sup>. Cohen, H. Y., Miller, C., Bitterman, K. J. et al., Calorie restriction promotes mammalian cell survival by inducing the sirt1 deacetylase, *Science* 305 (5682), 390-2, 2004.
- <sup>146</sup>. Yang, Y., Hou, H., Haller, E. M. et al., Suppression of foxo1 activity by fhl2 through sirt1-mediated deacetylation, *Embo J* 24 (5), 1021-32, 2005.
- <sup>147</sup>. Bouras, T., Fu, M., Sauve, A. A. et al., Sirt1 deacetylation and repression of p300 involves lysine residues 1020/1024 within the cell cycle regulatory domain 1, *J Biol Chem* 280 (11), 10264-76, 2005.
- <sup>148</sup>. Vaziri, H., Dessain, S. K., Ng Eaton, E. et al., Hsir2(sirt1) functions as an nad-dependent p53 deacetylase, *Cell* 107 (2), 149-59, 2001.
- <sup>149</sup>. Langley, E., Pearson, M., Faretta, M. et al., Human sir2 deacetylates p53 and antagonizes pml/p53-induced cellular senescence, *Embo J* 21 (10), 2383-96, 2002.
- <sup>150</sup>. Luo, J., Nikolaev, A. Y., Imai, S. et al., Negative control of p53 by sir2alpha promotes cell survival under stress, *Cell* 107 (2), 137-48, 2001.
- <sup>151</sup>. Fu, M., Rao, M., Wang, C. et al., Acetylation of androgen receptor enhances coactivator binding and promotes prostate cancer cell growth, *Mol Cell Biol* 23 (23), 8563-75, 2003.
- <sup>152</sup>. Fu, M., Liu, M., Sauve, A. A. et al., Hormonal control of androgen receptor function through sirt1, *Mol Cell Biol* 26 (21), 8122-35, 2006.
- <sup>153</sup>. Gaughan, L., Logan, I. R., Cook, S. et al., Tip60 and histone deacetylase 1 regulate androgen receptor activity through changes to the acetylation status of the receptor, *J Biol Chem* 277 (29), 25904-13, 2002.
- <sup>154</sup>. Gaughan, L., Logan, I. R., Neal, D. E. et al., Regulation of androgen receptor and histone deacetylase 1 by mdm2-mediated ubiquitylation, *Nucleic Acids Res* 33 (1), 13-26, 2005.
- <sup>155</sup>. Simonini, M. V., Camargo, L. M., Dong, E. et al., The benzamide ms-275 is a potent, long-lasting brain region-selective inhibitor of histone deacetylases, *Proc Natl Acad Sci U S A* 103 (5), 1587-92, 2006.

- <sup>156</sup>. Quivy, V. and Van Lint, C., Regulation at multiple levels of nf-kappab-mediated transactivation by protein acetylation, *Biochem Pharmacol* 68 (6), 1221-9, 2004.
- <sup>157</sup>. Greene, W. C. and Chen, L. F., Regulation of nf-kappab action by reversible acetylation, *Novartis Found Symp* 259, 208-17; discussion 218-25, 2004.
- <sup>158</sup>. Yeung, F., Hoberg, J. E., Ramsey, C. S. et al., Modulation of nf-kappab-dependent transcription and cell survival by the sirt1 deacetylase, *Embo J* 23 (12), 2369-80, 2004.
- <sup>159</sup>. Thevenet, L., Mejean, C., Moniot, B. et al., Regulation of human sry subcellular distribution by its acetylation/deacetylation, *Embo J* 23 (16), 3336-45, 2004.
- <sup>160</sup>. Matsuyama, A., Shimazu, T., Sumida, Y. et al., In vivo destabilization of dynamic microtubules by hdac6-mediated deacetylation, *Embo J* 21 (24), 6820-31, 2002.
- <sup>161</sup>. Zhang, Y., Li, N., Caron, C. et al., Hdac-6 interacts with and deacetylates tubulin and microtubules in vivo, *Embo J* 22 (5), 1168-79, 2003.
- <sup>162</sup>. Canettieri, G., Morantte, I., Guzman, E. et al., Attenuation of a phosphorylation-dependent activator by an hdac-pp1 complex, *Nat Struct Biol* 10 (3), 175-81, 2003.
- <sup>163</sup>. Atadja, P., Hsu, M., Kwon, P. et al., Molecular and cellular basis for the anti-proliferative effects of the hdac inhibitor laq824, *Novartis Found Symp* 259, 249-66; discussion 266-8, 285-8, 2004.

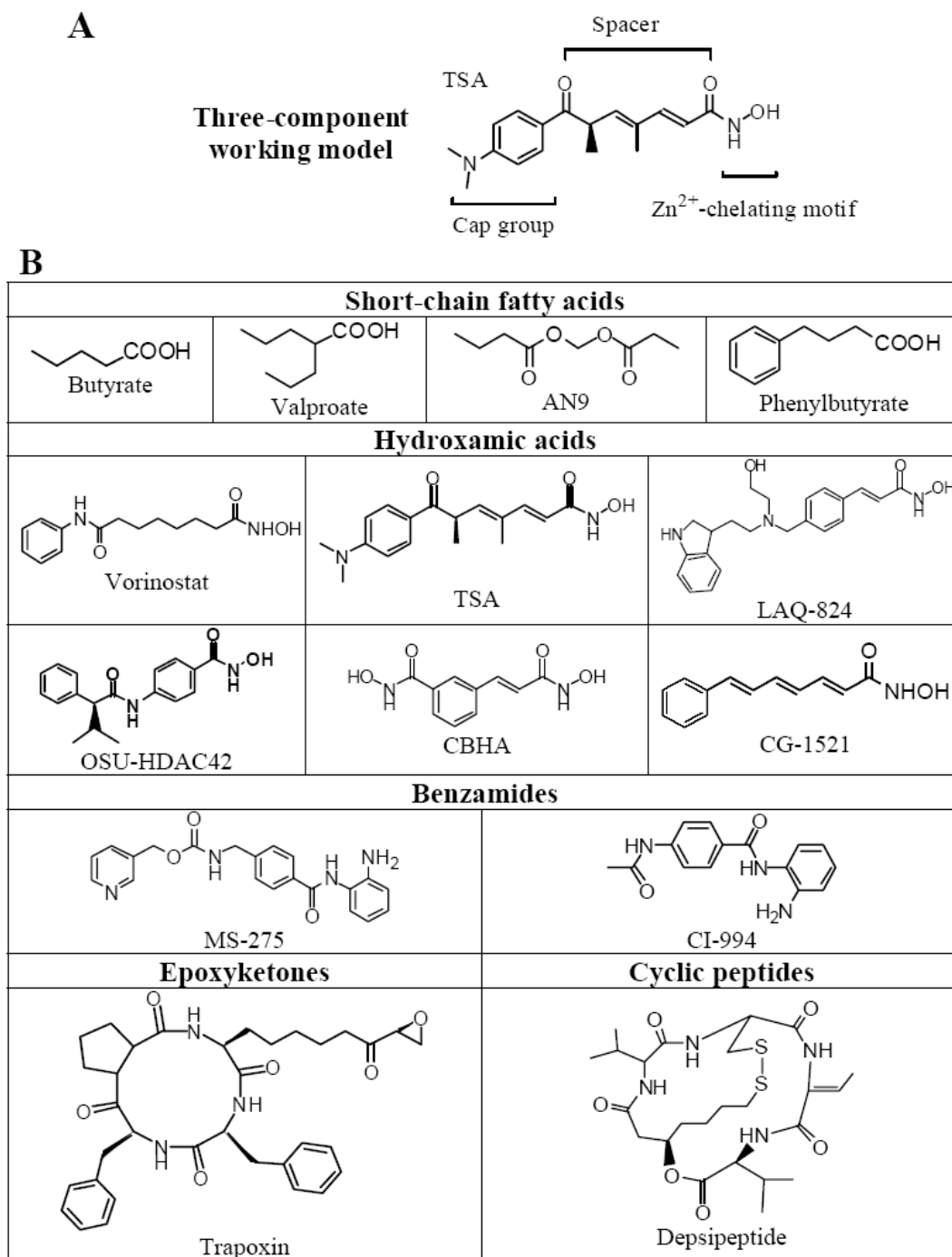


Fig. 1.1: Pharmacophore model (A) and chemical structures (B) of HDACi.

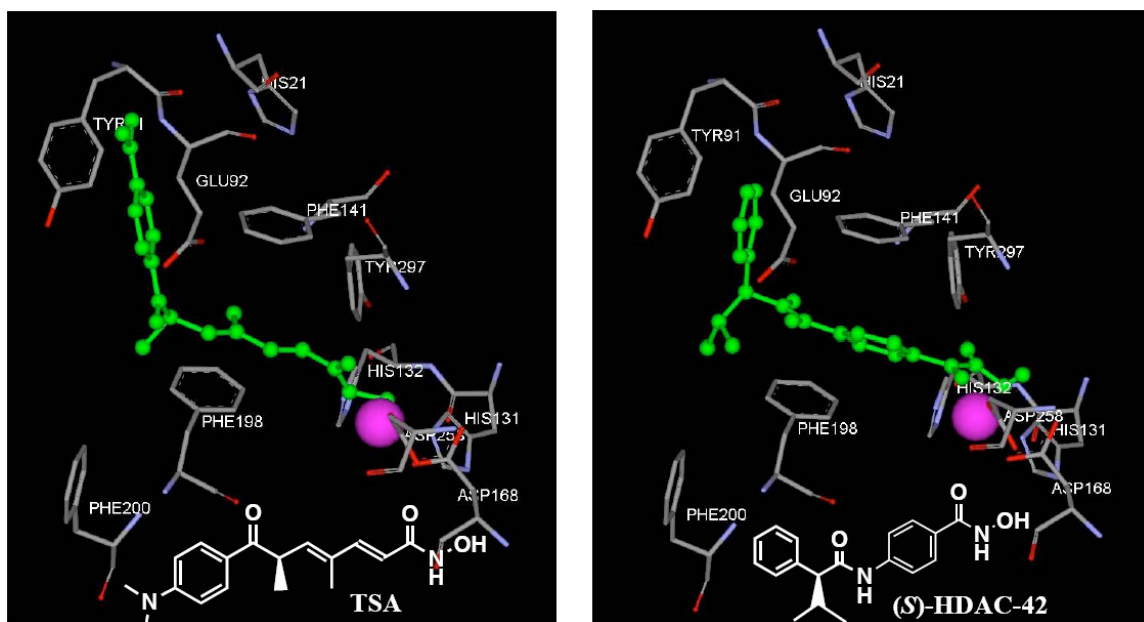


Fig. 1.2: Modeled docking of TSA (left) and (*S*)-HDAC42 (right) into the active site of histone deacetylase-like protein (HDLP). The small molecules are in the center of the images.

Substrate	Intracellular Function	Deacetylases	Ref.
Ku70	Anti-apoptosis	SIRT1, TSA-sensitive HDACs	61,62,144,145
FOXO1	Transcriptional factor	SIRT1	146
p300	Transcription factor	SIRT1	147
p53	Tumor suppressor	HDAC1, SIRT1	69-71,148-150
Androgen receptor	Hormone receptor	HDAC1, SIRT1	151-154
Smad7	Signal transducer of TGF- $\beta$	HDACs 1, 3, and 6	155
Stat3	Signal transducer of cytokines	HDACs 1, 2, and 3	89,91
NF- $\kappa$ B (RelA)	Nuclear transcription factor	HDAC3, SIRT1	96,156-158
SRY	Y-chromosome-encoded DNA-binding protein	HDAC3	159
$\alpha$ -Tubulin	Microtubule component	HDAC6, SIRT2	58,93,160-162
Hsp90	Molecular chaperone	HDAC6	80,87,163

Table 1.1: Representative non-histone substrates of HDACs.

HDACi	Other stimulus	Effect	Ref.
TSA, depsipeptide, vorinostat, sodium butyrate	5-aza-2-deoxycytidine	Enhanced apoptosis. Re-expression of hypermethylated genes.	123-127
CI-994, LAQ824, vorinostat	Gemcitabine, docetaxel	Enhanced cell cycle arrest and apoptosis.	19,85,128,130
Magnesium valproate	Neoadjuvant doxorubicin, cyclophosphamide	HDAC inhibition and gene reactivation.	131
OSU-HDAC42, TSA, vorinostat, MS-275	DNA-damaging agents bleomycin, doxorubicin, etoposide	Enhanced cell killing.	34,132
LAQ824, MS-275, sodium butyrate	TRAIL	Enhanced apoptosis. Apoptosis in TRAIL-resistant cells.	119,133,134
MS-275, vorinostat, sodium butyrate	LY294002	Enhanced apoptosis.	135
vorinostat	PD184352	Enhanced apoptosis.	136
vorinostat, depsipeptide, apicidin	Imatinib (STI571)	Enhanced apoptosis. Apoptosis in imatinib-resistant cells.	121,122,137,138
vorinostat, LBH589, sodium butyrate	17-AAG	Enhanced apoptosis and degradation of Hsp90 client proteins.	17,82,118
vorinostat, TSA, depsipeptide, MS-275, M344	Radiation	Enhanced radiosensitivity. Cell cycle arrest and inhibition of DNA synthesis.	120,139-141

Table 1.2: Combination strategies of HDACi and other anticancer agents.

## **CHAPTER 2**

### **OSU-HDAC42, A HISTONE DEACETYLASE INHIBITOR, BLOCKS TUMOR PROGRESSION IN THE TRANSGENIC ADENOCARCINOMA OF THE MOUSE PROSTATE MODEL**

#### **ABSTRACT**

Histone deacetylase (HDAC) inhibitors suppress tumor cell growth via a broad spectrum of mechanisms, which should prove advantageous in the context of cancer prevention. Here, we examined the effect of dietary administration of OSU-HDAC42, a novel HDAC inhibitor, on prostate tumor progression in the transgenic adenocarcinoma of the mouse prostate (TRAMP) model. Based on a series of pilot studies, an AIN-76A diet was formulated containing 208 ppm OSU-HDAC42, which was estimated to deliver approximately 25 mg/kg of drug per day to each mouse and found to cause a suppression of PC-3 xenograft tumor growth equivalent to that achieved by gavage administration of a similar dose. At 6 weeks of age, TRAMP mice received this drug-containing or control diet for 4 or 18 weeks, and were evaluated for prostatic intraepithelial neoplasia (PIN) and carcinoma development, respectively. OSU-HDAC42 not only decreased the severity of PIN and completely prevented its progression to poorly differentiated

carcinoma (74% incidence in controls vs. none in drug-treated mice), but also shifted tumorigenesis to a more differentiated phenotype, suppressing absolute and relative urogenital tract weights by 86% and 85%, respectively, at 24 weeks of age. This tumor suppression was associated with the modulation of intraprostatic biomarkers, including those indicative of HDAC inhibition, increased apoptosis and differentiation, and decreased proliferation. With the exception of completely reversible hematologic alterations and testicular degeneration, no significant changes in body weight or other indicators of general health were observed in drug-treated mice. These results suggest that OSU-HDAC42 has value in prostate cancer prevention.

## **INTRODUCTION**

Prostate cancer is the most commonly diagnosed noncutaneous cancer and the second leading cause of cancer death in men (1). Prostatic tumors often have a long initial latency period before becoming pathologically advanced, at which point they are invariably fatal (2, 3). Unfortunately, a consistently deregulated group of genes critical for malignant progression has not been identified for this disease (4). These attributes suggest a need to prevent prostate cancer, such as by chemopreventive agents capable of simultaneously modulating multiple cellular processes involved in prostate carcinogenesis.

Histone deacetylase (HDAC) inhibitors are appropriate candidates in this regard because of their ability to selectively induce apoptosis (5, 6), cell cycle arrest (7-9), and differentiation (10, 11) in cancer cells. These compounds have demonstrated pleiotropic

anticancer activities in many recent preclinical and clinical investigations of human cancers, including prostate cancer, through both histone acetylation-dependent and -independent mechanisms (12, 13, 10, 14). First, and representing the conventional rationale for their development, HDAC inhibitors induce the re-expression of growth arrest genes silenced in cancer through chromatin remodeling (15). Second, HDAC inhibitors modulate a growing list of nonhistone HDAC substrates including transcription factors and mediators of cell signaling in cancer cells, the immune system, and tumor vasculature (12, 16, 17). The paucity of knowledge of HDAC biology, however, has precluded a complete understanding of the anticancer mechanisms of these agents, and the toxicologic sequelae of chronic therapy are largely unknown (18).

We recently reported our development of a novel phenylbutyrate-based HDAC inhibitor, OSU-HDAC42, and demonstrated its potent and pleiotropic anticancer activities in models of human prostate and hepatic cancer *in vitro* and *in vivo* (19-24). Specifically, OSU-HDAC42 induces hallmark indicators of HDAC inhibition including histone H3 acetylation,  $\alpha$ -tubulin acetylation, and p21 upregulation, and modulates regulators of cell survival such as Akt, Bcl-xL, Bax, Ku70, survivin, and members of the inhibitor of apoptosis protein family (19-21, 24). In the present study, to evaluate these tumor suppressive effects in a chemopreventive context, we extended the use of OSU-HDAC42 to the transgenic adenocarcinoma of the mouse prostate (TRAMP) model, which mimics spontaneous tumor progression in man (25). Prostate lesion development in TRAMP is driven by the SV40 large T antigen (TAg) in the prostate epithelium (26). TAg disrupts cellular p53 and retinoblastoma functions, and is expressed upon activation

of an androgen response element in the probasin promoter (26). The ensuing tumorigenesis occurs in an age-dependent, multistage process including hyperplasia, prostatic intraepithelial neoplasia (PIN), and adenocarcinoma with distant metastasis (27).

Here, we employ an interdisciplinary approach entailing medicinal chemistry, molecular pharmacology, and veterinary pathology to assess the chemopreventive potential of OSU-HDAC42 concurrent with an investigation of whole-body ramifications of chronic therapy by using TRAMP mice as a model. Based on pilot studies demonstrating that dietary administration of OSU-HDAC42 suppressed PC-3 xenograft tumor growth, the drug was administered via diet to TRAMP mice to evaluate its inhibitory effects on PIN and prostate carcinoma. Collectively, our results show that OSU-HDAC42 achieves a remarkable suppression of prostate tumorigenesis in the absence of limiting toxicity.

## **MATERIALS AND METHODS**

**Reagents.** The HDAC inhibitors vorinostat (a.k.a., SAHA; suberoylanilide hydroxamic acid; Zolinza<sup>TM</sup>; Merck & Co. Inc., NJ, USA) and OSU-HDAC42 [a.k.a., (S)-HDAC-42; (S)-(+)-N-hydroxy-4-(3-methyl-2-phenylbutyrylamino)-benzamide] were synthesized in our laboratory with purities exceeding 99% as shown by nuclear magnetic resonance spectroscopy (300 MHz). OSU-HDAC42 (NSC D736012) is a novel hydroxamate-tethered phenylbutyrate derivative that had been evaluated preclinically by the Rapid Access to Intervention Development program at the National Cancer Institute

(NCI). Vorinostat is the first HDAC inhibitor to earn US Food and Drug Administration (FDA) approval and is marketed for the treatment of cutaneous T-cell lymphoma (10). AIN-76A rodent diet with and without 208 ppm OSU-HDAC42 was obtained from Research Diets, Inc. (New Brunswick, NJ). Mouse monoclonal antibodies against various target proteins were obtained from the following sources: p21 and TAg (Pab 101) (Santa Cruz Biotechnology, Inc., Santa Cruz, CA);  $\alpha$ -tubulin and acetylated (Ac)  $\alpha$ -tubulin (Sigma-Aldrich, St. Louis, MO); synaptophysin (Dako North America, Inc., Carpinteria, CA);  $\beta$ -actin (ICN Biomedicals, Irvine, CA). Rabbit polyclonal antibodies against various target proteins were obtained from the following sources: Acetylated histone H3 (Ac-H3) (Upstate Biotechnology Inc., Lake Placid, NY); Bax, Ki67, cleaved caspase-3, and E-cadherin (Cell Signaling Technology, Inc., Beverly, MA).

**Animals.** Male NCr athymic nude mice (5-7 weeks of age) were obtained from the NCI (Frederick, MD) and injected subcutaneously with PC-3 cells as described (21). Treatment was initiated 7 days following injection, with the gavage dose of drug adjusted twice weekly to mirror the dose of drug consumed in the diet. TRAMP mice (C57BL/6TRAMPxFVB) were generated and housed as previously reported (28). The reversibility of observed OSU-HDAC42-associated toxicity was determined in age-matched nontransgenic (wild-type) littermates of TRAMP, which included comparison of weights of the adrenal glands, brain, epididymides, epididymal fat pads, heart, kidneys, liver, pituitary gland, spleen, testes, and thymus. The procedures performed were in accordance with protocols approved by the Institutional Animal Care and Use Committee of The Ohio State University.

**Histopathology.** The entire carcass of each animal in all studies was evaluated for gross lesions and preserved in 10% formalin at necropsy. An extended set of tissues from representative animals (n = 3, 5, and 10 for the pharmacodynamic, xenograft, and TRAMP studies, respectively) was evaluated microscopically in accordance with Society of Toxicologic Pathology-proposed guidelines for repeat-dosing toxicity studies (29), with the exception of spinal cord and female reproductive organs. Dorsal (DP), lateral (LP), ventral (VP), and anterior (AP) prostate lobes, iliac lymph nodes, liver (left lobe), and lungs from each TRAMP mouse were collected, fixed, processed, and evaluated as described (28). Testes were fixed for 24 hours in Bouin's fixative, then transferred to 70% ethanol. The observer scoring the prostate slides (AS), via a TRAMP-specific grading scheme (30), was blinded to the treatment status.

**Immunodetection of biomarkers.** TRAMP prostate tissue homogenates were prepared and immunoblotted against Ac-H3, p21, Ac- $\alpha$ -tubulin,  $\alpha$ -tubulin, E-cadherin, synaptophysin, Bax, TAg, and  $\beta$ -actin as described (28). Immunohistochemical detection of Ac-H3, Ki67, cleaved caspase-3, E-cadherin, and synaptophysin was performed on four  $\mu$ M-thick, paraffin-embedded PC-3 xenograft tumor, TRAMP prostate, testis, spleen, and/or bone marrow tissue sections in accordance with the manufacturers' recommendations.

**Statistical analysis.** Satisfying the requisites of independence and normal distribution, a Student's *t*-test was used to determine if certain responses (immunoblotting and immunohistochemistry results, xenograft tumor volumes, body and tissue weights, and microscopic lesion scores and distributions) were influenced by drug treatment. The

incidences of prostate lesions and metastasis were compared with a Chi-square contingency analysis. Differences between groups were considered significant at  $P < 0.05$ .

## RESULTS

**Oral administration of OSU-HDAC42 modulates targets in TRAMP prostate with higher potency relative to vorinostat.** A series of pilot studies was carried out to identify an optimal dose and administration route of OSU-HDAC42 in preparation for a long-term prevention study in TRAMP mice. Considering the effect of dietary restriction on suppressed tumorigenesis in TRAMP mice (30, 31), a dose-ranging study was performed to identify a dosing schedule of OSU-HDAC42 that would not compromise body weight. Our data indicate that the doses of 25 mg/kg every day (QD) or 50 mg/kg every other day (QOD) by gavage had no significant effect on body weight, and exhibited no limiting toxicity in TRAMP mice. However, progressive weight losses were observed at higher doses including 40 mg/kg QD and 65 mg/kg QOD (data not shown).

To assess the HDAC inhibitory potency of these tolerated doses of OSU-HDAC42 *in vivo*, their pharmacodynamic effects vis-à-vis those of vorinostat on intraprostatic levels of histone H3 acetylation and p21 expression in the DPs of TRAMP mice were evaluated by Western blotting. Treatment with OSU-HDAC42 at both doses for 14 days caused greater increases in histone H3 acetylation than vorinostat at 50 mg/kg QD ( $P < 0.05$ ). A similar, but not statistically significant, trend occurred in p21 expression levels between OSU-HDAC42 and vorinostat (Fig. 2.1A). Together, these data indicate a higher HDAC

inhibitory potency for OSU-HDAC42 than for vorinostat at these dosing schedules.

**Dietary and gavage administrations of OSU-HDAC42 achieve equivalent suppression of PC-3 xenograft tumor growth.** To avoid repeated gavage-associated stressing of mice, feeding of drug in the diet represented a preferred route for long-term drug administration. To examine the feasibility of dietary delivery, the effect of OSU-HDAC42 administered via gavage versus diet on PC-3 tumor growth in nude mice was assessed. Accordingly, a diet was formulated to contain 208 ppm OSU-HDAC42, a concentration estimated by food consumption measurements to achieve an average dose of 25 mg/kg/day, which was previously reported to suppress PC-3 tumor growth when administered by gavage (21). PC-3 subcutaneous xenograft-bearing nude mice were treated with this diet or by daily gavage (with the gavage dose of OSU-HDAC42 adjusted twice weekly to mirror that consumed in the diet) for 6 weeks, and analyzed with respect to tumor volume and intratumoral target modulation.

The tumor growth curves for animals treated with drug in the diet and by gavage were nearly overlapping (Fig. 2.1B). Diet- and gavage-administered drug equivalently suppressed tumor volumes by 65.6% and 65.3%, respectively, compared to control animals (respective final volumes of  $190 \pm 17 \text{ mm}^3$  and  $183 \pm 29 \text{ mm}^3$  vs.  $424 \pm 51 \text{ mm}^3$  in controls, mean  $\pm$  SEM,  $P < 0.002$ ). The combined weights of the testes/epididymides were also comparably decreased by 64.5% and 61.8% in gavage- and diet-treated mice, respectively ( $101 \pm 8.4 \text{ mg}$  and  $108 \pm 13 \text{ mg}$  vs.  $284 \pm 26 \text{ mg}$  in controls, mean  $\pm$  SD,  $P < 0.0001$ ). Equivalent effects on blood cell counts and serum chemistry were also observed (data not shown; effects discussed in results of TRAMP studies below). Dietary drug

treatment did not significantly impact terminal body weight ( $30.3 \pm 3.8$  g in control mice versus  $30.4 \pm 2.5$  g in treated mice, mean  $\pm$  SD). Over the course of the study, mice consumed  $3.9 \pm 0.2$  g of diet per day, representing a  $28 \pm 3.3$  mg/kg/day dose of OSU-HDAC42 (means  $\pm$  SD).

**Suppression of PC-3 xenograft tumor growth is associated with target modulation by diet-administered OSU-HDAC42.** We previously reported that OSU-HDAC42 modulated a series of targets governing multiple aspects of prostate cancer cell survival *in vitro* and *in vivo* (21). To link the tumor suppressive activity of diet-administered OSU-HDAC42 with its effects on relevant biomarkers, immunohistochemical analyses were performed and indicate that the drug treatment significantly decreased the proliferation marker Ki67 concurrent with increased staining for Ac-H3 and the apoptosis marker cleaved caspase-3 (Fig. 2.1C and D).

**TRAMP mice develop prostatic hyperplasia and PIN at 6 weeks of age.** Having confirmed that the dietary administration of OSU-HDAC42 at 208 ppm was effective and safe in PC-3 tumor-bearing mice, we assessed its chemopreventive activity in the TRAMP model. Because TRAMP mice display an early stage of androgen-driven tumorigenesis by 6 weeks of age (26, 32), treatment was started at this age in our prevention study. The extent of lesions in prostate tissues of 6 week-old TRAMP mice was compared to that of age-matched wild-type mice with respect to urogenital tract (UGT) and prostate lobe weights, and microscopic lesion score and intra-lobe distribution. The weights of TRAMP UGT and prostate tissue were higher than that of wild-type mice, and this increase was attributable to epithelial hyperplasia and PIN, most

notably in the DPs and LPs (Fig. 2.2A, 2.3).

**OSU-HDAC42 decreases the severity of PIN in TRAMP mice at 10 weeks of age.**

PIN represents an opportune intervention point in man at which an effective therapeutic strategy could theoretically prevent or slow the progression to carcinoma (33-35). To assess the ability of OSU-HDAC42 to delay PIN development, 6-week-old TRAMP mice were treated with either control AIN-76A rodent diet or the diet containing 208 ppm OSU-HDAC42 through 10 weeks of age when control animals are expected to have developed advanced PIN and a low incidence of carcinoma (25). An approximate delivery of 19 mg OSU-HDAC42/kg/day to TRAMP mice over the course of the study was estimated by food consumption measurements.

PIN remained the most severe lesion in TRAMP mice following 4 weeks of treatment in both groups, with the exception of one poorly differentiated (PD) tumor in a control diet-fed mouse (Table 2.1). To ascertain subtle differences in lesion development between treatment groups, the weights of UGTs and prostate lobes, and microscopic lesion scores and intra-lobe distributions were compared. Fig. 2.2B and C show that OSU-HDAC42 suppressed the overall severity of PIN lesions as manifested in significant reductions in the weights of the UGTs and DPs, and significant decreases in the microscopic lesion scores in the LPs and VPs. The distribution of lesions within each prostate lobe was also affected, with a trend, as evident in the LPs and VPs and correlating with the decreased lesion score in these lobes, toward more normal epithelium and hyperplasia, and less PIN in drug-treated TRAMP mice (Fig. 2.2D). Seminal vesicle (SV) weights were also decreased by drug treatment [ $169 \pm 32$  mg in treated mice ( $n =$

15) versus  $193 \pm 31$  mg in control mice ( $n = 15$ ); mean  $\pm$  SD,  $P < 0.05$ ].

**OSU-HDAC42 prevents the progression of PIN to poorly differentiated carcinoma and shifts tumorigenesis to a more differentiated phenotype in TRAMP mice at 24 weeks of age.** We hypothesized that the suppressive effect of OSU-HDAC42 on the development of early proliferative lesions in TRAMP mice, as described above, would retard or prevent progression to carcinoma long-term. Accordingly, a larger numbers of animals ( $n = 23$ , to account for the expected increase in overall variation in lesion development in controls with age) were treated from 6 to 24 weeks of age when the majority of TRAMP mice will have developed advanced, metastatic tumors (25).

As summarized in Table 2.1, OSU-HDAC42 completely prevented the occurrence of macroscopic prostate tumors (78% of controls versus none in the drug-treated group) and of PD carcinoma (74% of controls versus none in the drug-treated group) after 18 weeks of treatment. Only 1 out of 23 drug-treated TRAMP mice had evidence of carcinoma microscopically (moderate differentiation). This profound inhibitory effect was reflected in the 86% and 85% reductions in absolute and relative UGT weights, respectively, in OSU-HDAC42-diet-fed mice relative to the controls. Specifically, the mean absolute and relative values of control versus drug-treated UGT weights were 3.1 grams versus 0.4 grams and 10% versus 1.5%, respectively (Fig. 2.4A and B; Table 2.1). The similarity in the reductions in absolute and relative UGT weights demonstrates that the antitumor effects occurred independent of an effect on body weight. Interestingly, the relative UGT weight of drug-treated TRAMP mice at 24 weeks of age was the same as that of control TRAMP mice at 10 weeks of age (1.5% of body weight).

Analysis of individual prostate lobes indicates that OSU-HDAC42 caused significant reductions in the weights of the DPs and microscopic lesion scores of the DPs, LPs, and VPs (Fig. 2.4B and C). As manifested in the lesion scores, the breakdown of lesion distribution by lobe shows that PIN remained the predominant lesion in the majority of OSU-HDAC42-treated mice at 24 weeks (Fig. 2.4D). In addition to the absence of PD tumors, drug-treated mice had significant increases in normal, hyperplastic, and/or PIN in all prostate lobes compared to control diet-fed mice. SV weights were also decreased by drug treatment [ $274 \pm 62$  mg in treated mice ( $n = 23$ ) versus  $377 \pm 147$  mg in control mice ( $n = 22$ ); mean  $\pm$  SD,  $P = 0.01$ ]. Control TRAMP mice developed palpable prostate tumors at  $19 \pm 2.7$  weeks of age; the tumors, including urinary bladder, weighed  $3.4 \pm 2.1$  grams at the time of sacrifice.

Interestingly, the incidence of adenomas at 24 weeks of age was greater in drug-treated TRAMP mice (43.5% versus 4.3% of controls, Table 2.1), and all adenomas occurred in the DPs (Fig. 3D). These tumors displayed characteristics consistent with adenoma according to terminology proposed by the Mouse Models of Human Cancer Consortium Prostate Pathology Committee (36). They consisted of focally distinct, intraluminal projections of well-differentiated epithelium arranged in papillary projections on hypocellular and non-edematous connective tissue scaffolds (Fig. 2.5C; lower left panel). A supportive fibrovascular stalk and compression atrophy of adjacent epithelium were present in some sections. Nuclear and cellular atypia, mitotic figures, and destructive invasion were lacking. Arising within a background of PIN, the adenomas generally occupied a small percentage of total lobe area ( $8.3 \pm 2.5\%$ , mean  $\pm$

SEM).

To shed light onto the latency of the adenomas after agent withdrawal, two TRAMP mice were returned to control diet at 24 weeks of age. These mice were sacrificed at 42 weeks of age with palpable tumors arising in the SVs that were determined microscopically to be epithelial-stromal tumors (37). The prostate lobes were variably expanded by phyllodes-like tumors (APs, DPs), PIN (VPs), and well-differentiated carcinoma (LPs) with no evidence of metastasis (Fig. 2.6).

**Tumor suppression in TRAMP mice by OSU-HDAC42 is associated with target modulation and biomarkers of differentiation.** Relevant HDAC inhibition-associated and cell survival biomarkers were assessed in the PIN lesions of TRAMP mice after treatment from 6–10 weeks of age. Drug treatment significantly altered the proliferation and apoptotic indices in PIN, as demonstrated by immunohistochemical staining of Ki67 and cleaved caspase-3 (Fig. 2.5A). OSU-HDAC42 induced 2.6-fold and 2-fold increases ( $P < 0.01$ ) in the acetylation of  $\alpha$ -tubulin and the expression of Bax compared to controls, respectively (Fig. 2.5B). An increase in histone H3 acetylation was also noted, but was not statistically significant due to greater variation in this biomarker.

The marked disparity in prostate morphology at 24 weeks of age between the two treatment groups, i.e., PD tumors in controls versus PIN and adenomas in drug-treated mice, suggested a shift to a more differentiated phenotype in response to OSU-HDAC42. While this disparity precluded a morphology-matched comparison of biomarkers between treatment groups, an effort was made to evaluate the expression of biomarkers of differentiation in representative tissue samples by using immunohistochemistry and

immunoblotting analyses. Distinct differences in the expression levels of E-cadherin and synaptophysin were noted between the treatment groups, both of which were reported to be dysregulated with lesion progression in TRAMP mice (38, 25). In 24-week-old TRAMP mice, OSU-HDAC42 maintained E-cadherin expression, which was lost in controls, and prevented the expression of synaptophysin (an indicator of the neuroendocrine phenotype), which was increased in controls (Fig. 2.5C and D). The increased Ac-H3 levels in adenomas confirmed the HDAC-inhibitory effect of OSU-HDAC42 in the prostate (Fig. 2.5C).

**OSU-HDAC42 causes reversible hematologic alterations and testicular degeneration.** Toxicologic effects of OSU-HDAC42 in TRAMP mice were assessed by hematologic, histopathologic, and body and organ weight evaluations. There was no significant difference in the body weight after 18 weeks of treatment [ $31 \pm 3.6$  g for treated mice ( $n = 23$ ) versus  $29 \pm 2.7$  g for control mice ( $n = 23$ ); mean  $\pm$  SD,  $P = 0.6$ ]. The weights of epididymal fat pads, measured as an assessment of body fat and additional indicator of general health, were also not significantly altered [ $549 \pm 349$  mg in treated mice ( $n = 23$ ) versus  $625 \pm 282$  mg in control mice ( $n = 18$ ); mean  $\pm$  SD,  $P = 0.5$ ]. After 4 weeks of treatment with OSU-HDAC42 (i.e., 10 weeks of age), a significant leukopenia characterized by a mature neutropenia and lymphopenia was present, and red cell numbers were decreased (Table 2.2). All blood cell counts returned to control levels upon withdrawal of drug in wild-type littermates of TRAMP mice. Femoral and sternebral bone marrow of 4-week-treated animals was of comparable cellularity and proliferative status to controls with all cell types and stages of maturation

present (Fig. 2.7). None of the hematologic abnormalities observed after 4 weeks of treatment was noted after 18 weeks of treatment, i.e., 24 weeks of age (Table 2.2). Extramedullary hematopoiesis (EMH) was increased in the spleens of mice treated for both 4 and 18 weeks, and reversible thymic atrophy, demonstrated by histology and organ weight data, occurred in association with OSU-HDAC42 treatment (Fig. 2.7 and Table 2.3).

Significant effects on serum chemistry after 4 weeks of treatment included increased AST, total bilirubin, and albumin, and decreased ALP and cholesterol, all of which, like the blood cell count alterations, returned to controls levels upon discontinuation of the drug. At 18 weeks of treatment, significant decreases remained in ALP and cholesterol, as well as decreased potassium and increased protein that appeared to be due to elevated albumin (Table 2.2).

Other than effects on the prostate, spleen (EMH), and thymus (atrophy), the only lesion detected by gross or histopathologic examination was severe testicular degeneration in drug-treated mice. A marked bilateral reduction in the size of the testes was noted after two weeks of repeated dosing of OSU-HDAC42, but not with vorinostat (Fig. 2.8A). Weights of the testes and epididymides decreased progressively in TRAMP mice after 4 and 18 weeks of treatment, and eventually returned to control levels upon withdrawal of the drug after each treatment period (Fig. 2.8C). Mice were able to achieve litters within 6-8 weeks of drug withdrawal following both 4 and 18 weeks of treatment, and the sizes of these litters (9 and 11 pups for the first litters of two recovered mice following 4 weeks of treatment, and 8 and 13 pups for the first litters of two

recovered mice following 18 weeks of treatment) were estimated to be normal for their strain background.

Histologically, the seminiferous tubules of drug-treated mice were devoid of spermatozoa and lined predominantly by Sertoli cells, spermatogonia, and variable numbers of primary spermatocytes up to the leptotene-zygotene stage. Immunostaining of Ki67 demonstrates that actively dividing spermatogonia remained even after 18 weeks of drug treatment (Fig. 2.8B). No morphologic abnormalities of the Sertoli or Leydig cells were noted.

**Tumor suppression by OSU-HDAC42 in TRAMP mice is not associated with disruption of large T antigen expression.** Given the consistent and marked drug effect on the testes, an effort was made to determine whether the dramatic suppression of tumorigenesis in TRAMP was associated with disruption of TAG expression or androgen production. Immunoblotting of prostate tissue homogenates shows that TAG was expressed at similar levels in OSU-HDAC42-diet- and control-diet-fed mice both at 10 and 24 weeks of age. Moreover, serum testosterone levels in drug-treated mice were not significantly different from those in controls, refuting the involvement of altered TAG expression or androgen production in the suppressive effects of OSU-HDAC42 on tumorigenesis (Fig. 2.8D).

## **DISCUSSION**

The intensity of efforts to develop HDAC inhibitors for cancer therapy is reflected by the recent FDA approval of vorinostat (10) and the current use of at least ten different

HDAC inhibitors in more than eighty clinical cancer trials ([www.clinicaltrials.gov](http://www.clinicaltrials.gov)). Far fewer studies, however, address the chemopreventive activities of these agents (38). The features of HDAC inhibitors that underlie their preclinical and clinical successes to date as cancer therapeutic agents, such as their broad spectrum of activities against regulators of cellular differentiation, cell cycle, and apoptosis, as well as their differential toxicity (8, 39) for transformed cells, also predict favorably for their chemopreventive activity, and are especially fitting for the molecularly heterogeneous and initially latent disease of prostate cancer. However, lack of full understanding of HDAC biology precludes the complete mechanistic characterization of HDAC inhibitors and hinders the prediction of drug-associated toxicity (18). Consequently, this study is aimed at providing insight into both the chemopreventive efficacy and toxicity of chronic therapy of OSU-HDAC42 by examining its *in vivo* impact on tumorigenic and phenotypic endpoints in TRAMP mice.

To establish the anti-tumor efficacy of the dietary administration of OSU-HDAC42, the *in vivo* effects of dietary delivery were compared to that of gavage administration in PC-3 tumor-bearing mice. Despite the presumed differences in the pharmacokinetic behaviors of OSU-HDAC42 administered by these two methods of drug delivery, the effect on endpoints of efficacy (PC-3 tumor volume) and toxicity (testis/epididymis weight, hematologic parameters) were, nevertheless, equivalent. This finding established the feasibility of dietary administration of OSU-HDAC42 and suggests a desirable pharmacokinetic feature of the drug, which provides flexibility in its delivery method in cancer treatment.

Targeting PIN as a method to control prostate cancer was recently validated by the

association of finasteride's cancer preventive activity with reduced risk of PIN in the Prostate Cancer Prevention Trial (35). Similarly, in our study, the suppression of PIN in TRAMP mice by OSU-HDAC42 correlated with a marked retardation of prostate tumorigenesis. It is noteworthy that in 24-week old TRAMP mice, OSU-HDAC42 completely inhibited the occurrence of PD carcinoma and suppressed the relative UGT weight to that of 10-week-old control TRAMP mice. To our knowledge, this is the most potent chemopreventive effect achieved by a small-molecule agent in TRAMP mice with documentation of the effects on body weight. The class I HDAC inhibitor, MS-275, induced much smaller reductions in macroscopic tumor incidence (9/10 controls versus 5/11 drug-treated animals) and UGT weights of TRAMP mice treated over an age interval and with a drug dose similar to those in our study (5-7 weeks to 27 weeks of age and 20 mg/kg/day) (40). Considering that OSU-HDAC42 affects both class I and II HDAC substrates (20) and that the clinical significance of improving HDAC isoform selectivity is undetermined (41), these findings support a role for broad spectrum HDAC inhibitors in prostate cancer chemoprevention.

The high incidence of adenomas in OSU-HDAC42-treated TRAMP mice is noteworthy. The adenoma phenotype is not included in the spectrum of lesions described by the founders of the model (25), and is rarely reported in TRAMP by other investigators. While the mechanistic basis for adenoma formation in response to drug treatment is uncertain, the pro-differentiation effects attributed to HDAC inhibitors are potentially involved. Consistent with this notion are the changes in E-cadherin and synaptophysin expression observed in representative prostate tissue from control and

OSU-HDAC42-treated TRAMP mice at 24 weeks. Although these adenomas were limited to the DPs, the reported location of phyllodes-like tumors in TRAMP mice (25), their morphology was distinctly different from phyllodes-like lesions in that they contained a scant stromal compartment. The single phyllodes-like tumor detected in this study occurred concomitantly with an adenoma in the same DP of a drug-treated mouse. While these adenomas could be interpreted to represent a drug-induced alteration of phyllodes-like tumor growth, the coexistence of these lesions suggests they were unrelated.

The exact cause of OSU-HDAC42-induced testicular degeneration remains undetermined; however, based on unchanged serum levels of testosterone and TAg expression in treated TRAMP mice, this toxicity does not appear to involve disrupted androgen production. This is an important point since carcinogenesis in the TRAMP model is initially dependent on androgen to induce TAg expression through the probasin promoter. Thus, unlike flutamide, which decreased prostate lesion development in TRAMP mice in association with its antiandrogen activity and suppression of TAg (42), the potent chemopreventive effects observed in our study are attributed to the direct effects of OSU-HDAC42 on the prostate. The sparing of spermatogonia in the degenerative testes of treated mice correlates well with the reversible nature of the lesion. Since the leptotene-zygotene spermatocytes are the most progressed cell types of the spermatogenic cycle remaining in drug-treated testis, OSU-HDAC42 likely disrupts the successional stage of meiotic prophase, the pachytene-diplotene primary spermatocytes.

The lack of testicular degeneration in vorinostat-treated mice in our pilot study shows

that this toxicity is not common to all agents in this class. To our knowledge, the only other report of HDAC inhibitor-associated testicular degeneration involved trichostatin-A (TSA), which was also concluded to target spermatocytes (43). Although a direct link to testicular HDAC inhibition has not been demonstrated with TSA or OSU-HDAC42, this association is plausible given the critical role of HDACs in the control of chromatin condensation during spermatogenesis (44). Differences in HDAC isoform selectivity could play a role in this toxicity given the high expression of HDAC6, against which OSU-HDAC42 and TSA have potent inhibitory activity (20, 45), in normal testis compared to other tissues (46). In any event, it should be noted that OSU-HDAC42 has not been evaluated clinically yet, thus its effect on human testis is unknown and a conclusion regarding the risk-efficacy ratio for this toxicity in man would be speculative at this time. In fact, the consistent, potent, and reversible effect of OSU-HDAC42 on the testes, with sparing of major organ histology and weight, may warrant its evaluation for the treatment of testicular cancer.

The transient decrease in circulating blood cells that occurred in OSU-HDAC42-treated mice without effects on bone marrow cellularity is different from the myelosuppression observed with cytotoxic agents currently in clinical use, and, as is suspected with other HDAC inhibitors, suggests a mechanism other than toxicity to early hematopoietic precursors (47). Compensatory EMH in the spleens of OSU-HDAC42-treated mice may explain the absence of leukopenia following 18 weeks of treatment. The significance of these hematologic alterations, which must be interpreted in light of their magnitude and in conjunction with all pathology parameters and in-life observations

(48), requires further preclinical evaluation and dose titration to assess potential implications for human patients. Importantly, no lesions were detected in major organs, either by histologic assessment or by organ weight evaluation (Table 2.3), including heart, liver, kidney, lung, adrenal gland, pituitary gland, and brain, that correlated with the hematologic abnormalities.

In summary, OSU-HDAC42 suppressed the severity of PIN and completely blocked the progression of PIN to PD carcinoma in the TRAMP model. The tumor suppressive effects were associated with intraprostatic modulation of HDAC and targets regulating cancer cell survival and differentiation. These results suggest clinical value in incorporating OSU-HDAC42 into the management regimen of patients with PIN. In addition to effects of drug treatment on the prostate, we partially characterized reversible testicular degeneration and identified hematologic alterations that should be considered for monitoring in the future preclinical and clinical use of this and other HDAC inhibitors.

## **LIST OF REFERENCES**

1. Jemal A, Siegel R, Ward E, et al. Cancer statistics, 2007. *CA Cancer J Clin* 2007;57:43-66.
2. Crawford ED Epidemiology of prostate cancer. *Urology* 2003;62:3-12.
3. Sheldon CA, Williams RD, and Fraley EE Incidental carcinoma of the prostate: a review of the literature and critical reappraisal of classification. *J Urol* 1980;124:626-31.
4. Sander M, Trump BF, and Harris CC The Twenty-First Aspen Cancer Conference: Mechanisms of Toxicity, Carcinogenesis, Cancer Prevention, and Cancer Therapy, 2006. *Mol Carcinog* 2007;46:415-35.

5. Marks PA and Dokmanovic M Histone deacetylase inhibitors: discovery and development as anticancer agents. *Expert Opin Investig Drugs* 2005;14:1497-511.
6. Rosato RR, Maggio SC, Almenara JA, et al. The histone deacetylase inhibitor LAQ824 induces human leukemia cell death through a process involving XIAP down-regulation, oxidative injury, and the acid sphingomyelinase-dependent generation of ceramide. *Mol Pharmacol* 2006;69:216-25.
7. Nimmanapalli R, Fuino L, Stobaugh C, et al. Cotreatment with the histone deacetylase inhibitor suberoylanilide hydroxamic acid (SAHA) enhances imatinib-induced apoptosis of Bcr-Abl-positive human acute leukemia cells. *Blood* 2003;101:3236-9.
8. Ungerstedt JS, Sowa Y, Xu WS, et al. Role of thioredoxin in the response of normal and transformed cells to histone deacetylase inhibitors. *Proc Natl Acad Sci U S A* 2005;102:673-8.
9. Xu W, Ngo L, Perez G, et al. Intrinsic apoptotic and thioredoxin pathways in human prostate cancer cell response to histone deacetylase inhibitor. *Proc Natl Acad Sci U S A* 2006;103:15540-5.
10. Marks PA and Breslow R Dimethyl sulfoxide to vorinostat: development of this histone deacetylase inhibitor as an anticancer drug. *Nat Biotechnol* 2007;25:84-90.
11. Marks PA, Richon VM, and Rifkind RA Cell cycle regulatory proteins are targets for induced differentiation of transformed cells: Molecular and clinical studies employing hybrid polar compounds. *Int J Hematol* 1996;63:1-17.
12. Bolden JE, Peart MJ, and Johnstone RW Anticancer activities of histone deacetylase inhibitors. *Nat Rev Drug Discov* 2006;5:769-84.
13. Drummond DC, Noble CO, Kirpotin DB, et al. Clinical development of histone deacetylase inhibitors as anticancer agents. *Annu Rev Pharmacol Toxicol* 2005;45:495-528.
14. Minucci S and Pelicci PG Histone deacetylase inhibitors and the promise of epigenetic (and more) treatments for cancer. *Nat Rev Cancer* 2006;6:38-51.
15. Glaser KB, Staver MJ, Waring JF, et al. Gene expression profiling of multiple histone deacetylase (HDAC) inhibitors: defining a common gene set produced by HDAC inhibition in T24 and MDA carcinoma cell lines. *Mol Cancer Ther* 2003;2:151-63.
16. Qian DZ, Kato Y, Shabbeer S, et al. Targeting tumor angiogenesis with histone

- deacetylase inhibitors: the hydroxamic acid derivative LBH589. *Clin Cancer Res* 2006;12:634-42.
17. Wang XQ, Alfaro ML, Evans GF, et al. Histone deacetylase inhibition results in decreased macrophage CD9 expression. *Biochem Biophys Res Commun* 2002;294:660-6.
  18. Garber K HDAC inhibitors overcome first hurdle. *Nat Biotechnol* 2007;25:17-9.
  19. Chen CS, Wang YC, Yang HC, et al. Histone deacetylase inhibitors sensitize prostate cancer cells to agents that produce DNA double-strand breaks by targeting Ku70 acetylation. *Cancer Res* 2007;67:5318-27.
  20. Chen CS, Weng SC, Tseng PH, et al. Histone acetylation-independent effect of histone deacetylase inhibitors on Akt through the reshuffling of protein phosphatase 1 complexes. *J Biol Chem* 2005;280:38879-87.
  21. Kulp SK, Chen CS, Wang DS, et al. Antitumor effects of a novel phenylbutyrate-based histone deacetylase inhibitor, (S)-HDAC-42, in prostate cancer. *Clin Cancer Res* 2006;12:5199-206.
  22. Lu Q, Wang DS, Chen CS, et al. Structure-based optimization of phenylbutyrate-derived histone deacetylase inhibitors. *J Med Chem* 2005;48:5530-5.
  23. Lu Q, Yang YT, Chen CS, et al. Zn<sup>2+</sup>-chelating motif-tethered short-chain fatty acids as a novel class of histone deacetylase inhibitors. *J Med Chem* 2004;47:467-74.
  24. Lu YS, Kashida Y, Kulp SK, et al. Efficacy of a novel histone deacetylase inhibitor in murine models of hepatocellular carcinoma. *Hepatology* 2007; 46:1119-30.
  25. Kaplan-Lefko PJ, Chen TM, Ittmann MM, et al. Pathobiology of autochthonous prostate cancer in a pre-clinical transgenic mouse model. *Prostate* 2003;55:219-37.
  26. Greenberg NM, DeMayo F, Finegold MJ, et al. Prostate cancer in a transgenic mouse. *Proc Natl Acad Sci U S A* 1995;92:3439-43.
  27. Klein RD The use of genetically engineered mouse models of prostate cancer for nutrition and cancer chemoprevention research. *Mutat Res* 2005;576:111-9.
  28. Sargeant AM, Klein RD, Rengel RC, et al. Chemopreventive and bioenergetic signaling effects of PDK1/Akt pathway inhibition in a transgenic mouse model of prostate cancer. *Toxicol Pathol* 2007;35:549-61.
  29. Bregman CL, Adler RR, Morton DG, et al. Recommended tissue list for

- histopathologic examination in repeat-dose toxicity and carcinogenicity studies: a proposal of the Society of Toxicologic Pathology (STP). *Toxicol Pathol* 2003;31:252-3.
30. Suttie A, Nyska A, Haseman JK, et al. A grading scheme for the assessment of proliferative lesions of the mouse prostate in the TRAMP model. *Toxicol Pathol* 2003;31:31-8.
  31. Suttie AW, Dinse GE, Nyska A, et al. An investigation of the effects of late-onset dietary restriction on prostate cancer development in the TRAMP mouse. *Toxicol Pathol* 2005;33:386-97.
  32. Greenberg NM, DeMayo FJ, Sheppard PC, et al. The rat probasin gene promoter directs hormonally and developmentally regulated expression of a heterologous gene specifically to the prostate in transgenic mice. *Mol Endocrinol* 1994;8:230-9.
  33. Clark LC and Marshall JR Randomized, controlled chemoprevention trials in populations at very high risk for prostate cancer: Elevated prostate-specific antigen and high-grade prostatic intraepithelial neoplasia. *Urology* 2001;57:185-7.
  34. Sakr WA and Partin AW Histological markers of risk and the role of high-grade prostatic intraepithelial neoplasia. *Urology* 2001;57:115-20.
  35. Thompson IM, Lucia MS, Redman MW, et al. Finasteride decreases the risk of prostatic intraepithelial neoplasia. *J Urol* 2007;178:107-9; discussion 10.
  36. Shappell SB, Thomas GV, Roberts RL, et al. Prostate pathology of genetically engineered mice: definitions and classification. The consensus report from the Bar Harbor meeting of the Mouse Models of Human Cancer Consortium Prostate Pathology Committee. *Cancer Res* 2004;64:2270-305.
  37. Tani Y, Suttie A, Flake GP, et al. Epithelial-stromal tumor of the seminal vesicles in the transgenic adenocarcinoma mouse prostate model. *Vet Pathol* 2005;42:306-14.
  38. Huss WJ, Lai L, Barrios RJ, et al. Retinoic acid slows progression and promotes apoptosis of spontaneous prostate cancer. *Prostate* 2004;61:142-52.
  39. Warrenner R, Beamish H, Burgess A, et al. Tumor cell-selective cytotoxicity by targeting cell cycle checkpoints. *Faseb J* 2003;17:1550-2.
  40. Qian DZ, Wei YF, Wang X, et al. Antitumor activity of the histone deacetylase inhibitor MS-275 in prostate cancer models. *Prostate* 2007;67:1182-93.
  41. Karagiannis TC and El-Osta A Will broad-spectrum histone deacetylase inhibitors be

- superseded by more specific compounds? *Leukemia* 2007;21:61-5.
42. Raghoebar S, Kuliiev E, Steakley M, et al. Efficacious chemoprevention of primary prostate cancer by flutamide in an autochthonous transgenic model. *Cancer Res* 2000;60:4093-7.
  43. Fenic I, Sonnack V, Failing K, et al. In vivo effects of histone-deacetylase inhibitor trichostatin-A on murine spermatogenesis. *J Androl* 2004;25:811-8.
  44. Hazzouri M, Pivot-Pajot C, Faure AK, et al. Regulated hyperacetylation of core histones during mouse spermatogenesis: involvement of histone deacetylases. *Eur J Cell Biol* 2000;79:950-60.
  45. Matsuyama A, Shimazu T, Sumida Y, et al. In vivo destabilization of dynamic microtubules by HDAC6-mediated deacetylation. *Embo J* 2002;21:6820-31.
  46. Seigneurin-Berny D, Verdel A, Curtet S, et al. Identification of components of the murine histone deacetylase 6 complex: link between acetylation and ubiquitination signaling pathways. *Mol Cell Biol* 2001;21:8035-44.
  47. Sandor V, Bakke S, Robey RW, et al. Phase I trial of the histone deacetylase inhibitor, depsipeptide (FR901228, NSC 630176), in patients with refractory neoplasms. *Clin Cancer Res* 2002;8:718-28.
  48. Boone L, Meyer D, Cusick P, et al. Selection and interpretation of clinical pathology indicators of hepatic injury in preclinical studies. *Vet Clin Pathol* 2005;34:182-8.

Figure 2.1: Pilot studies done in preparation for a chemoprevention trial in the TRAMP model. *A*, representative immunoblots of prostate tissue lysates from 10-week-old TRAMP mice treated as indicated for 14 days. Orally administered OSU-HDAC42 induced the expression of Ac-H3 and p21 in the prostate more potently than vorinostat. The values in fold, quantified by densitometry, denote the intensity of protein bands relative to that of  $\beta$ -actin and standardized to the vehicle control group (means  $\pm$  SD,  $n = 3$ ). The fold increases in Ac-H3 by both doses of OSU-HDAC42 were significant at  $P < 0.05$ . *B*, diet and gavage-administered OSU-HDAC42 equivalently suppressed the growth of subcutaneous PC-3 xenograft tumors in nude mice treated from 7 to 49 days following engraftment ( $P < 0.002$  compared to controls). Values represent means  $\pm$  SEM ( $n = 10$ ) of tumor volumes calculated using the standard formula: length  $\times$  width<sup>2</sup>  $\times$  0.52. The gavage dose of drug was adjusted twice weekly to mirror the dose consumed in the diet, the latter of which was calculated from the difference in the mass of food per mouse in 24 hours divided by body weight. 42, OSU-HDAC42. *C*, photomicrographs (400x mag.) of representative Ac-H3, Ki67, and cleaved caspase-3-immunostained sections of PC-3 tumors from mice treated via experimental diet as described in *B*. *D*, quantification of immunostaining in *C* shows that OSU-HDAC42 induced histone H3 hyperacetylation, decreased the proliferation index, and increased the apoptotic index. Ac-H3 staining was quantified using Image-Pro Plus software (Media Cybernetics, Inc., Bethesda, MD) from 10 randomly chosen 400x fields. The percentages of Ki67- and cleaved caspase-3-positive cells were manually counted from 10 randomly chosen 400x fields. Values represent means  $\pm$  SD. \* $P < 0.05$ , \*\* $P < 0.01$ .

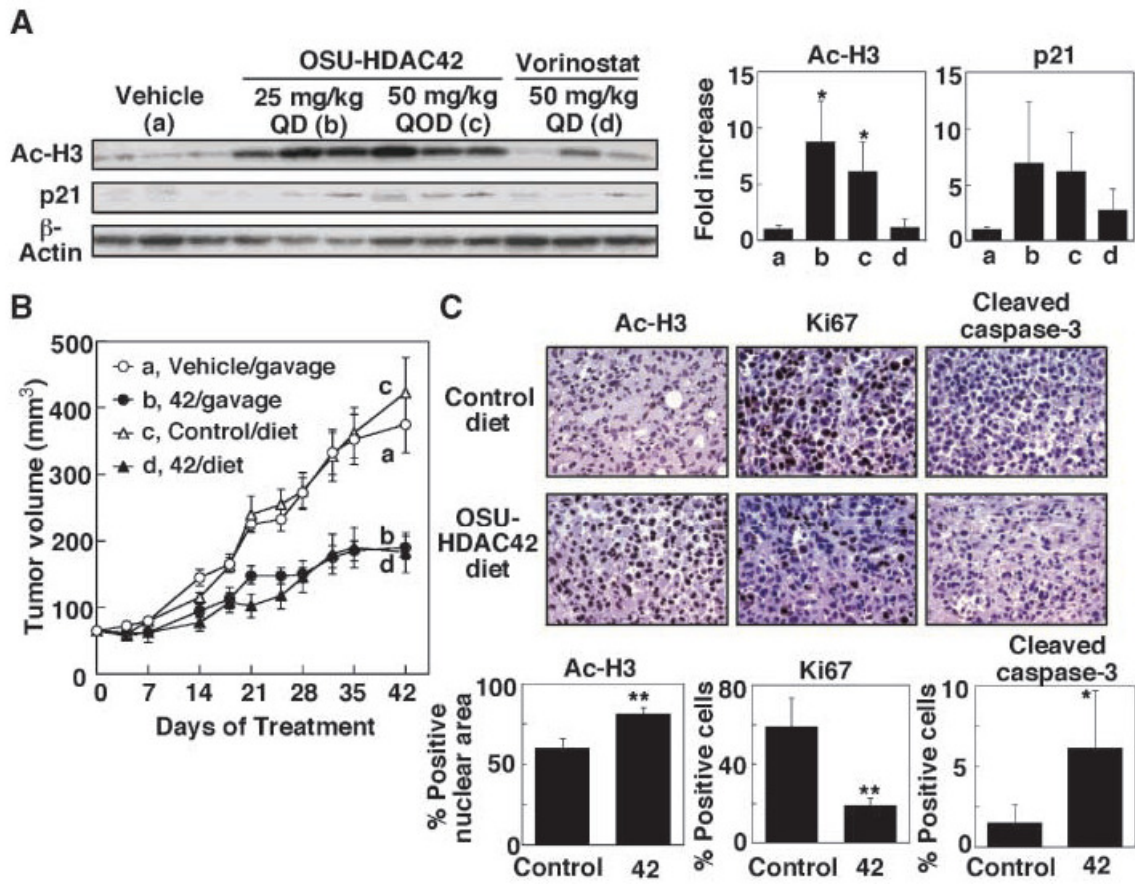


Figure 2.1

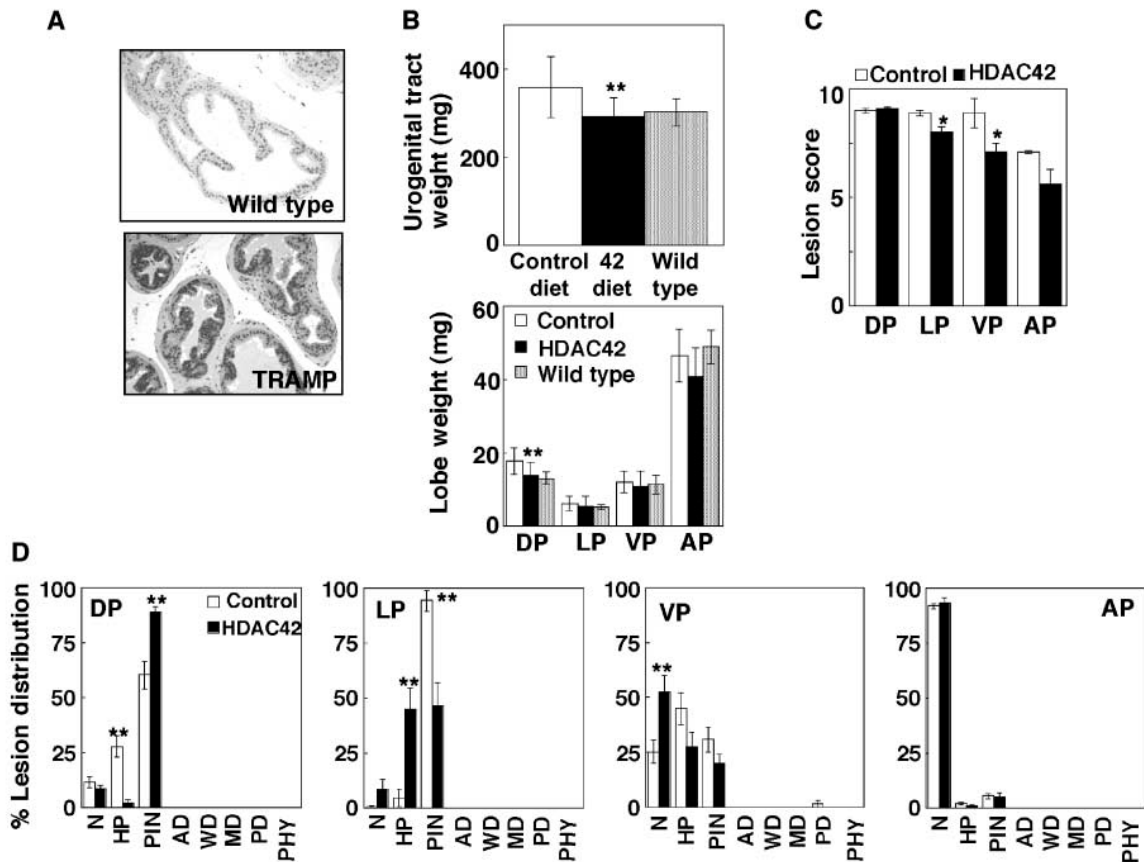


Figure 2.2: OSU-HDAC42 suppressed the development of prostate lesions in 10-week-old TRAMP mice. *A*, photomicrographs of representative dorsal prostate tissue from TRAMP and wild-type mice at the beginning of treatment (6 weeks of age) (H&E stain, 200x mag.). Note the histologic spectrum of normal epithelium, simple hyperplasia, and PIN in the TRAMP prostate at 6 weeks. *B*, urogenital tract and individual prostate lobe weights of TRAMP mice fed an AIN-76A rodent diet with or without 208 ppm OSU-HDAC42 from 6 to 10 weeks of age, compared to wild-type littermates fed a control diet. *C*, scoring of lesion severity in individual prostate lobes of control and OSU-HDAC42-treated TRAMP mice. *D*, distribution of lesions within the prostate lobes of control and OSU-HDAC42-treated TRAMP mice. Values represent means  $\pm$  SD ( $n = 15$  TRAMP and 5 wild-type mice). \* $P < 0.05$ , \*\* $P < 0.01$ . HDAC42, OSU-HDAC42; N, normal; HP, hyperplasia; PIN, prostatic intraepithelial neoplasia; AD, adenoma; WD, MD, and PD, well, moderate, and poorly differentiated carcinoma; PHY, phyllodes-like tumor.

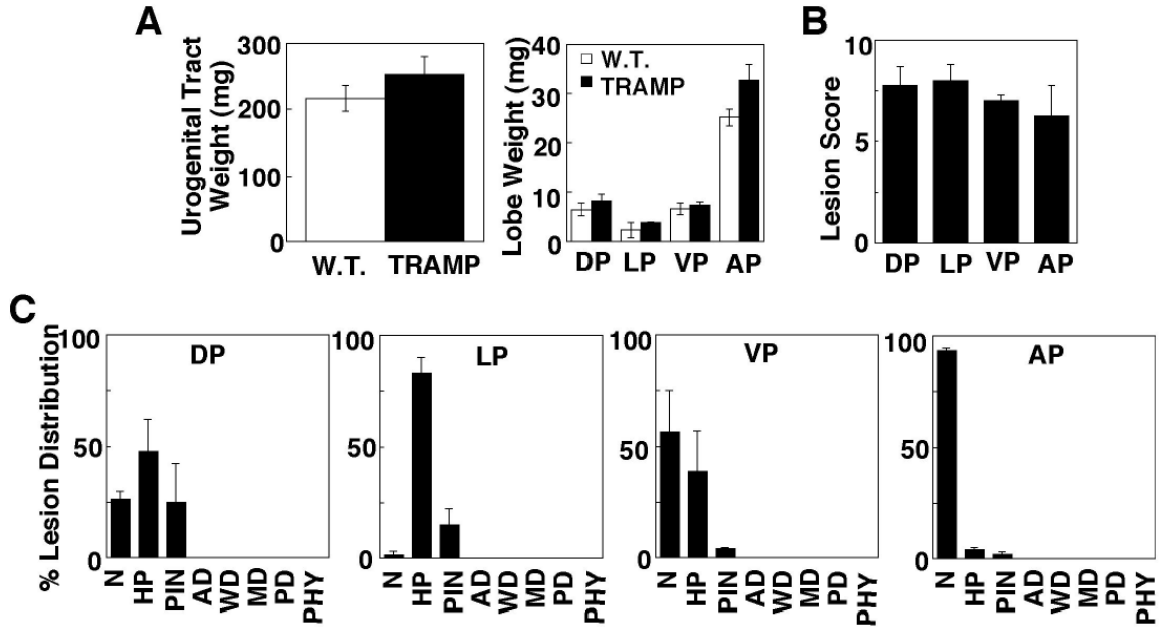


Figure 2.3: Characterization of lesions in the prostates of 6-week-old TRAMP mice shows that hyperplasia and PIN are present at this age. *A*, urogenital tract and individual prostate lobe weights of TRAMP mice and wild-type littermates. *B*, lesion scores for individual prostate lobes of TRAMP mice at 6 weeks. *C*, distribution of lesions within the prostate lobes of TRAMP mice. Lesion scoring and distribution were determined as described in the Materials and Methods. Values represent means  $\pm$  SD ( $n = 4$ ). DP, dorsal prostate; LP, lateral prostate; VP, ventral prostate; AP, anterior prostate; N, normal; HP, hyperplasia; PIN, prostatic intraepithelial neoplasia; AD, adenoma; WD, MD, and PD, well, moderate, and poorly differentiated carcinoma; PHY, phyllodes-like tumor.

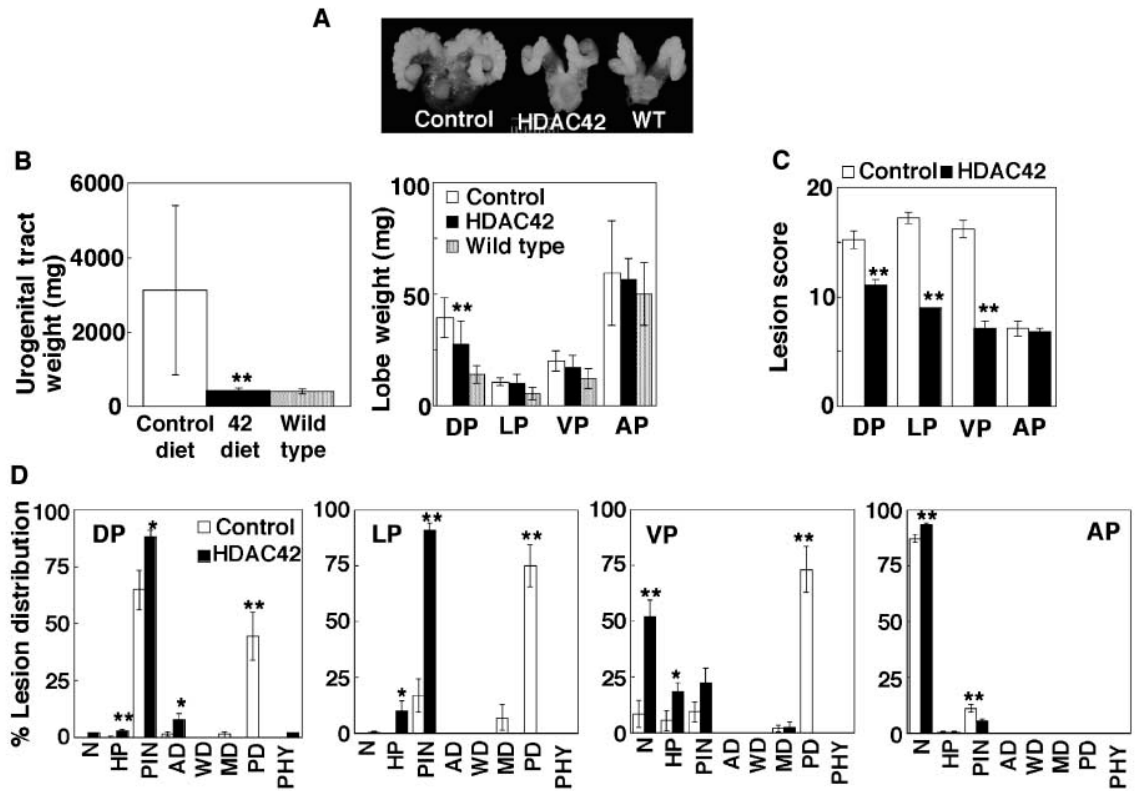


Figure 2.4: OSU-HDAC42 prevented the progression of prostate lesions to poorly differentiated carcinoma in 24-week-old TRAMP mice. *A*, photograph showing the representative gross appearance of urogenital tracts from control and OSU-HDAC42-treated TRAMP mice, and a wild-type littermate. The control TRAMP prostate is symmetrically expanded by a poorly differentiated carcinoma. *B*, urogenital tract and individual prostate lobe weights of TRAMP mice fed an AIN-76A rodent diet with or without 208 ppm OSU-HDAC42 from 6 to 24 weeks of age, compared to wild-type littermates fed a control diet. Values represent means  $\pm$  SD ( $n = 23$  TRAMP and 8 wild-type mice). For the individual prostate lobe weights of control TRAMP mice, the “ $n$ ” varied [ $n = 8$  (DP), 5 (LP), 5 (VP), and 14 (AP)] since tumor expansion precluded the microdissection of some prostate lobes. *C*, scoring of lesion severity in individual prostate lobes of control and OSU-HDAC42-treated TRAMP mice. *D*, distribution of lesions within the prostate lobes of control and OSU-HDAC42-treated TRAMP mice. Values represent means  $\pm$  SD ( $n = 23$ ). \* $P < 0.05$ , \*\* $P < 0.01$ .

Figure 2.5: Histology and immunochemical analysis of biomarkers in the prostates of TRAMP mice fed an AIN-76A rodent diet with or without 208 ppm OSU-HDAC42 from 6 to 10 (A and B) or 24 (C and D) weeks of age. A, Immunohistochemical evaluation of Ki67 and cleaved caspase-3 in prostates of TRAMP mice treated via experimental diet as described above. Decreased Ki67 and increased cleaved caspase-3 immunopositivities (400x mag.) were associated with a lesser degree of epithelial proliferation in the lateral prostates of drug-treated TRAMP mice (score 8) compared to controls (score 9) (*Left panels*, H&E-stain, 200x mag.). The percentages of positive-staining cells were  $20.7 \pm 3.1$  vs.  $13.9 \pm 3.1$  for Ki67 ( $P < 0.01$ ), and  $1.4 \pm 1.0$  vs.  $2.0 \pm 1.0$  for cleaved caspase-3 ( $P < 0.05$ ) in control vs. drug-treated prostate, respectively (means  $\pm$  SD from 10 randomly chosen 400x mag. fields). B, representative immunoblots of prostate tissue lysates shows increases in the acetylation of  $\alpha$ -tubulin and histone H3, and Bax expression in OSU-HDAC42-treated TRAMP mice. The values in fold, quantified by densitometry, denote the intensity of protein bands relative to that of  $\alpha$ -tubulin (Ac- $\alpha$ -tubulin) or  $\beta$ -actin (Ac-H3, Bax) and standardized to the control diet group (means  $\pm$  SD, n = 3). The fold increases in Ac- $\alpha$ -tubulin and Bax were significant at  $P < 0.01$ . C, Immunohistochemical evaluation of differentiation markers (E-cadherin and synaptophysin) and Ac-H3 in prostates of TRAMP mice treated via experimental diet as described above. H&E-stained sections (200x mag.) show a poorly differentiated carcinoma (score 18) and an adenoma (score 13) in the dorsal prostates of control and drug-treated TRAMP, respectively. Immunohistochemistry (400x mag.) shows that this tumor suppression was associated with retention of E-cadherin and prevention of synaptophysin expression, and increased acetylation of histone H3. D, Immunoblotting of prostate tissue lysates confirms the effects of OSU-HDAC42 on E-cadherin and synaptophysin expression demonstrated immunohistochemically in C.

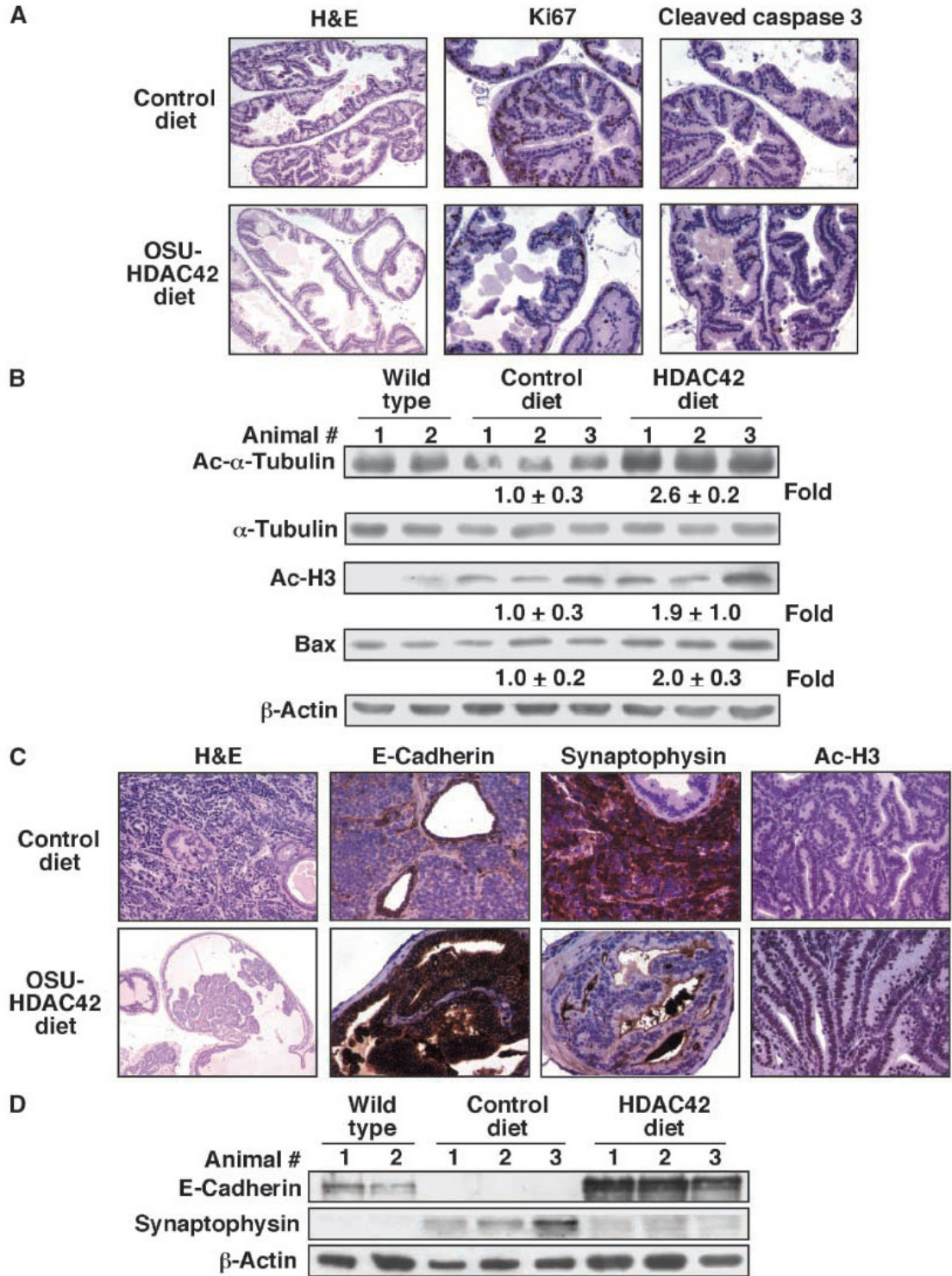


Figure 2.5

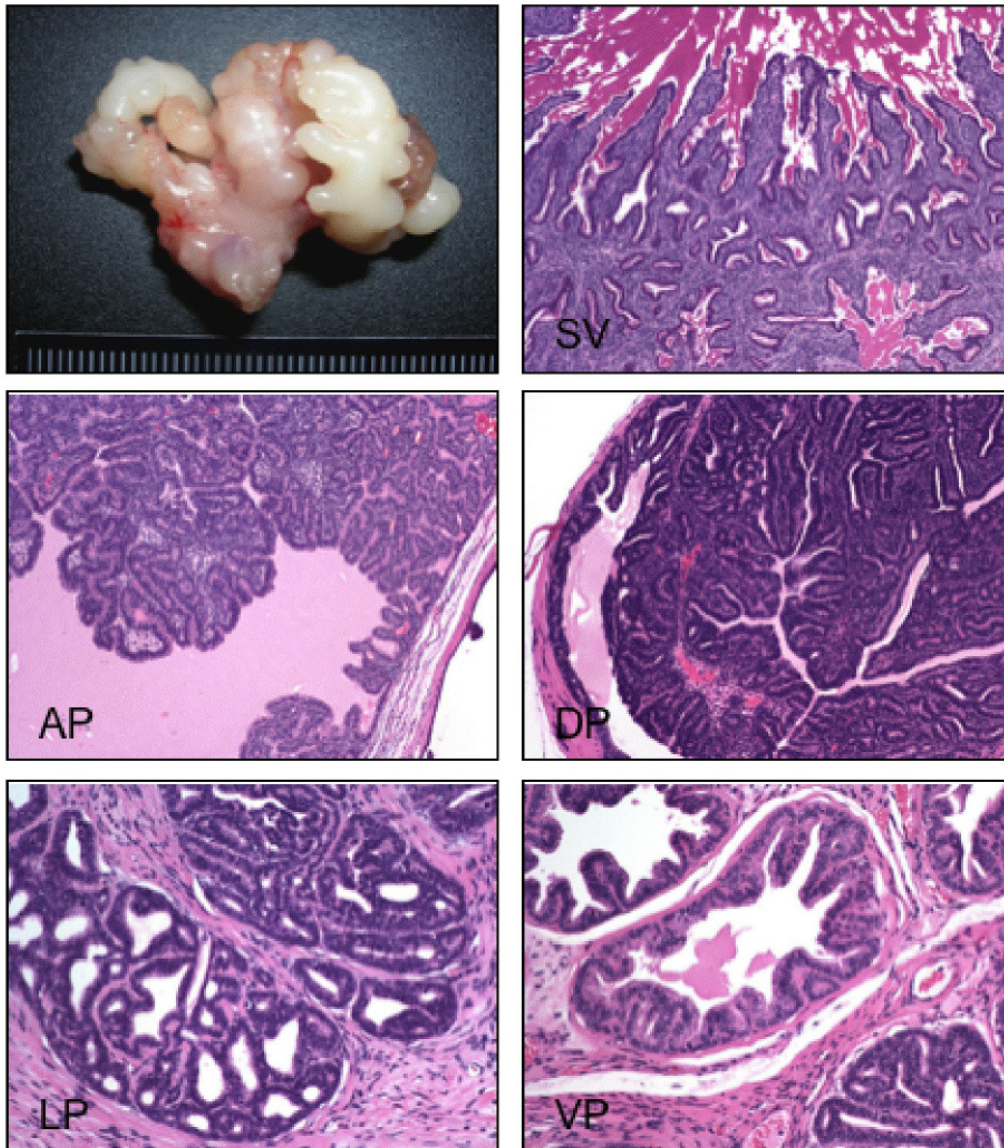


Figure 2.6: Effect of withdrawal of OSU-HDAC42 on lesion progression in the TRAMP model. *Top left panel*, gross image of the urogenital tract from a TRAMP mouse that was treated with 208 ppm OSU-HDAC42 in the diet from 6-24 weeks of age and then off treatment from 24-42 weeks of age. Note the unilateral expansion of the left seminal vesicle and anterior prostate lobe. Microscopically, the lesions consisted of an epithelial-stromal tumor in the seminal vesicle (*top right panel*), phyllodes-like tumors in the AP and DP (*middle panels*), well-differentiated carcinoma in the LP (*bottom left panel*) and PIN in the VP (*bottom right panel*). H&E-stain, 100x mag. SV, AP, DP, and 200x mag. LP, VP. SV, seminal vesicle; AP, anterior prostate; DP, dorsal prostate; LP, lateral prostate; VP, ventral prostate.

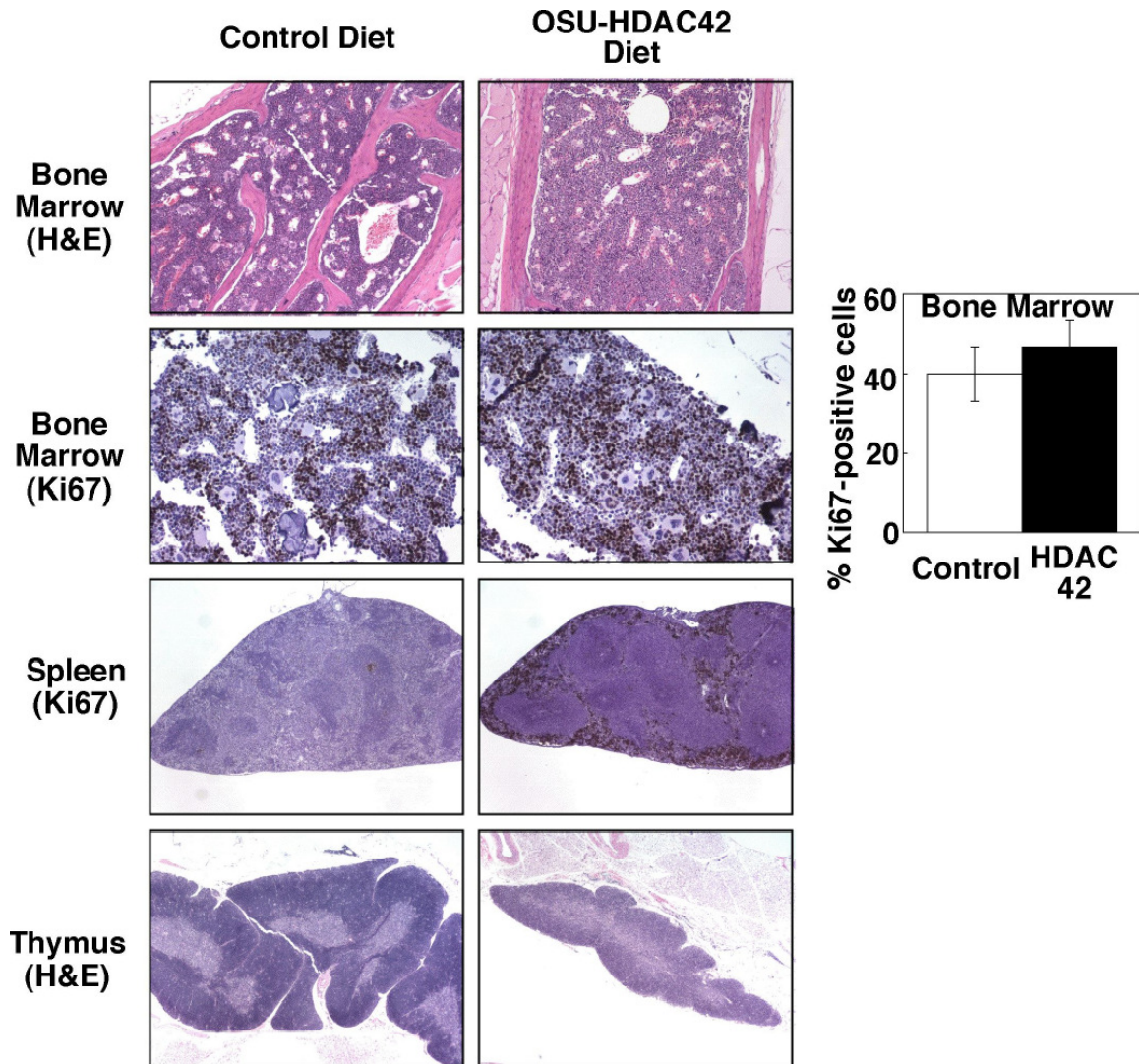


Figure 2.7: Effects of OSU-HDAC42 on lymphoid organs. Photomicrographs of representative H&E- (100x mag.) and Ki67-stained (200x mag.) sections of sternbral bone marrow show that marrow cellularity and proliferation of drug-treated mice are similar to those of controls. Ki67-positive cells in the spleens of drug-treated mice indicate extramedullary hematopoiesis within the splenic red pulp (40x mag.). Photomicrographs of representative H&E-stained sections of thymus, all at the same magnification (40x), show drug-induced thymic atrophy, which was determined to be reversible (Supplementary Table 2). *Right panel*, percentages of Ki67-immunopositive cells in sternbral bone marrow. Values represent means  $\pm$  SD (n = 10). Tissues were from mice treated with AIN-76A rodent diet with or without 208 ppm OSU-HDAC42 from 6 to 24 weeks of age.

Figure 2.8: Characterization of OSU-HDAC42-associated testicular degeneration. *A*, photograph showing the representative gross appearances of testes/epididymides from TRAMP mice treated as indicated for 14 days. Note the reduction in size of OSU-HDAC42-, but not vorinostat-treated testes. *B*, histological evaluation of the seminiferous tubules of control and OSU-HDAC42-treated TRAMP mice. The tubules of drug-treated mice are lined by Sertoli cells, spermatogonia (Ki67 immunopositive cells), and variable numbers of spermatocytes up to the leptotene-zygotene stage (Bouin's-fixed, H&E stain, 400x mag.). *C*, weights of testes and epididymides after OSU-HDAC42 treatment from 6 to 10 (*left panel*) or 24 (*right panel*) weeks of age, and 5 weeks or 6 months after drug withdrawal. OSU-HDAC42 significantly reduced testis and epididymis weights in treated TRAMP mice. Tissue weights were restored in similarly treated wild-type mice after withdrawal of the drug. Values represent means  $\pm$  SD (n = 15 and 23 TRAMP mice at 10 and 24 weeks, respectively; n = 5 wild-type mice in the recovery groups). \*\* $P < 0.01$ . *D*, *Left panel*, Western blot analysis of TAg expression in the prostates of wild-type mice and TRAMP mice treated from 6 to 10 or 24 weeks of age. Prostatic TAg expression is retained in drug-treated TRAMP mice. *Right panel*, serum total testosterone levels in control and treated TRAMP mice. Testosterone levels were unaltered by drug treatment. Testosterone levels were measured using an enzyme immunoassay kit (Cayman Chemical Company, Ann Arbor, MI) according to the manufacturer's recommendations. Values represent means  $\pm$  SD (n = 5). T, testosterone.

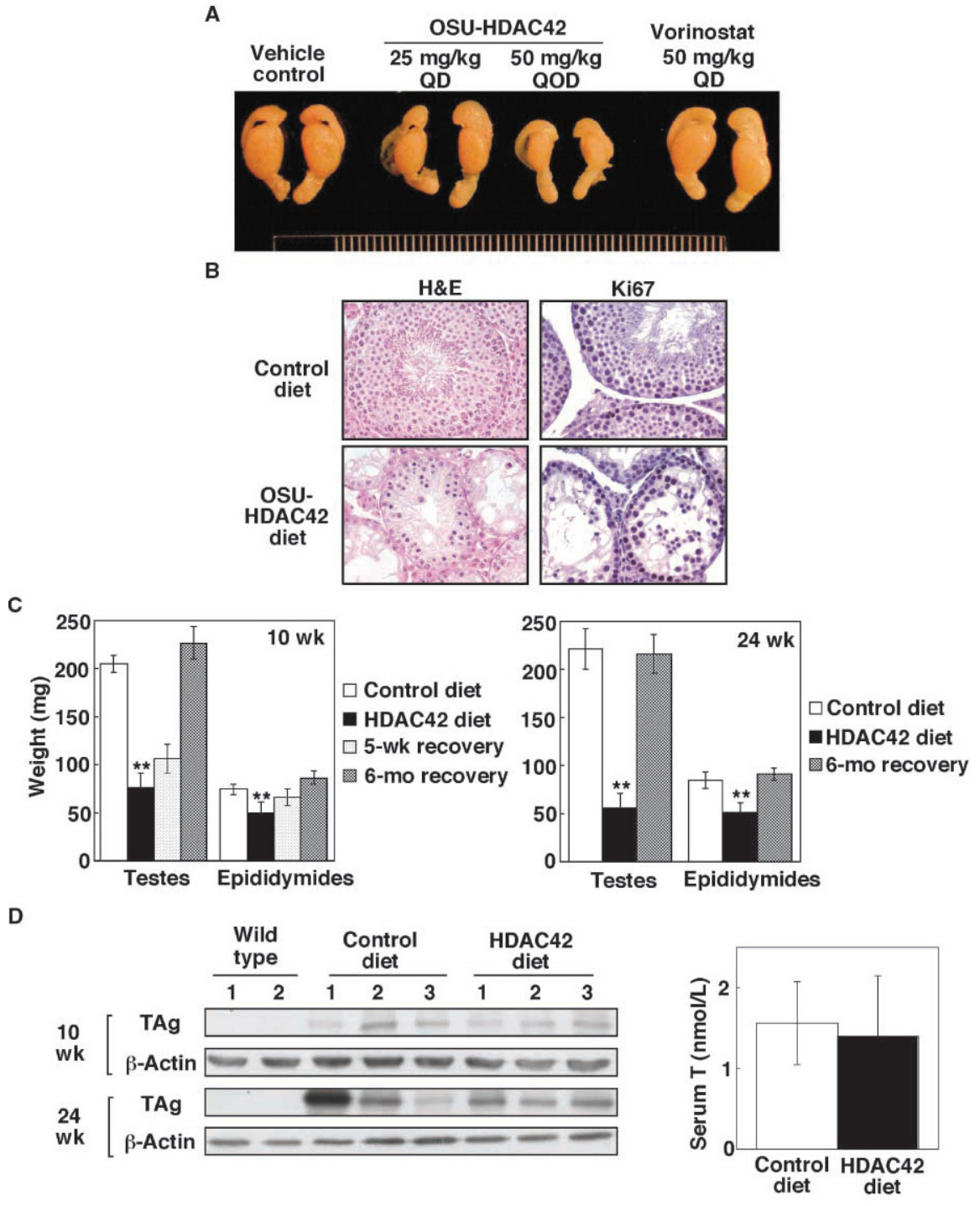


Figure 2.8

Treatment		n	Relative UGT weight <sup>b</sup>	Macroscopic tumors	Most severe lesion in any prostate lobe					Metastases	
Wks	Group				PIN	AD	WD	MD	PD	LN	Others <sup>c</sup>
10	Control	15	1.5±0.0	1 (6.7%)	14 (93.3%)	0	0	0	1 (6.7%)	0	0
	HDAC42	15	1.2±0.0 <sup>g</sup>	0	15 (100%)	0	0	0	0	0	0
24	Control	23	10.0±1.7	18 (78.3%)	3 13%	1 (4.3%)	0	2 (8.7%)	17 (73.9%)	15 (65.2%)	4 (17.4%)
	HDAC42	23	1.5±0.0 <sup>g</sup>	0 <sup>f</sup>	12 (52.2%) <sup>e</sup>	10 (43.5%) <sup>e</sup>	0	1 (4.3%)	0 <sup>f</sup>	0 <sup>f</sup>	0 <sup>d</sup>

<sup>a</sup>number of animals affected with percent of total indicated in parentheses

<sup>b</sup>values represent percentages calculated as UGT weight/body weight x 100, mean ± SEM; values at 6 weeks of age (initiation of treatment) = 0.9 ± 0.0

<sup>c</sup>lung and/or liver

<sup>d, e, f, g</sup>difference from control group is significant at <sup>d</sup> $P < 0.05$ , <sup>e</sup> $P < 0.01$ , and <sup>f</sup> $P < 0.001$  by Chi-square analysis, and <sup>g</sup> $P < 0.001$  by Student t-test

UGT, urogenital tract; PIN, prostatic intraepithelial neoplasia; AD, adenoma; WD, well differentiated carcinoma; MD, moderately differentiated carcinoma; PD, poorly differentiated carcinoma; LN, lymph node; HDAC-42, OSU-HDAC42

Table 2.1: Relative urogenital tract weight and incidence<sup>a</sup> of prostate lesions in TRAMP mice treated from 6 to 10 or 24 weeks of age.

<b>Hematology</b>	<u>10 weeks</u>		5-week recovery <sup>b</sup>	<u>24 weeks</u>	
	Control	HDAC42		Control	HDAC42
PCV (%)	45.5 ± 6.4	38.8 ± 2.6	52.6 ± 1.7	41.0 ± 10.2	41.2 ± 4.0
RBC (x 10 <sup>6</sup> /μl)	10.6 ± 1.3	<sup>c</sup> 9.0 ± 0.4	11.6 ± 0.5	8.9 ± 2.0	8.6 ± 0.3
Nucleated cells (x 10 <sup>3</sup> /μl)	2.4 ± 1.5	<sup>c</sup> 0.7 ± 0.1	2.8 ± 1.1	3.0 ± 0.3	2.6 ± 2.0
Segmented neutrophils (x 10 <sup>3</sup> /μl)	0.2 ± 0.1	0.1 ± 0.1	0.2 ± 0.1	0.3 ± 0.2	0.5 ± 0.7
Lymphocytes (x 10 <sup>3</sup> /μl)	2.1 ± 1.4	<sup>c</sup> 0.5 ± 0.1	2.5 ± 1.2	2.5 ± 0.5	1.7 ± 1.1
Platelets (x 10 <sup>3</sup> /μl)	332.4 ± 342.2	256.7 ± 261.4	779.5 ± 524.1	860.4 ± 819.1	861.0 ± 371.0
<b>Serum Chemistry</b>					
BUN (mg/dl)	25.7 ± 4.0	23.0 ± 8.3	26.6 ± 2.6	21.0 ± 6.7	18.7 ± 3.2
Creatinine (mg/dl)	0.5 ± 0.1	0.4 ± 0.0	0.4 ± 0.0	0.3 ± 0.1	0.4 ± 0.0
Phosphorus (mg/dl)	9.5 ± 1.4	10.7 ± 1.3	7.3 ± 1.6	7.6 ± 2.3	8.4 ± 1.2
Calcium (mg/dl)	10.1 ± 1.0	11.2 ± 1.0	10.7 ± 1.6	11.2 ± 1.8	11.0 ± 1.1
Potassium (mEq/L)	6.5 ± 1.5	5.1 ± 0.4	5.4 ± 1.0	6.2 ± 0.7	<sup>d</sup> 3.8 ± 0.3
ALT (iu/L)	33.7 ± 14.4	37.0 ± 4.0	28.8 ± 7.4	29.2 ± 11.3	27.7 ± 6.0
AST (iu/L)	116.5 ± 47.9	<sup>c</sup> 198.2 ± 42.4	110.8 ± 43.5	222.7 ± 225.2	154.5 ± 144.4
ALP (iu/L)	105.7 ± 24.0	<sup>d</sup> 50.0 ± 8.7	100.2 ± 12.9	57.7 ± 12.6	<sup>c</sup> 34.7 ± 9.5
CK (iu/L)	203.3 ± 235.3	341.0 ± 371.9	359.6 ± 186.0	269.7 ± 281.1	147.0 ± 44.1
Cholesterol (mg/dl)	177.5 ± 24.0	<sup>d</sup> 125.4 ± 15.6	192.2 ± 51.2	154.7 ± 17.7	<sup>c</sup> 121.2 ± 5.4
Total Bilirubin (mg/dl)	0.1 ± 0.0	<sup>c</sup> 0.2 ± 0.0	0.1 ± 0.0	0.2 ± 0.0	0.2 ± 0.1
Total Protein (g/dl)	6.4 ± 0.8	6.7 ± 0.6	6.3 ± 1.0	5.5 ± 0.3	<sup>c</sup> 6.4 ± 0.6
Albumin (g/dl)	3.9 ± 0.3	<sup>d</sup> 4.6 ± 0.3	4.0 ± 0.7	3.7 ± 0.3	4.1 ± 0.3
Globulin (g/dl)	2.5 ± 1.0	1.8 ± 0.9	2.3 ± 0.4	1.8 ± 0.2	1.9 ± 1.3
Glucose (mg/dl)	205.8 ± 29.7	191.6 ± 22.0	250.2 ± 69.9	236.5 ± 76.3	197.2 ± 33.3

<sup>a</sup>values represent means (n=5) ± SD

<sup>b</sup>Mice were fed a diet containing 208 ppm OSU-HDAC42 from 6-10 weeks of age, then placed on a control diet through 15 weeks of age.

<sup>c</sup>difference from control group is significant at <sup>c</sup>P<0.05 and <sup>d</sup>P<0.01 by Student t-test HDAC42, OSU-HDAC42; PCV, packed cell volume; RBC, red blood cells; BUN, blood urea nitrogen; ALT, alanine aminotransferase; AST, aspartate aminotransferase; ALP, alkaline phosphatase; CK, creatine kinase

Table 2.2: Hematology and serum chemistry values<sup>a</sup> of TRAMP mice treated from 6 to 10 or 24 weeks of age.

Organ	10 weeks		5-week recovery <sup>c</sup>	24 weeks	
	Control	HDAC42		Control	HDAC42
Adrenal glands (mg)	4.0 ± 0.4 (0.0 ± 0.0)	4.4 ± 0.5 (0.0 ± 0.0)	3.8 ± 0.8 (0.0 ± 0.0)	4.4 ± 1.2 (0.0 ± 0.0)	4.3 ± 0.5 (0.0 ± 0.0)
Brain (mg)	474.1 ± 24.5 (1.9 ± 0.2)	476.4 ± 5.5 (2.0 ± 0.1)	467.7 ± 16.4 (1.7 ± 0.1)	489.3 ± 15.2 (1.5 ± 0.1)	483.3 ± 22.3 (1.6 ± 0.2)
Epididymides (mg)	70.0 ± 5.0 (0.3 ± 0.0)	<sup>e</sup> 54.1 ± 4.6 ( <sup>d</sup> 0.2 ± 0.0)	66.7 ± 8.6 (0.2 ± 0.0)	83.6 ± 8.1 (0.2 ± 0.0)	<sup>e</sup> 54.9 ± 7.7 ( <sup>e</sup> 0.2 ± 0.0)
Epididymal fat pad (mg)	560.0 ± 162.7 (2.2 ± 0.5)	388.5 ± 131.4 (1.6 ± 0.5)	469.7 ± 57.1 (1.8 ± 0.1)	790.2 ± 236.1 (2.5 ± 0.6)	556.2 ± 182.5 (1.8 ± 0.5)
Heart (mg)	123.4 ± 11.4 (0.5 ± 0.0)	121.6 ± 4.9 (0.5 ± 0.0)	125.3 ± 8.1 (0.5 ± 0.0)	138.2 ± 11.6 (0.4 ± 0.0)	142.2 ± 14.8 (0.5 ± 0.0)
Kidneys (mg)	351.7 ± 33.0 (1.4 ± 0.2)	387.4 ± 17.5 (1.6 ± 0.1)	382.4 ± 39.6 (1.4 ± 0.1)	388.2 ± 58.8 (1.3 ± 0.1)	393.8 ± 33.7 (1.4 ± 0.1)
Liver (g)	1.2 ± 0.1 (4.7 ± 0.6)	1.3 ± 0.1 (4.4 ± 2.5)	1.4 ± 0.2 (5.3 ± 0.4)	1.2 ± 0.2 (3.8 ± 0.3)	1.3 ± 0.2 (4.3 ± 0.6)
Pituitary gland (mg)	1.7 ± 0.2 (0.0 ± 0.0)	1.6 ± 0.3 (0.0 ± 0.0)	1.9 ± 0.1 (0.0 ± 0.0)	1.7 ± 0.2 (0.0 ± 0.0)	1.7 ± 0.3 (0.0 ± 0.0)
Spleen (mg)	61.3 ± 2.9 (0.2 ± 0.0)	64.5 ± 7.4 (0.3 ± 0.0)	60.8 ± 9.6 (0.2 ± 0.0)	78.0 ± 19.4 (0.2 ± 0.1)	77.6 ± 14.4 (0.2 ± 0.0)
Testes (mg)	205.5 ± 7.9 (0.8 ± 0.0)	<sup>e</sup> 90.2 ± 13.0 ( <sup>e</sup> 0.4 ± 0.0)	107.1 ± 15.0 (0.4 ± 0.0)	211.3 ± 11.6 (0.6 ± 0.0)	<sup>e</sup> 52.6 ± 5.1 ( <sup>e</sup> 0.2 ± 0.0)
Thymus (mg)	34.6 ± 7.1 (0.1 ± 0.0)	<sup>e</sup> 14.0 ± 4.2 ( <sup>e</sup> 0.1 ± 0.0)	36.6 ± 20.4 (0.1 ± 0.1)	31.0 ± 5.7 (0.1 ± 0.0)	<sup>e</sup> 12.2 ± 2.8 ( <sup>e</sup> 0.0 ± 0.0)

<sup>a</sup>values represent means [n=5 (10-week-old mice and recovery mice) and n=8 (24-week-old mice)] ± SD; relative values are indicated in parentheses after the absolute weights and represent percentages calculated as organ weight/body weight x 100; post-fix weights were obtained for brain and pituitary gland; paired organs were weighed together and evaluations were done in accordance with guidelines proposed by Sellers RS, Morton D, Michael B, Roome N, Johnson JK, Yano BL, Perry R, Schafer K. Society of Toxicologic Pathology position paper: organ weight recommendations for toxicology studies. *Toxicol Pathol.* 2007;35(5):751-5.

<sup>b</sup>C57BL/6xFVB

<sup>c</sup>Mice were fed a diet containing 208 ppm OSU-HDAC42 from 6-10 weeks of age, then placed on a control diet through 15 weeks of age.

<sup>d,e</sup>difference from control group is significant at <sup>d</sup>P<0.05 and <sup>e</sup>P<0.01 by Student t-test HDAC42, OSU-HDAC42

Table 2.3: Absolute and relative organ weight values<sup>a</sup> of wild type<sup>b</sup> mice treated from 6 to 10 or 24 weeks of age.

## **CHAPTER 3**

# **CHEMOPREVENTIVE AND BIOENERGETIC SIGNALING EFFECTS OF PDK1/AKT PATHWAY INHIBITION IN A TRANSGENIC MOUSE MODEL OF PROSTATE CANCER**

### **ABSTRACT**

The phosphoinositide-dependent kinase 1 (PDK1)/Akt pathway is an important regulator of multiple biological processes including cell growth, survival, and glucose metabolism. In light of the mechanistic link between Akt signaling and prostate tumorigenesis, we evaluated the chemopreventive relevance of inhibiting this pathway in the transgenic adenocarcinoma of the mouse prostate (TRAMP) mouse with OSU03012, a celecoxib-derived, but COX-2-inactive, PDK1 inhibitor. Beginning at ten weeks of age when prostatic intraepithelial neoplasia (PIN) lesions are well developed, TRAMP mice received OSU03012 via daily oral gavage for eight weeks. The drug treatment significantly decreased the weight of all four prostate lobes as well as the grade of epithelial proliferation in the dorsal and lateral lobes compared to vehicle-treated control mice. The incidences of carcinoma and metastasis were decreased, although not to statistically significant levels. Treated mice lost body fat and failed to gain weight

independent of food intake. This change and periportal hepatocellular atrophy can be linked to sustained PDK1 inhibition through downstream inactivation of glycogen synthase. Centrilobular hepatocellular hypertrophy and necrosis of Type II skeletal myofibers were also compound-related effects. We conclude that targeting of the PDK1/Akt pathway has chemopreventive relevance in prostate cancer and causes other *in vivo* effects mediated in part by an alteration of bioenergetic signaling.

## **INTRODUCTION**

The 3-phosphoinositide-dependent protein kinase-1 (PDK1)/Akt signaling pathway is an important regulator of multiple biological cellular processes and is widely conserved across species. In addition to influencing cell proliferation and survival, and energy metabolism in normal cells, the role of Akt in carcinogenesis and tumor progression, including that of the prostate, has been firmly established (Li et al., 2005). Accordingly, a number of small-molecule inhibitors of Akt signaling have emerged in recent years with promising efficacy against prostate, breast, hematopoietic, and ovarian cancer among others (Komander et al., 2003; Yang et al., 2004; Zhu et al., 2004; Ihle et al., 2005; Kucab et al., 2005, Mimeault et al., 2006; Xie et al., 2006). While these studies demonstrate the cancer therapeutic success of Akt-inhibiting agents, either alone or in combination with currently used drugs, few draw conclusions about their cancer preventability. Regarding prostate cancer, Akt is an especially attractive target since deregulation of the PI3-K/PDK1/Akt cascade correlates with an increased Gleason score and androgen-independent phenotype with a poor prognosis (Edwards et al., 2003; Liao

et al., 2003). Using Akt antagonists to prevent or delay the onset of prostate cancer is logical considering the implication of this protein in the progression of prostate intraepithelial neoplasia (PIN) to carcinoma (Narayanan et al., 2004), together with the long initial latency of prostate cancer in men (Gupta, 2004).

Among the animal models available to study the efficacy of prostate chemopreventive candidates, the transgenic adenocarcinoma of the mouse prostate (TRAMP) has received much attention because it involves defined stages of spontaneous tumor progression similar to that in man (Klein, 2005). Paramount to this multi-stage escalation from simple hyperplasia to carcinoma is the development of PIN lesions, which represent a key intervention point at which a molecularly targeted agent could potentially prevent or slow the progression of prostate epithelial cells to a malignant phenotype. The term chemoprevention here is applied to the chemotherapy of these precancerous PIN lesions (Gupta, 2004). The TRAMP model has been used extensively in chemoprevention studies, including the evaluation of celecoxib, flutamide, R-flurbiprofen, toremifene, decitabine, and green tea polyphenols (Raghow et al., 2000; Wechter et al., 2000; Gupta et al., 2001; Raghow et al., 2002; Gupta, 2004; Narayanan et al., 2004, McCabe et al., 2006).

Although the anti-cancer activity of signaling pathway inhibitors is often well characterized, less is known about mechanism-based, *in vivo* sequelae of chronic pathway inhibition. Identification and characterization of these effects are appropriate prior to human use since their overall significance may be considered greater in a chemopreventive (vs. cancer therapeutic) context due to an increased patient risk-to-

benefit ratio. An opportune time to realize many of these mechanism-based or off-target effects is early in the drug discovery process by thorough phenotyping of animals used in efficacy studies. Albeit ultimately designed to evaluate cancer endpoints, these studies can provide toxicologic information that allows researchers to predict the impact of chronic therapy.

Here we exemplify an approach of combining the disciplines of medicinal chemistry, biochemistry, and veterinary pathology to thoroughly evaluate the prostate chemopreventive ability of a novel compound concurrent with an investigation of whole-body ramifications. Specifically, TRAMP mice were treated with OSU03012, an orally bioavailable, celecoxib-derived PDK1 inhibitor, to determine its suppressive effects in the progression of PIN to carcinoma and analyzed with respect to prostate and phenotype endpoints. Retardation of prostate lesions was anticipated in light of the mechanistic link between PDK1/Akt signaling and prostate tumorigenesis. Systemic effects were difficult to predict given the limited safety information of similarly targeted agents in the literature, but were suspected to be minimal based on shorter-duration efficacy studies completed in our laboratory. It is noteworthy that OSU03012 is currently undergoing preclinical evaluations in the Rapid Access to Intervention Development (RAID) program at NCI. The chemopreventive activity of OSU03012 is described here in addition to an alteration of bioenergetic signaling linked to PDK1/Akt pathway inhibition. Our results show evidence of a negative effect on prostate epithelial lesion development and reveal systemic non-cancer parameters that should be considered for monitoring in future preclinical/clinical evaluation of this and similarly targeted agents.

## MATERIALS AND METHODS

**Animals.** Hemizygous C57BL/6 TRAMP mice from our own colony were cross-bred with FVB/n mice to generate F1 litters. Tail tips from all F1 male offspring were genotyped by polymerase chain reaction (PCR) to identify mice carrying the transgene as described (Greenberg et al., 1995). These TRAMP mice (C57BL/6TRAMPxFVB) were housed in cages with corncob bedding under a constant photoperiod (12 hours light: 12 hours dark) in a temperature- and humidity-controlled room (68°F-72°F and 45-55% respectively) with *ad libitum* access to pelleted rodent chow and water. The procedures performed were in accordance with protocols approved by the Institutional Laboratory Animal Care and Use Committee of The Ohio State University.

**Reagents.** OSU03012, a novel celecoxib-derived, COX-2-inactive PDK-1 inhibitor, was synthesized in our laboratory as described previously (Zhu et al., 2004). This compound is currently undergoing preclinical evaluation through the National Cancer Institute's RAID Program. OSU03012 was prepared as a suspension in vehicle consisting of 0.5% methylcellulose (w/v) and 0.1% Tween 80 (v/v) in sterile water for oral administration. Treatment volumes remained constant at 0.01 ml per gram of body weight. Rabbit polyclonal antibodies against  $\beta$ -Actin, Akt, phospho-Thr308-Akt, glycogen synthase (GS) kinase 3 beta (GSK3 $\beta$ ), phospho-Ser9-GSK3 $\beta$ , and phospho-Ser641-GS were purchased from Cell Signaling Technology (Beverly, MA).

**Study Design and Experimental Procedure.** Ten-week-old TRAMP mice were randomly assigned to experimental (n = 31) and control (n = 30) groups and treated once

daily by oral gavage with either 200 mg/kg OSU03012 or vehicle alone under isoflurane anesthesia using a flexible gavage needle. Treatment was initiated at 10 weeks of age when 100% of animals have PIN lesions, and continued through 18 weeks of age when a high percentage (~60%) have developed prostate carcinoma (Kaplan-Lefko et al., 2003). The mice were sacrificed at 18 weeks of age by CO<sub>2</sub> inhalation, which was performed approximately 8 hours post-treatment corresponding to the time of peak plasma concentration<sup>1</sup>. Throughout the study, all mice were weighed once per week and daily food consumption was monitored in a representative group (n=9 control, 14 treated animals). Food consumption was measured as the difference in the mass of food per mouse in 24 hours. The age at which palpable tumors developed was determined for each mouse by daily palpation at the time of gavage. At sacrifice following 8 weeks of treatment, the dorsal (DP), lateral (LP), ventral (VP), and anterior (AP) prostate lobes were microdissected and weighed, with one lobe of each pair saved in formalin and the other frozen in liquid nitrogen.

**Histopathology.** Individual prostate lobes, iliac lymph nodes, liver (left lobe), and lung from each TRAMP mouse were fixed overnight in 10% formalin then transferred to 70% ethanol. Four μm-thick, paraffin-embedded tissue sections were stained with hematoxylin and eosin (H&E) by standard procedures. All tissues were evaluated microscopically by a veterinary anatomic pathology resident consulting with board-

---

<sup>1</sup> Compound Summary, August 1, 2006, NCI RAID Initiative for NSC D728209, Contract No. N01-CM-07019.

certified veterinary pathologists about relevant lesions. A TRAMP-specific grading scheme (Suttie et al., 2003) was employed to semi-quantitatively compare proliferative prostate lesions between groups. The observer scoring the prostate slides was blinded to the treatment status. The grading scheme, which assigns a single number 1-18 to each prostate lobe, accounts for the entire spectrum of proliferative lesions, from simple hyperplasia to poorly differentiated carcinoma, with adjustment for lesion distribution. In addition to these tissues, the remainder of each carcass excluding skin and vertebral column was saved in 10% formalin; tissues from representative animals (n=7 control, 12 treated mice) were evaluated microscopically with respect to Society of Toxicologic Pathology-proposed guidelines for repeat-dose toxicity studies (Bregman et al., 2003).

**Immunohistochemistry.** Immunohistochemical detection of proteins using the antibodies indicated in Figures 3.2, 3.4, and 3.6 was performed on four  $\mu\text{m}$ -thick, paraffin-embedded prostate, liver, and skeletal muscle tissue sections as described (Tomita et al., 2006). For muscle fiber typing, paraffin sections of mouse muscle were deparaffinized with Ventana EZ Prep (Tucson, AZ) and treated with CC1 antigen retrieval on a Ventana Discovery autostainer. Slides were rinsed in  $\text{dH}_2\text{O}$ , placed on the DAKO autostainer plus (Carpinteria, CA), then dual stained with Novocastra Laboratories Ltd. Myosin Heavy Chain (MHC) slow and fast mouse monoclonal antibodies (Newcastle upon Tyne NE12 8EW, UK). The DAKO ARK (Animal Research Kit) kit peroxidase was used to reduce reactivity of the two mouse antibodies with endogenous immunoglobulin. The volumes of primary antibody, biotinylation, DAKO diluent, and blocking reagents needed for the biotinylated primary antibody were

calculated with ARKulator software and reagents included in the ARK kit. The procedure outlined in this kit was duplicated for use on the DAKO autostainer. The sections were first tested with a peroxidase block for five minutes then the biotinylated MHCs antibody (1:40) for 1 hour followed by streptavidin-HRP for thirty minutes and DAB+ for fifteen minutes. The slides were tested again with peroxidase block for five minutes then the biotinylated MHCf antibody (1:40) for 1 hour followed by KPL streptavidin-phosphatase (Gaithersburg, MD) for thirty minutes. DAKO wash buffer was used for all rinse steps in the procedure. DAKO permanent red was manually applied to the sections for six minutes, rinsed and dipped in DAKO Hematoxylin for twenty seconds then air dried overnight and cover-slipped.

**Immunoblotting for Molecular Targets.** Total protein was extracted from tissue homogenates of dorsal, lateral, ventral, and anterior prostate lobes from 18-week-old vehicle-control and treated TRAMP mice. Briefly, prostate tissues were mechanically homogenized in 16  $\mu$ l of lysis buffer (20 mM tris pH 8, 20 mM EDTA, 0.5% NP-40) per mg of tissues, and left on ice for 30 minutes. Protein concentrations were determined in duplicate using a BCA assay (Pierce) with LC software and samples were prepared so that 20  $\mu$ l containing 40  $\mu$ g of protein per sample were loaded in each lane. The samples were fractionated on 4-15% gradient SDS-PAGE gels (Criterion Precast Gel, BioRad) and transferred to nitrocellulose membranes. Western blotting was accomplished as done previously (Kulp et al., 2004) with the antibodies indicated in Figure 3.2, using  $\beta$ -Actin as an internal control. A chemiluminescence detection reagent (Western Lightning, Perkin Elmer Life Sciences) was used to visualize protein bands developed on Kodak

Biomax light film.

**Transmission Electron Microscopy.** Primary fixation of liver samples was done with 1.75% glutaraldehyde, 25 mM Na-phosphate buffer (pH 7.4), 5 mM sucrose, and 0.5 mM  $\text{NaN}_3$ . Post-fixation was accomplished with 1%  $\text{OsO}_4$ . Following dehydration, infiltration and embedding were carried out in an epon resin. Thin sections were cut for toluidine blue staining. For EM analysis, thin sections were double stained with 1 % uranylacetate in aqua and lead citrate, then observed by a Philips 300 Transmission EM at an accelerating voltage of 60 kV. Photographs were taken on Kodak Electron image films.

**Statistical Analysis.** A Student's t-Test was used to compare the means of 2 samples of independent, normally-distributed observations. Specifically, this test was used to determine if certain responses (prostate lobe and epididymal fat pad weight, prostate lesion score, immunoblotting results) were influenced by drug treatment. A Chi-square contingency analysis was used to determine if drug treatment affected the incidences of carcinoma and metastases, which were evaluated as discrete, whole number values. Differences between groups were considered significant at  $P < 0.05$ .

## **RESULTS**

**OSU03012 Decreases Prostate Lobe Weight and the Grade of Epithelial Proliferation.** The weights of all 4 paired lobes of drug-treated animals were significantly less than those of control mice (Fig. 3.1a) following 8 weeks of repeat dosing. Seminal vesicle weights were also significantly decreased in drug-treated

TRAMP mice with an average weight of  $279 \pm 107$  mg compared to  $445 \pm 185$  mg in controls [ $P = 0.0001$ , mean  $\pm$  standard deviation (SD)].

The TRAMP-specific grading scheme (Suttie et al., 2003) showed a significant reduction in lesion score in the DP and LP of drug-treated mice (Fig. 3.1b), with an average score for the DP and LP of  $9.0 \pm 2.7$  and  $9.2 \pm 3.4$ , respectively, in drug-treated mice compared to  $10.5 \pm 2.7$  and  $11.4 \pm 4.2$  in control mice (mean  $\pm$  SD). Fig. 3.2a and b demonstrate a representative histologic appearance of this suppressive effect. The grade of epithelial lesion development was also decreased in the VP and AP, although not to statistically significant levels.

**OSU03012 Decreases the Incidences of Prostate Carcinoma and Metastasis, Although not to Statistically Significant Levels.** After 8 weeks of daily oral treatment with 200 mg/kg OSU03012, carcinoma was detected in 8 of 31 (25.8%) mice compared to 12/30 (40%) of vehicle control mice. Metastasis was limited to the iliac lymph nodes and was decreased from 9 of 12 (75%) control mice to 3 of 8 (37.5%) drug-treated mice. Although the difference in tumor size was often striking at necropsy, neither of these differences was statistically significant ( $P = 0.24$  and  $0.09$ , respectively). No metastases were observed in the liver, lung, or other tissues of any TRAMP mice. There were no significant differences in age at development of palpable tumors. Prostate tumors could be palpated at approximately 8 mm-diameter or 400 mg weight. OSU03012-treated mice developed palpable tumors at  $14.5 \pm 2.3$  weeks of age compared to  $15.5 \pm 4.8$  weeks of age in control mice (mean  $\pm$  SD).

**OSU03012 Inhibits the Phosphorylation of Akt and the Downstream Effector**

**GSK3 $\beta$ .** Overexpression of p-Akt in proliferative prostate epithelium of TRAMP mice was demonstrated in a proof-of-principle study that preceded the longer-term drug treatment study. Fig. 3.2c demonstrates this dramatic increase in p-Akt immunostaining in hyperplastic epithelial cells that are sharply demarcated from non-staining normal epithelium. After 8 weeks of treatment with OSU03012, immunostaining for p-Thr308-Akt revealed a sharp decrease in reactivity in the prostate epithelium compared to that of vehicle-treated control mice (Fig. 3.2d and e). Because Akt is a major regulator of GSK3 $\beta$  activity (Cross et al., 1995), we assessed the phosphorylation status of GSK3 $\beta$ , an Akt substrate, as a functional consequence of diminished Akt phosphorylation. As shown in Fig. 3.2f, levels of phosphorylated GSK3 $\beta$  were markedly decreased in samples from OSU03012-treated mice without changes in the expression of total GSK3 $\beta$  protein. This treatment-induced activation of GSK3 $\beta$  correlates with the observed phosphorylating inactivation of GS, the downstream regulator of glycogen synthesis. In principle, OSU03012-mediated deactivation of Akt led to GSK3 $\beta$  dephosphorylation, thereby increasing the level of p-GS.

**OSU03012 Decreases Body Fat and Prevents Body Weight Gain Independent of Food Intake, and Alters the Serum Chemistry Profile.** The body weight of treated mice remained relatively constant throughout the 8-week treatment period compared to a gradual weight gain in control mice (Fig. 3.3a). The overall reduction in body fat of drug-treated animals was quantified by weighing epididymal fat pads, which was significantly decreased compared to controls (Fig. 3.3b). Food intake was estimated to be equal between the groups by serial measurements of daily food consumption. This

observation suggested a shift towards higher bioenergetic metabolism in the drug-treated animals and encouraged continued phenotyping of the drug-treated and control mice.

Serum chemistry revealed a modest, but significant reduction in blood glucose and cholesterol, and a significant increase in aspartate aminotransferase (AST) in treated mice (Table 3.1). Elevations in creatine kinase (CK), alanine aminotransferase (ALT), and alkaline phosphatase (ALP) were also noted in OSU03012-treated TRAMP mice. Hemograms of animals in both groups were unremarkable with the exception of a relative lymphopenia in drug-treated mice (Table 3.2). The overall significance of the decreased lymphocyte count is uncertain since, although decreased compared to controls, the count lies within the normal reference range determined for various mouse strains and ages (Suckow et al., 2001).

**OSU03012 Causes Hepatic Lesions that can be Linked in Part with Target Pathway Inhibition.** A distinct accentuation of lobular architecture, characterized by atrophy of zone 1 (periportal) cells and hypertrophy of zone 3 (centrilobular) cells, was evident histologically in the livers of drug-treated mice (Fig. 3.4b). Considering that the liver is a main site of glycogen synthesis and storage in the body, together with the role of PDK1/Akt signaling in glycogen metabolism, an effort was made to determine if these changes could be mechanism-based effects of drug administration. Accordingly, periodic acid-Schiff (PAS) staining of the liver was employed and revealed a dramatic reduction in glycogen storage in drug-treated TRAMP livers compared to controls (Fig 3.4d). Moreover, intense immunostaining for the inactive, phosphorylated form of GS was detected in the atrophic zone 1 cells in the livers of drug-treated mice (Fig. 3.4f).

To further characterize centrilobular hypertrophy, and specifically to investigate if cytochrome P450 induction was responsible for hypertrophy, toluidine blue staining and transmission electron microscopy (EM) of livers from control and treated mice were performed. A finely stippled, ground glass-like appearance of hepatocellular cytoplasm of drug-treated TRAMP mice was evident in toluidine blue-stained sections (Fig. 3.5b). Ultrastructurally, this finely granular material corresponds to focal clusters of tightly packed smooth ER mixed with dispersed arrangements of rough ER and mitochondria within a glycogen-poor cytoplasm (Fig. 3.5d). This pattern contrasts sharply with the deep blue, clumped foci observed in control TRAMP mice (Fig. 3.5a) that correspond to large aggregations of mitochondria and rough ER ultrastructurally within a glycogen-rich cytoplasm (Fig. 3.5c). EM also revealed an apparent increase in the number of canalicular microvilli in OSU03012-treated TRAMP, the cause of which is uncertain but is not an uncommon alteration in experimental or spontaneous disease states in rodents (Ghadially, 1982).

**A Multifocal, Multiphasic Skeletal Myopathy Targeting Type II Fibers is Observed in Drug-Treated TRAMP Mice.** Multifocal segmental myonecrosis was noted in various skeletal muscles of treated mice including biceps femoris, parasternal, masseter, and occipital muscles. Fig. 3.6b demonstrates a spectrum of lesions from acute myofiber degeneration and necrosis to myofiber loss with macrophage infiltration and regeneration of myofibers. Intense immunostaining for p-GS was demonstrated in affected skeletal muscle of drug-treated TRAMP mice (Fig. 3.6d) similar to that observed in periportal cells of the liver. Immunohistochemical typing of myofibers revealed

targeting of Type II (glycolytic/fast) fibers with sparing of Type I (oxidative/slow) fibers (Fig. 3.6e).

## **DISCUSSION**

The PI3-K pathway is known to play a major role in prostate tumorigenesis, owing much of its oncogenicity to activation of Akt through PDK1 (Li et al., 2005). We have previously reported potent anti-cancer effects of OSU03012, our novel, celecoxib-derived, PDK1/Akt-targeted agent, in a variety of human malignancies *in vitro*, including prostate, breast, glioblastoma, and hematopoietic cancers (Zhu et al., 2004; Johnson et al., 2005; Kucab et al., 2005, Tseng et al., 2005, McCubrey et al., 2006, Tseng et al., 2006). In this report, we describe onco-suppressive effects of PDK1/Akt inhibition by repeat oral dosing of TRAMP mice with OSU03012 on the progression of PIN to carcinoma. In addition to prostate endpoints, an alteration in energy metabolism was observed and linked to inactivation of GS in normal cells.

Evaluation of endpoints for prostate lobe weight and the severity of epithelial proliferative lesions revealed that OSU03012 is able to suppress the overall grade of lesion development in TRAMP mice when treatment is initiated after marked hyperplasia (PIN) is well established. Significant decreases of these parameters in the dorsal and lateral lobes are especially noteworthy since this part of the rodent prostate is believed to mimic the peripheral zone of the human prostate in its disposition to develop malignancy (Abate-Shen and Shen, 2002). Although food consumption was considered equal between the groups, the influence of decreased body weight on prostate lesion

development in drug-treated mice cannot be discounted. Diet restriction in this model has been shown to retard lesion development (Suttie et al., 2003; Suttie et al., 2005). However, TRAMP mice in the present study exhibit at most a 6% decrease in body weight, the effect of which on tumorigenesis is unclear. Despite large numbers of experimental animals (n = 30 per group), we were unable to demonstrate strong evidence for a decrease in the incidence of carcinoma in the treatment group. The data indicate that, considering all alveoli that comprise a prostate lobe, OSU03012 has a general negative effect on epithelial lesion development (the decreased lobe weights in treated animals correlate with the reduction in microscopic lesion score), but the transformation of certain cells to neoplasia is not substantially affected. It appears that once a clonal population of cells is established, the tumors grow quickly and aggressively regardless of treatment.

Two explanations of this failure to stop the progression to malignancy are possible. First, the TRAMP model is characterized by a strong oncogenic stimulus that drives the rapid progression from non-invasive, low-grade lesions, which were present at the time treatment was started, to aggressive carcinoma. This rapid tumorigenic progression is a considerable drawback of the model (Gupta, 2004) and may counter chemopreventive effects of single agent treatment with OSU03012 that would be evident in an *in vivo* system that more closely models the slower progression of the human disease. Secondly, although we demonstrated Akt activation in hyperplastic prostate epithelium in TRAMP mice prior to this study (Fig. 2c), the exact transition point in the prostate at which Akt activation leads to tumor growth remains unclear (Narayanan et al., 2004). The

promotion of cell proliferation by viral T antigens, and subsequent inhibition of retinoblastoma and p53 (Greenberg et al., 1995), may override the necessity of Akt signaling in progressed lesions in this model.

This apparent time-dependency of Akt modulation in TRAMP is further demonstrated by Natarayanan et al. in which Akt suppression was correlated with reduced PIN lesions when TRAMP mice were treated with celecoxib beginning at 6 weeks of age (Narayanan et al., 2004). This study also reflects the COX-2-independent anti-tumor activity of COX-2 antagonists, which have been previously described (Hsu et al., 2000), as does our study since OSU03012 is a celecoxib analogue in which COX-2 targeting has been removed (Zhu et al., 2004).

A treatment-associated, food intake-independent reduction in body fat, observed in otherwise apparently healthy TRAMP mice prompted detailed phenotyping and comparison of experimental groups. This analysis revealed hepatic lesions suggestive of altered glycogen metabolism and of a link to target pathway inhibition. Glycogen synthase is a pivotal regulator of glucose storage (Plyte et al., 1992) and is controlled by PDK1/Akt/GSK3 signaling in liver, striated muscle, and fat (Mora et al., 2005). As GSK3 $\beta$  is an important inhibitor of GS activity, and inhibition of PDK1 promotes GSK3 $\beta$  function by inactivation of both Akt and p70 ribosomal S6 kinase (S6K) (Zhu et al., 2004), it not surprising that chronic, systemic PDK1 inhibition could influence basic energy metabolism by depleting liver and muscle glycogen stores. A subsequent increase in  $\beta$ -oxidation of fatty acids to maintain ATP production could, in principle, account for the observed decrease in body fat of the treated mice.

Supportive evidence of an effect on glycogen synthesis was determined by histopathology, immunohistochemistry, and electron microscopy of liver, and immunohistochemistry of skeletal muscle. Evidence of decreased hepatocellular glycogen content concurrent with inactivation of GS correlates well with the proposed pharmacologic effect of OSU03012 (Fig. 3.7) and suggests a cause of the zonal pattern of hepatocellular atrophy. The increased intrahepatic level of p-GS in association with decreased glycogen content strongly suggest a pharmacological effect of OSU03012 treatment since GS activity and glycogen content exhibit an inverse relationship under normal physiologic conditions (Nielsen JN, 2001).

Inactivation of GS in skeletal muscle is supported by the intense immunohistochemical staining of p-GS and suggests that generalized suppression of GS occurred in mice subsequent to OSU03012 treatment. This is the first report, to our knowledge, of a systemic effect on glycogen synthase activity secondary to chronic PDK1 targeting by an orally administered compound. There are no reports of this effect by celecoxib, the parent compound, which is fitting since PDK1 inhibition by celecoxib is modest in comparison to that caused by OSU03012. Adverse effects by celecoxib are largely associated with its nonsteroidal anti-inflammatory properties and include cardiovascular and gastrointestinal events (Food and Drug Administration, 2004). 7-hydroxystaurosporine (UCN-01), a broad-acting kinase inhibitor of which PDK1/Akt is a target, has been reported to modulate bioenergetic signaling in Phase I clinical trials (Kondapaka et al., 2004). This effect, however, is one of insulin resistance and appears to be much different than that observed here. Similar phenotypic sequelae of chronic

PI3-K inhibition, the upstream kinase, have been described and include hyperglycemia associated with perturbations of insulin signaling in adipocytes and myotubes. Effects on glucose metabolism in the liver, however, remain unexplored (Knight et al., 2006).

Considering that genetically engineered animals designed to predict the efficacy of therapeutic agents may provide ancillary information about toxicity (Bolon, 2004), conditional liver and skeletal muscle PDK1 knockout animals would be useful for further investigation of the causal relationship proposed here. Lawlor et. al. found that PDK1 is an essential regulator of cell size and is required for embryonic development. Although homozygous PDK1 deletion is embryonically lethal, hypomorphic mutant PDK1 mice are viable, fertile, and 40-50% smaller than control animals (Lawlor et al., 2002). In a conditional knockout model, Mora et. al. showed that insulin could not activate GS or cause its dephosphorylation at GSK3-phosphorylated residues in cardiac muscle from PDK1<sup>-/-</sup> or double GSK3alpha/GSK3beta knock-in mice. Perhaps surprisingly, normal levels of cardiac glycogen were detected in these mice suggesting a more complex regulation of GS activity in the heart (Mora et al., 2005). It would be interesting to know total hepatic and skeletal muscle glycogen content in animals from these studies. Regarding GS specifically, humans with congenital deficiencies of GS are reported to develop fasting hypoglycemia (Orho et al., 1998), and knockout mice lacking muscle GS are smaller than wild-type littermates and have less body fat (Pederson et al., 2005).

Additional *in vivo* studies are needed to further characterize cytochrome P450 induction associated with hypertrophy of zone 3 cells. For our purposes, smooth ER proliferation detected by EM is compatible with phenobarbitone-like P450 induction and

rules out peroxisome proliferation as the cause of hypertrophy (Greaves, 2000). The observed focal clusters of tightly packed smooth ER may represent a late stage of hepatocellular drug tolerance by drug-handling enzymes (Ghadially, 1982). The enlarged zone 3 cells at least partly explain the elevated ALP detected in these mice via cholestasis. Both the centrilobular and periportal changes likely contributed to the increases in ALT and AST, however, overt hepatocellular necrosis was not observed. A similar pattern of centrilobular hypertrophy was associated with a dose-dependent increase in liver weight in nude mice treated with OSU03012 for 6 weeks at 100 and 200 mg/kg/day (unpublished research). These results provide guidelines for future toxicity assays that may include specific time-course characterization, enzyme activity analysis, and profiling of P450 isozymes. The latter will be important for inferring human risk (Watanabe et al., 1998; Greaves, 2000), especially since xenobiotic-induced activity of mixed function oxidases may affect the metabolism of other administered compounds, or may be a compensatory response with little clinical significance (Greaves, 2000).

Skeletal myonecrosis in treated TRAMP mice correlates with the elevated CK and AST levels detected in these animals. This lesion is intriguing considering that skeletal muscle diagnoses in general are very rare in National Toxicology Program studies in mice (Leininger, 1999), and that the literature contains very few reports of such lesions in the nonclinical and clinical safety evaluation of pharmaceutical candidates. Potential drug associations in our study include altered muscle homeostasis secondary to impaired glycogen metabolism, or a disturbance of Akt/GSK3 signaling, which regulates myofiber size and hypertrophic responses (Bodine et al., 2001; Rommel et al., 2001). As other Akt

inhibitors have been reported to target glycolytic cells [in the context of cancer cells dependent on glucose (Elstrom et al., 2004; Plas and Thompson, 2005; Thompson, 2005)], it is also possible that Akt inhibition can affect glycolytic Type II myocytes, which we have shown to be targeted in our drug-treated mice. It is noteworthy that the pattern of myonecrosis observed here is reminiscent of that induced by statins, the exact mechanism of which remains unknown but was recently shown to involve targeting of type IIB fibers (Westwood et al., 2005) and has been linked directly to cholesterol lowering, as detected in our mice, by an alteration of myocyte lipid/protein organization (Draeger et al., 2006). A mechanistic link to cholesterol lowering, shared by the statins and the present study of OSU03012, is also supported by reports of skeletal muscle necrosis with other hypocholesterolemic drugs including clofibrate in rats (McDonald and Hamilton, 1990).

We hope to demonstrate here that complete phenotyping of animals used in early efficacy studies may reveal unanticipated effects that could facilitate lead optimization, assist protocol design in toxicology, and provide additional biomarkers for further *in vivo* testing. This approach will undoubtedly improve the efficiency of preclinical evaluation of drug candidates, which remains a substantial roadblock in drug development partly due to the time and money required for performing both therapeutic and toxicologic studies in animals. Given that elucidating the exact mechanisms of the changes observed here requires toxicology-specific animal assays, we demonstrate evidence for association with target pathway inhibition. Fresh tissue obtained from animals in future studies will permit quantitative analysis of glycogen content, for example. It is important to note that

the 200 mg/kg/day dose used in this study is the highest dose of OSU03012 to be administered to xenograft-bearing mice in our work (unpublished data). Moreover, the reversibility and specific dose-dependency of the observed effects are unknown. Although OSU03012 potently inhibits PDK1 (Zhu et al., 2004), other effects likely contribute to its anti-cancer activity and must also be considered as potential influencers of phenotypic changes.

In conclusion, inhibition of the PDK1/Akt pathway during the progression of advanced PIN to carcinoma reduces the overall severity of epithelial lesion development as determined by lobe weight and lesion score endpoints, but is insufficient to significantly decrease the incidence of carcinoma and metastasis in TRAMP mice. In addition to effects on the prostate, chronic oral administration of OSU03012 caused phenotypic changes at least in part associated with inactivation of the enzyme responsible for glycogen synthesis. As the rational design and development of PDK1- and Akt-targeted small molecules is an active focus of research in the field of anticancer drug discovery, our study reveals important non-cancer parameters, namely body fat/weight along with markers of liver and skeletal muscle health, that should be considered for monitoring in future preclinical and clinical evaluations of these agents.

## **LIST OF REFERENCES**

- Abate-Shen, C. and Shen, M. M. (2002). Mouse models of prostate carcinogenesis. *Trends Genet* **18**(5), S1-5.
- Bodine S. C., Stitt, T. N., Gonzalez, M., Kline, W. O., Stover, G. L., Bauerlein, R., Zlotchenko, E., Scrimgeour, A., Lawrence, J. C., Glass, D. J., and Yancopoulos, G. D. (2001). Akt/mTOR pathway is a crucial regulator of skeletal muscle

- hypertrophy and can prevent atrophy *in vivo*. *Nat Cell Biol* **3**, 1014-1019.
- Bolon, B. (2004). Genetically engineered animals in drug discovery and development: a maturing resource for toxicologic research. *Basic Clin Pharmacol Toxicol* **95**(4), 154-61.
- Bregman, C. L., Adler, R. R., Morton, D. G., Regan, K. S., and Yano, B. L. (2003). Recommended tissue list for histopathologic examination in repeat-dose toxicity and carcinogenicity studies: a proposal of the Society of Toxicologic Pathology (STP). *Toxicol Pathol* **31**(2), 252-3.
- Cross, D. A., Alessi, D. R., Cohen, P., Andjelkovich, M., Hemmings, B. A. (1995). Inhibition of glycogen synthase kinase-3 by insulin mediated by protein kinase B. *Nature* **378**(6559): 785-9.
- Draeger, A., Monastyrskaya, K., Mohaupt, M., Hoppeler, H., Savolainen, H., Allemann, C., Babiyshuk, E. B. (2006). Statin therapy induces ultrastructural damage in skeletal muscle in patients without myalgia. *J Pathol* **210**(1), 94-102.
- Edwards, J., Krishna, N. S., Witton, C. J., and Bartlett, J. M. (2003). Gene amplifications associated with the development of hormone-resistant prostate cancer. *Clin Cancer Res* **9**(14), 5271-81.
- Elstrom, R. L., Bauer, D. E., Buzzai, M., Karnauskas, R., Harris, M. H., Plas, D. R., Zhuang, H., Cinalli, R. M., Alavi, A., Rudin, C. M., and Thompson, C. B. (2004). Akt stimulates aerobic glycolysis in cancer cells. *Cancer Res* **64**(11), 3892-9.
- Food and Drug Administration. Celebrex label (2005): <http://www.fda.gov/cder/foi/label/2005/020998s018,019lbl.pdf>
- Ghadially, F. N. (1982). Endoplasmic reticulum. In *Ultrastructural Pathology of the Cell and Matrix*, 2<sup>nd</sup> ed., pp. 370, 838. William Clowes (Beccles) Limited, Beccles and London, Great Britain.
- Greaves, P. (2000). Digestive System 2. In *Histopathology of Preclinical Toxicity Studies. Interpretation and Relevance in Drug Safety Evaluation*, 2<sup>nd</sup> ed., p. 435-52. Elsevier.
- Greenberg, N. M., DeMayo, F., Finegold, M. J., Medina, D., Tilley, W. D., Aspinall, J. O., Cunha, G. R., Donjacour, A. A., Matusik, R. J., and Rosen, J. M. (1995). Prostate cancer in a transgenic mouse. *Proc Natl Acad Sci U S A* **92**(8), 3439-43.
- Gupta, S. (2004). Prostate cancer chemoprevention: models, limitations and potential (Review). *Int J Oncol* **25**(4), 1133-48.

- Gupta, S., Hastak, K., Ahmad, N., Lewin, J. S., and Mukhtar, H. (2001). Inhibition of prostate carcinogenesis in TRAMP mice by oral infusion of green tea polyphenols. *Proc Natl Acad Sci U S A* **98**(18), 10350-5.
- Hsu, A. L., Ching, T. T., Wang, D. S., Song, X., Rangnekar, V. M., and Chen, C. S. (2000). The cyclooxygenase-2 inhibitor celecoxib induces apoptosis by blocking Akt activation in human prostate cancer cells independently of Bcl-2. *J Biol Chem* **275**(15), 11397-403.
- Ihle, N. T., Paine-Murrieta, G., Berggren, M. I., Baker, A., Tate, W. R., Wipf, P., Abraham, R. T., Kirkpatrick, D. L., and Powis, G. (2005). The phosphatidylinositol-3-kinase inhibitor PX-866 overcomes resistance to the epidermal growth factor receptor inhibitor gefitinib in A-549 human non-small cell lung cancer xenografts. *Mol Cancer Ther* **4**(9), 1349-57.
- Johnson, A. J., Smith, L. L., Zhu, J., Heerema, N. A., Jefferson, S., Mone, A., Grever, M., Chen, C. S., and Byrd, J. C. (2005). A novel celecoxib derivative, OSU03012, induces cytotoxicity in primary CLL cells and transformed B-cell lymphoma cell line via a caspase- and Bcl-2-independent mechanism. *Blood* **105**(6), 2504-9.
- Klein, R. D. (2005). The use of genetically engineered mouse models of prostate cancer for nutrition and cancer chemoprevention research. *Mutation Res* **576**, 111-119.
- Knight, Z. A., Gonzalez, B., Feldman, M. E., Zunder, E. R., Goldenberg, D. D., Williams, O., Loewith, R., Stokoe, D., Balla, A., Toth, B., Balla, T., Weiss, W. A., Williams, R. L., and Shokat, K. M. (2006). A pharmacological map of the PI3-K family defines a role for p110alpha in insulin signaling. *Cell* **125**(4), 733-47.
- Komander, D., Kular, G. S., Bain, J., Elliott, M., Alessi, D. R., and Van Aalten, D. M. (2003). Structural basis for UCN-01 (7-hydroxystaurosporine) specificity and PDK1 (3-phosphoinositide-dependent protein kinase-1) inhibition. *Biochem J* **375**(Pt 2), 255-62.
- Kondapaka, S. B., Zarnowski, M., Yver, D. R., Sausville, E. A., and Cushman, S. W. (2004). 7-hydroxystaurosporine (UCN-01) inhibition of Akt Thr308 but not Ser473 phosphorylation: a basis for decreased insulin-stimulated glucose transport. *Clin Cancer Res* **10**(21), 7192-8.
- Kucab, J. E., Lee, C., Chen, C. S., Zhu, J., Gilks, C. B., Cheang, M., Huntsman, D., Yorida, E., Emerman, J., Pollak, M., and Dunn, S. E. (2005). Celecoxib analogues disrupt Akt signaling, which is commonly activated in primary breast tumours. *Breast Cancer Res* **7**(5), R796-807.

- Kulp, S. K., Yang, Y. T., Hung, C. C., Chen, K. F., Lai, J. P., Tseng, P. H., Fowble, J. W., Ward, P. J., and Chen, C. S. (2004). 3-phosphoinositide-dependent protein kinase-1/Akt signaling represents a major cyclooxygenase-2-independent target for celecoxib in prostate cancer cells. *Cancer Res* **64**(4), 1444-51.
- Lawlor, M. A., Mora, A., Ashby, P. R., Williams, M. R., Murray-Tait, V., Malone, L., Prescott, A. R., Lucocq, J. M., and Alessi, D. R. (2002). Essential role of PDK1 in regulating cell size and development in mice. *Embo J* **21**(14), 3728-38.
- Leininger, J. R. (1999). Skeletal muscle. In *Pathology of the Mouse* (R. R. Maronpot, G. A. Boorman, B. W. Gaul, eds.) 1<sup>st</sup> ed, p. 637. Cache River Press, Vienna, IL.
- Li, L., Ittmann, M. M., Ayala, G., Tsai, M. J., Amato, R. J., Wheeler, T. M., Miles, B. J., Kadmon, D. and Thompson, T. C. (2005). The emerging role of the PI3-K-Akt pathway in prostate cancer progression. *Prostate Cancer Prostatic Dis* **8**(2), 108-18.
- Liao, Y., Grobholz, R., Abel, U., Trojan, L., Michel, M. S., Angel, P., and Mayer, D. (2003). Increase of AKT/PKB expression correlates with Gleason pattern in human prostate cancer. *Int J Cancer* **107**(4), 676-80.
- McCabe, M. T., Low, J. A., Daignault, S., Imperiale, M. J., Wojno, K. J., Day, M. L. (2006). Inhibition of DNA methyltransferase activity prevents tumorigenesis in a mouse model of prostate cancer. *Cancer Res* **66**(1), 385-92.
- McCubrey, J. A., LaHair, M. M., Franklin, R. A. (2006). OSU-03012 in the treatment of glioblastoma. *Mol Pharmacol* **70**(2), 437-39.
- McDonald, M. M., and Hamilton, B. F. (1990). Skeletal muscle. In *Pathology of the Fischer Rat* (G. A. Boorman, S. L. Eustis, M. R. Elwell, C. A. Montgomery, W. F. MacKenzie, eds.) p. 202. Academic Press, Inc., San Diego, CA.
- Mimeault, M. and Batra, S. K. (2006). Recent advances on multiple tumorigenic cascades involved in prostatic cancer progression and targeting therapies. *Carcinogenesis* **27**(1), 1-22.
- Mora, A., K. Sakamoto, McManus, E. J., and Alessi, D. R. (2005). Role of the PDK1-PKB-GSK3 pathway in regulating glycogen synthase and glucose uptake in the heart. *FEBS Lett* **579**(17), 3632-8.
- Narayanan, B. A., Narayanan, N. K., Pittman, B., and Reddy, B. S. (2004). Regression of mouse prostatic intraepithelial neoplasia by nonsteroidal anti-inflammatory drugs in the transgenic adenocarcinoma mouse prostate model. *Clin Cancer Res* **10**(22),

7727-37.

- Nielsen., J. N., Derave, W., Kristiansen, S., Ralston, E., Ploug, T., and Richter, E. A., (2001). Glycogen synthase localization and activity in rat skeletal muscle is strongly dependent on glycogen content. *J Physiol* (531), 757-769.
- Orho, M., Bosshard, N. U., Buist, N. R., Gitzelmann, R., Aynsley-Green, A., Blumel, P., Gannon, M. C., Nuttall, F. Q., Groop, L. C. (1998). Mutations in the liver glycogen synthase gene in children with hypoglycemia due to glycogen storage disease type 0. *J Clin Invest* **102**(3), 507-15.
- Pederson, B. A., Schroeder, J. M., Parker, G. E., Smith, M. W., Depaoli-Roach, A. A., and Roach, P. J. (2005). Glucose metabolism in mice lacking muscle glycogen synthase. *Diabetes* **54**(12), 3466-73.
- Plas, D. R. and Thompson, C. B. (2005). Akt-dependent transformation: there is more to growth than just surviving. *Oncogene* **24**(50), 7435-42.
- Plyte, S. E., Hughes, K., Nikolakaki, E., Pulverer, B. J., and Woodgett, J. R. (1992). Glycogen synthase kinase-3: functions in oncogenesis and development. *Biochem Biophys Acta* **1114**(2-3), 147-62.
- Raghow, S., Hooshdaran, M.Z., Katiyar, S., Steiner, M.S. (2002). Toremifene prevents prostate cancer in the transgenic adenocarcinoma of mouse prostate model. *Cancer Res* **62**(5), 1370-6.
- Raghow, S., Kuliyeve, E., Steakley, M., Greenberg, N., and Steiner, M. S. (2000). Efficacious chemoprevention of primary prostate cancer by flutamide in an autochthonous transgenic model. *Cancer Res* **60**(15), 4093-7.
- Rommel, C., Bodine, S. C., Clarke, B. A., Rossman, R., Nunez, L., Stitt, T. N., Yancopoulos, G. D., and Glass, D. J. (2001). Mediation of IGF-1-induced skeletal myotube hypertrophy by PI(3)K/Akt/mTOR and PI(3)K/Akt/GSK3 pathways. *Nat Cell Biol* **3**(11): 1009-13.
- Suckow, M. A., Danneman, P., Brayton, C. (2001). Important biological features. In *The Laboratory Mouse*, p. 12. CRC Press LLC, Boca Raton, Florida.
- Suttie, A. W., Dinse, G. E., Nyska, A., Moser, G. J., Goldsworthy, T. L., and Maronpot, R. R. (2005). An investigation of the effects of late-onset dietary restriction on prostate cancer development in the TRAMP mouse. *Toxicol Pathol* **33**(3), 386-397.
- Suttie, A., Nyska, A., Haseman, J. K., Moser, G. J., Hackett, T. R., and Goldsworthy, T.

- L. (2003). A grading scheme for the assessment of proliferative lesions of the mouse prostate in the TRAMP model. *Toxicol Pathol* **31**(1), 31-8.
- Thompson, C. B. (2005). Metabolic regulation of cancer cell survival. In Mechanisms of toxicity, carcinogenesis, cancer prevention and cancer therapy. The Twentieth Aspen Cancer Conference. Session 8. Apoptosis. *Toxicol Pathol* **33**(7), 829-31.
- Tomita, Y., Morooka, T., Hoshida, Y., Zhang, B., Qiu, Y., Nakamichi, I., Hamada, K., Ueda, T., Naka, N., Kudawara, I., Aozasa, K. (2006). Prognostic significance of activated AKT expression in soft-tissue sarcoma. *Clin Cancer Res* **12**, 3070-3077.
- Tseng, P. H., Lin, H. P., Zhu, J., Chen, K. F., Hade, E. M., Young, D. C., Byrd, J. C., Grever, M., Johnson, K., Druker, B. J., Chen, C. S. (2005). Synergistic interactions between imatinib mesylate and the novel phosphoinositide-dependent kinase-1 inhibitor OSU-03012 in overcoming imatinib mesylate resistance. *Blood* **105**, 4021-27.
- Tseng, P. H., Weng, S. C., Wang, Y. C., Weng, J. R., Chen, C. S., Brueggemeier, R. W., Shapiro, C. L., Chen, C. Y., Dunn, S. E., Pollak, M., Chen, C.S. (2006). Overcoming trastuzumab resistance in HER2-overexpressing breast cancer cells by using a novel celecoxib-derived PDK-1 inhibitor. *Mol Pharmacol* **70**(5), 1534-41.
- Watanabe, T., Manabe, S., Ohashi, Y., Okamiya, H., Onodera, H., and Mitsumori, K. (1998). Comparison of the induction profile of hepatic drug-metabolizing enzymes between piperonyl butoxide and phenobarbital in rats. *J Toxicol Pathol* **11**, 1-10.
- Wechter, W. J., Leipold, D. D., Murray, E. D., Jr., Quiggle, D., McCracken, J. D., Barrios, R. S., and Greenberg, N. M. (2000). E-7869 (R-flurbiprofen) inhibits progression of prostate cancer in the TRAMP mouse. *Cancer Res* **60**(8), 2203-8.
- Westwood, F. R., Bigley, A., Randall, K., Marsden, A. M., and Scott, R. C. (2005). Statin-induced muscle necrosis in the rat: distribution, development, and fibre selectivity." *Toxicol Pathol* **33**(2), 246-57.
- Xie, Z., Yuan, H., Yin, Y., Zeng, X., Bai, R., and Glazer, R. I. (2006). 3-phosphoinositide-dependent protein kinase-1 (PDK1) promotes invasion and activation of matrix metalloproteinases. *BMC Cancer* **6**, 77.
- Yang, L., Dan, H. C., Sun, M., Liu, Q., Sun, X. M., Feldman, R. I., Hamilton, A. D., Polokoff, M., Nicosia, S. V., Herlyn, M., Sebt, S. M., and Cheng, J. Q. (2004). Akt/protein kinase B signaling inhibitor-2, a selective small molecule inhibitor of Akt signaling with antitumor activity in cancer cells overexpressing Akt. *Cancer*

*Res* **64**(13), 4394-9.

Zhu, J., Huang, J. W., Tseng, P. H., Yang, Y. T., Fowble, J., Shiau, C.W., Shaw, Y. J., Kulp, S. K., and Chen, C.S. (2004). From the cyclooxygenase-2 inhibitor celecoxib to a novel class of 3-phosphoinositide-dependent protein kinase-1 inhibitors. *Cancer Res* **64**(12), 4309-18.

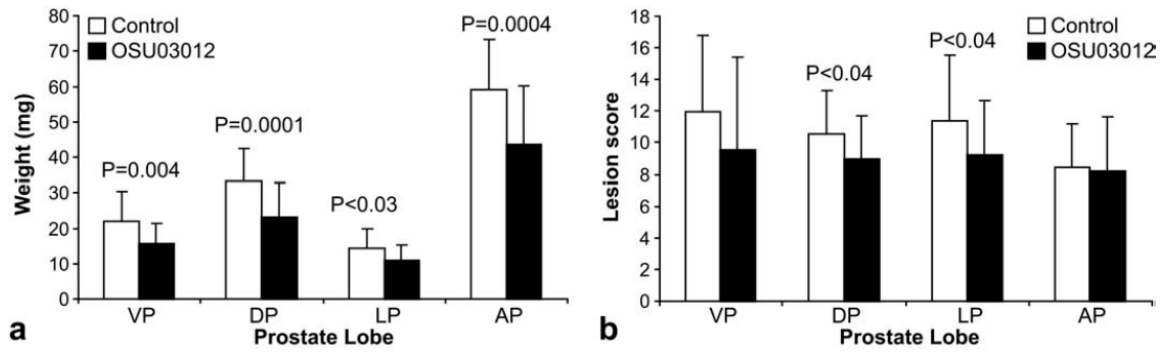


Figure 3.1: OSU03012 decreased prostate lobe weights and the severity of epithelial proliferation. (a) The weights of all prostate lobes of TRAMP mice were significantly decreased following 8 weeks of OSU03012 treatment (200 mg/kg/day) compared to vehicle-treated controls. (b) Assessed by a TRAMP-specific grading scheme, the severity of prostate epithelial lesion development was significantly decreased in the dorsal and lateral lobes. VP: ventral prostate, DP: dorsal prostate, LP: lateral prostate, AP: anterior prostate. Values reported as mean  $\pm$  SD, n=30 control, 31 treated mice.

Figure 3.2: OSU03012 decreased prostate epithelial lesion development and inhibited the phosphorylation of Akt and the downstream effector GSK3 $\beta$ . (a) DP from a control mouse with diffuse grade 3 epithelial hyperplasia or PIN compared to multifocal grade 3 hyperplasia from a drug-treated mouse (b) at 18 weeks of age. The difference in distribution here of the same proliferative grade lesion accounts for one less score point in the treated mouse (score 9) compared to control (score 8). H&E; Bars = 200  $\mu$ m. (c) P-Thr308-Akt immunohistochemistry of the DP from an untreated, 7-week-old TRAMP mouse demonstrates increased staining in hyperplastic epithelium (arrows) compared to adjacent normal epithelium. A dramatic decrease in immunostaining is evident in the DP of 18-week-old, OSU03012-treated TRAMP (e) compared to control TRAMP (d). Bars = 30  $\mu$ m. (f). Representative immunoblots of DP tissue lysate, quantitated by densitometry, shows a significant decrease in the phosphorylation of GSK3 $\beta$ , a downstream effector of Akt, and a significant increase in the phosphorylation of GS in drug-treated TRAMP. P-GSK3 $\beta$  and p-GS were normalized against total GSK3 $\beta$  and  $\beta$ -Actin, respectively. Data points represent mean  $\pm$  SD, n = 5 per group. C: vehicle-control, O: OSU03012-treated, GSK3 $\beta$ : glycogen synthase kinase 3 beta, GS: glycogen synthase.

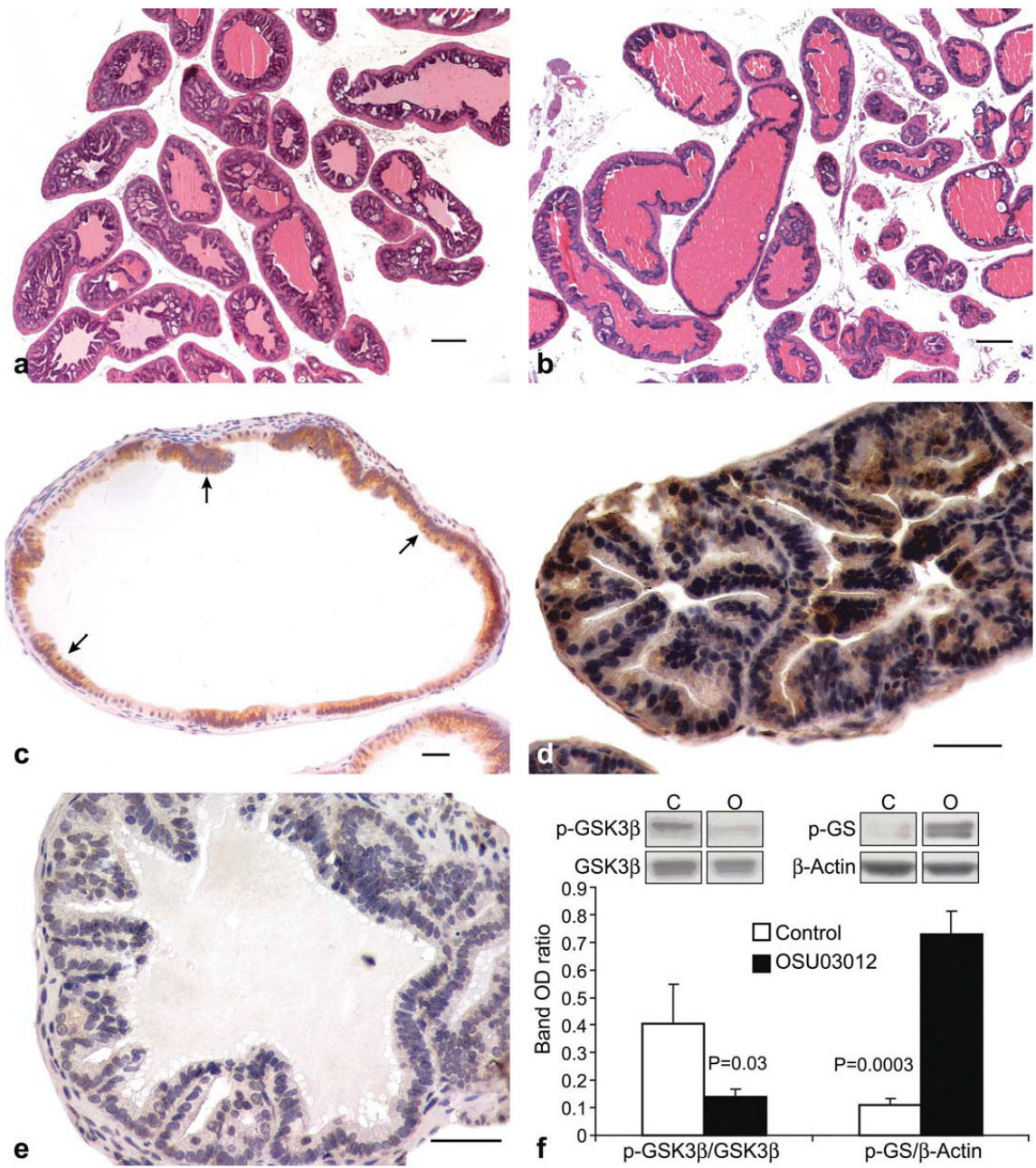


Figure 3.2

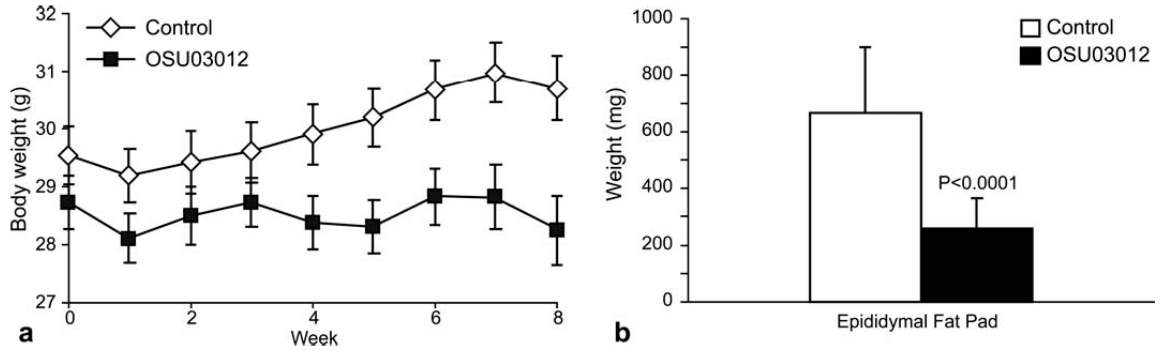


Figure 3.3: OSU03012 decreased body fat and prevented body weight gain independent of food intake. (a) The body weights of drug-treated TRAMP mice remained relatively constant during the 8-week treatment period compared to a gradual increase in vehicle-treated control TRAMP mice. Data points represent mean  $\pm$  standard error, n = 30 control, 31 treated mice. (b) This failure of weight gain was at least in part due to a significant decrease in body fat which was quantified by the weights of epididymal fat pads. Values reported as mean  $\pm$  SD, n = 21 control, 16 treated mice.

Figure 3.4: OSU03012 caused hepatic lesions that can be linked in part to target pathway inhibition. (a,b) An accentuation of lobular architecture characterized by zone 3 hypertrophy (black arrows) and zone 1 atrophy (white arrows) was observed in the livers of TRAMP following 8 weeks of treatment with OSU03012 (b), compared to a uniformity in hepatocellular size across the hepatic lobule in vehicle-treated control TRAMP (a). Bars = 50  $\mu\text{m}$ . (c,d). PAS-stained sections show a decrease in and altered distribution of glycogen in drug-treated TRAMP hepatocytes (d) compared to controls (c). PAS: periodic acid-Schiff; Bar = 100  $\mu\text{m}$ . (e,f) P-GS immunohistochemistry shows increased staining in atrophic zone 1 cells (white arrows) in drug-treated TRAMP (f) with a lack of staining in zone 3 cells (black arrows), compared to a uniform, less intense degree of staining across the lobule in control TRAMP (e). Bars = 100  $\mu\text{m}$ .

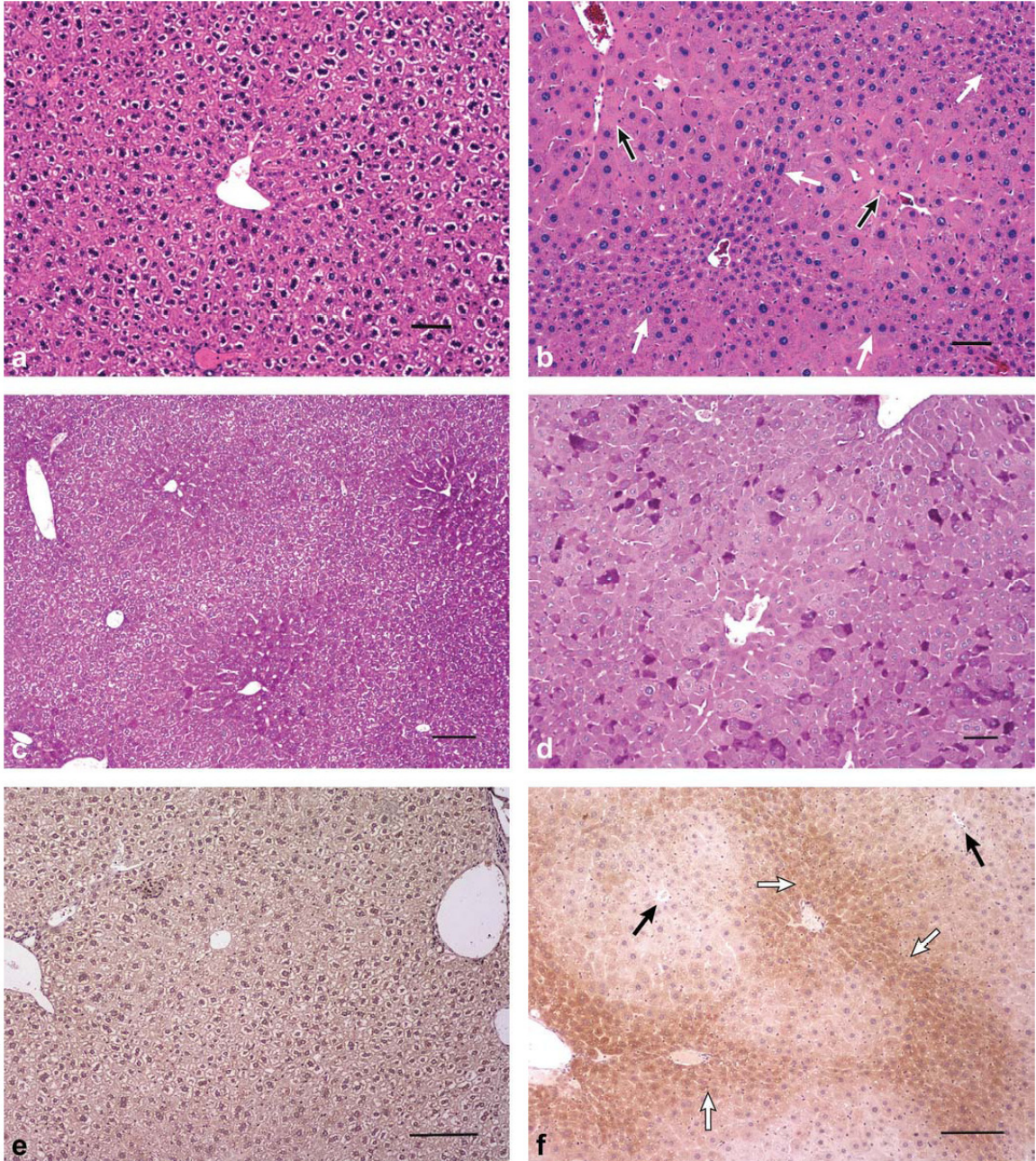


Figure 3.4

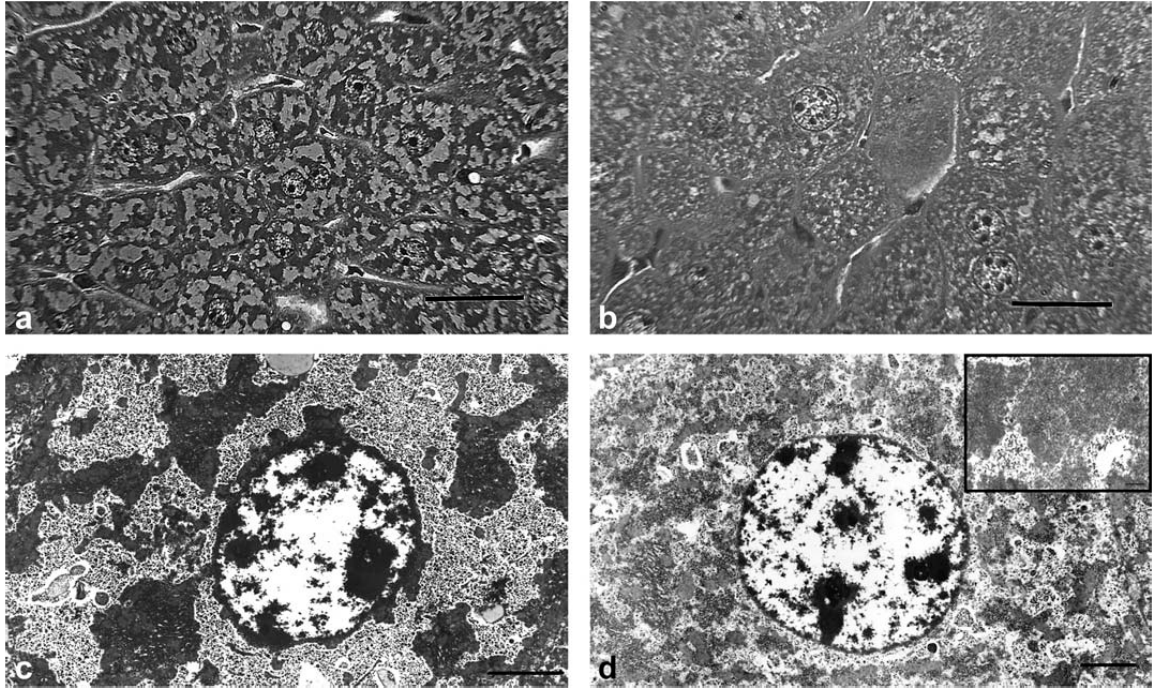


Figure 3.5: Toluidine blue staining and transmission electron microscopy of hypertrophic zone 3 hepatocytes. (a) Hepatocyte cytoplasm of control TRAMP contains dark, clumped foci separated by pale-staining material that corresponds ultrastructurally to large aggregations of rough ER and mitochondria mixed with abundant glycogen (c). This pattern sharply contrasts with the finely stippled, ground-glass like cytoplasm of drug-treated TRAMP hepatocytes (b) that corresponds ultrastructurally to focal, tightly packed proliferations of smooth ER (inset), smaller aggregations of rough ER and mitochondria, and glycogen-poor cytoplasm (d). Bars = 30  $\mu\text{m}$  (a,b), 3  $\mu\text{m}$  (c,d), 0.4  $\mu\text{m}$  (inset).

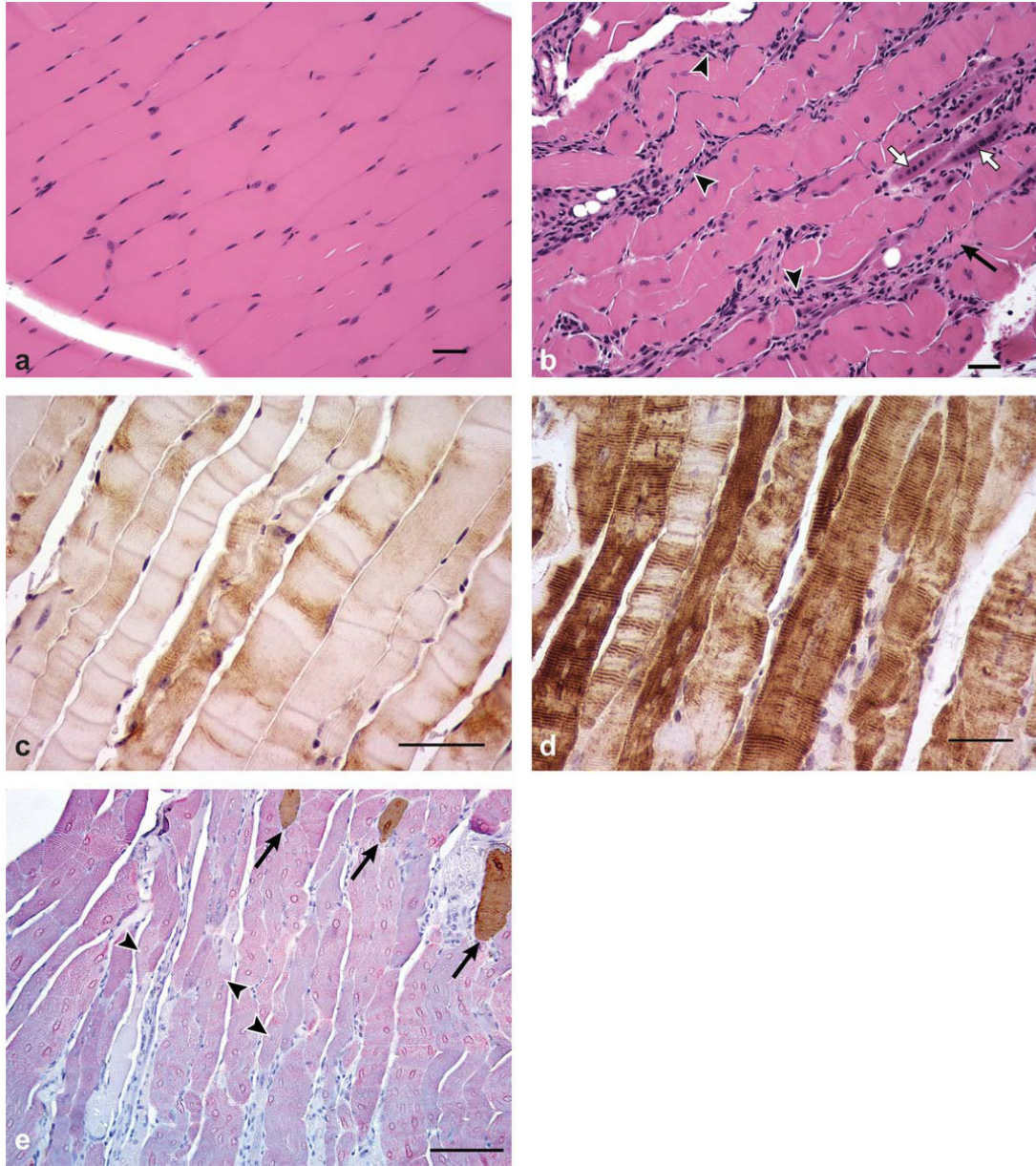


Figure 3.6: Multifocal, multiphasic necrosis of Type II skeletal myofibers was observed in drug-treated TRAMP mice, and GS was inactivated in skeletal muscle. (a) Unaffected biceps femoris muscle of a vehicle-treated control TRAMP. (b) Drug-treated TRAMP muscle showing a spectrum of lesions including acute segmental necrosis (black arrow), loss of myofibers with infiltration of macrophages (arrowheads), and regenerative rowing of nuclei (white arrows). H&E. P-GS immunostaining is increased in drug-treated TRAMP muscle (d) compared to control TRAMP muscle (c). Bars = 50  $\mu$ m. (e) Dual labelling for slow and fast myosin shows targeting of Type II fibers (pink fibers/arrowheads) with sparing of Type I fibers (black fibers/arrows). Bar = 100  $\mu$ m.

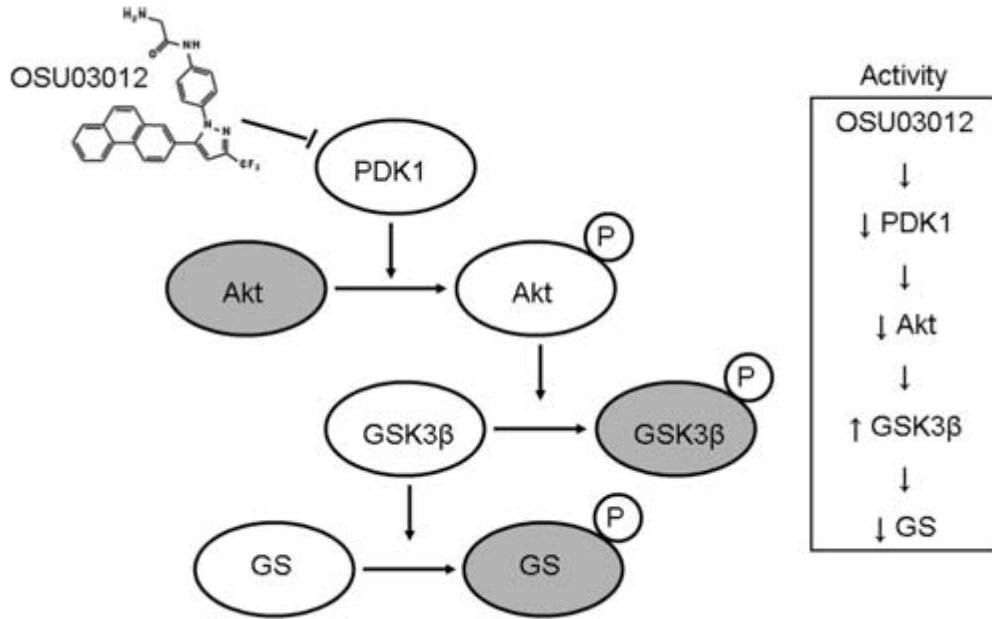


Figure 3.7: Signaling pathway of PDK1/Akt  $\rightarrow$  GS, and proposed protein activity induced by OSU03012 treatment. Inactive proteins are shaded gray.

Dose Group	BUN (mg/dl)	Creatinine (mg/dl)	ALT (iu/L)	AST <sup>b</sup> (iu/L)	ALP (iu/L)	CK (iu/L)	Cholesterol <sup>c</sup> (mg/dl)	TBILI (mg/dl)	Glucose <sup>d</sup> (mg/dl)
Control	21.2 ± 5.6	0.44 ± 0.21	90.7 ± 88.7	152.7 ± 128.7	41.4 ± 29.6	517.9 ± 621.2	154.4 ± 10.9	0.23 ± 0.09	193.6 ± 23.5
OSU-03012	21.2 ± 2.1	0.29 ± 0.06	298.7 ± 375.8	420.8 ± 168.7	71.6 ± 59.7	922.6 ± 433.9	112.1 ± 19.6	<0.22 ± 0.05	155.7 ± 27.7
Fold increase	-	-	3.3	2.8	1.7	1.8	-	-	-

<sup>a</sup>Values are expressed as averages (n = 8) ± standard deviation.

<sup>b</sup>P = 0.003

<sup>c</sup>P = 0.0001

<sup>d</sup>P = 0.01

BUN: blood urea nitrogen, ALT: alanine aminotransferase, AST: aspartate aminotransferase, ALP: alkaline phosphatase, CK: creatine kinase, TBILI: total bilirubin

Table 3.1: Serum chemistry values<sup>a</sup> of TRAMP mice after 8 weeks of treatment.

Dose Group	PCV (%)	RBC (x 10 <sup>6</sup> /μl)	Nucleated cells (x 10 <sup>3</sup> /μl)	Segmented neutrophils (x 10 <sup>3</sup> /μl)	Lymphocytes <sup>b</sup> (x 10 <sup>3</sup> /μl)	Platelets (x 10 <sup>3</sup> /μl)
Control	43.3 ± 3.8	9.9 ± 0.9	14.5 ± 3.1	1.7 ± 1.4	10.4 ± 2.7	1240.7 ± 417.3
OSU-03012	41.0 ± 5.2	9.3 ± 1.4	10.2 ± 1.7	5.5 ± 2.3	4.5 ± 1.8	1000.7 ± 766.2

<sup>a</sup>Values are expressed as averages (n = 3) ± standard deviation.

<sup>b</sup>P = 0.03

PCV: packed cell volume, RBC: red blood cells

Table 3.2: Hematology values<sup>a</sup> of TRAMP mice after 8 weeks of treatment.

## **CHAPTER 4**

# **PRECLINICAL INVESTIGATION OF NOVEL INDOLE-3-CARBINOL ANALOGS FOR THE PREVENTION AND TREATMENT OF PROSTATE CANCER**

### **ABSTRACT**

We recently reported the anticancer activity of OSU-A9, a novel small-molecule agent which retains the broad-spectrum of antitumor activity of its parent compound indole-3-carbinol but with enhanced metabolic stability and two orders of magnitude greater potency in prostate cancer. Here, we assess both the efficacy and safety of orally-administered OSU-A9 vis-à-vis two slightly modified agents in a series of preclinical studies carried out, in part, in preparation for prevention and regression trials in the transgenic adenocarcinoma of the mouse prostate (TRAMP) model. Histopathology and body and organ weight evaluations of mice treated in a dose-ranging study demonstrated additional advantages of OSU-A9 over indole-3-carbinol including an absence of toxicity up to 200 mg/kg/day and a lack of hepatic cytochrome P450 induction. When administered daily to PC-3 xenograft tumor-bearing nude mice and TRAMP-C2 tumor-bearing C57BL/6 mice at 25, 50, and 100 mg/kg, the drug achieved significant

suppressions of tumor growth in association with increased apoptosis and decreased proliferation. However, a dose-response was not observed. Methylated OSU-A9 demonstrated a therapeutic advantage in potency *in vitro* and *in vivo* in the absence of toxicity. An experimental diet formulated with this agent targeting a daily dose of 50 mg/kg suppressed the growth of PC-3 tumors by 60% ( $P < 0.05$ ) and increased the tumor-defined lifespan of the TRAMP-C2 tumor model by 77% ( $P < 0.01$ ). A pilot study with this diet validates its safe use in the TRAMP model whereby the drug's molecular and morphologic effects on the development of prostatic intraepithelial neoplasia and carcinoma will be assessed.

## **INTRODUCTION**

Prostate cancer is a molecularly heterogeneous disease second only to lung cancer in the cancer-related death of men in the United States (Society AC, 2008). Although fatal in advanced cases, a potential for successful intervention strategies is suggested by the high incidence of precursor lesions and age-dependent nature and environmental influence on disease progression (Shirai, 2008). Accordingly, the development of broadly-targeted agents capable of simultaneously combating an assortment of genomic and cellular aberrations that occur with the progression of prostate cancer is warranted. The phytochemical indole-3-carbinol has received much recent attention in this regard because of its pleiotropic anticancer effects, ability to inhibit the viability of various cancer cells *in vitro*, and ability to suppress carcinogenesis in animal studies (Chinni et al., 2001; He et al., 2000; Bradlow et al., 1991; Kojima et al., 1994).

Although the ability of indole-3-carbinol to target a broad spectrum of signaling pathways predicts favorably for cancer therapy and prevention, its chemical instability in an acidic milieu, unpredictable pharmacokinetic properties, and low *in vitro* antiproliferative potency limit its use in clinical settings (reviewed by Bradlow, 2008). Furthermore, oral use of indole-3-carbinol is associated with hepatocellular hypertrophy due to the induction of the cytochrome P450 enzymatic system, which has been linked with activation of the aryl hydrocarbon receptor and modulation of estrogen metabolism (Crowell et al., 2006; Yoshida et al., 2004). Collectively, these drawbacks create uncertainty in the potential clinical application of indole-3-carbinol.

Using indole-3-carbinol as a scaffold, we have developed a series of pleiotropic anticancer agents which retain the broad-spectrum of antitumor activity of the parental compound but with enhanced metabolic stability and two orders of magnitude greater potency in prostate cancer (Weng et al., 2007). Specifically, OSU-A9, the lead compound of our structural optimization efforts, regulates cell cycle and apoptosis at multiple levels through the modulation of intracellular kinase signaling, transcriptional activation of gene expression, cell cycle checkpoint control, mitochondrial integrity, and caspase activation (Weng et al., 2007).

Here, in a continued effort to further optimize the efficacy and pharmacokinetic features of OSU-A9, we report the synthesis of two slightly modified compounds with greater potency in suppressing prostate cancer cell viability and tumor growth: its fluorinated derivative OSU-A9F and methylated derivative OSU-A9M. Both the efficacy and safety of orally-administered OSU-A9 is evaluated vis-à-vis these slightly modified

agents in a series of preclinical studies carried out, in part, in preparation for prevention and regression trials in the transgenic adenocarcinoma of the mouse prostate (TRAMP) model. Our data demonstrate a therapeutic advantage of OSU-A9M in potency in both human and murine prostate cancer cell models that warrants the selection of this compound for continued development for prostate cancer prevention and therapy.

## **MATERIALS AND METHODS**

**Reagents.** Indole-3-carbinol and its derivative OSU-A9 were synthesized as described (Weng et al., 2007). Fluorinated OSU-A9 (OSU-A9F) and methylated OSU-A9 (OSU-A9M) were synthesized in our laboratory with purities exceeding 99% as shown by nuclear magnetic resonance spectroscopy (300 MHz), high-resolution mass spectrometry, and elemental analysis. For the treatment of cancer cells *in vitro*, stock solutions of these compounds were prepared in DMSO and diluted in culture medium with a < 0.1% final concentration of DMSO. For repeat gavage dosing of mice, the compounds were prepared as solutions in vehicle (0.5% methylcellulose w/v, 0.1% Tween 80 v/v, in sterile water) and administered at a constant volume of 10  $\mu$ L/g body weight. Rabbit polyclonal antibodies against Ki67 and cleaved caspase-3 were obtained from Cell Signaling Technology, Inc. (Beverly, MA). AIN-76A rodent diets with and without 450 ppm OSU-A9M were obtained from Research Diets, Inc. (New Brunswick, NJ).

**Cell culture.** Human PC-3 and murine TRAMP-C2 prostate cancer cell lines were purchased from the American Type Tissue Collection and cultured, respectively, in

RPMI 1640 or DMEM high glucose with L-glutamine and without sodium pyruvate media (Life Technologies, Inc., Grand Island, NY). The media were supplemented with 10% fetal bovine serum (Life Technologies).

**Cell viability analysis.** The 3-(4,5-dimethylthiazol-2-yl)-2,5-diphenyl-2H-tetrazolium bromide (MTT) assay was performed to measure the effect of test agents on cell viability as reported (Weng et al., 2007). Six to 12 replicates were used per data point with 8,000 PC-3 cells and 4,000 TRAMP-C2 cells seeded per well on 96-well plates.

**Animals.** For the OSU-A9 dose-ranging study, young adult male C57BL/6 mice were obtained from NCI (Frederick, MD) and randomly assigned to one of six indicated experimental groups (n = 3 per group). Mice were gavaged under isoflurane anesthesia with vehicle alone or OSU-A9 at 10, 25, 50, 100, or 200 mg/kg once daily in the morning.

For the PC-3 xenograft study, 5-7-week-old male NCr athymic nude mice were obtained from the NCI (Frederick, MD) and injected subcutaneously with PC-3 cells as described (Kulp et al., 2006). Beginning 14 days following inoculation, mice (n = 8 per group) were treated with vehicle alone or OSU-A9, OSU-A9F, or OSU-A9M at 25, 50, or 100 mg/kg/day. Subcutaneous tumors were measured weekly with calipers and volumes were calculated by the standard formula: length x width<sup>2</sup> x 0.52.

For the TRAMP-C2 syngeneic model, C57BL/6 mice were obtained as for the dose-ranging study above and inoculated subcutaneously in the right flank with  $5 \times 10^6$  TRAMP-C2 cells in a total volume of 0.1 mL serum-free medium containing 50%

Matrigel (BD Biosciences). Eight mice per group were treated with vehicle alone or OSU-A9, OSU-A9F, or OSU-A9M at 25, 50, or 100 mg/kg/day when tumors reached a volume of approximately 100 mm<sup>3</sup>. Treatment was continued until tumors reached an approximate volume of 2,000 mm<sup>3</sup>, thereby defining the lifespan of this model. For the PC-3 and TRAMP-C2 tumor studies involving OSU-A9M, an additional treatment group (n = 8) received OSU-A9M at 450 ppm in the diet. Mice in all other experimental groups in these OSU-A9M studies were fed an isocaloric control diet without drug.

TRAMP mice (C57BL/6TRAMPxFVB) were generated and housed as previously reported (Sargeant et al., 2007). To validate the safety of the experimental diet in this strain background prior to use in TRAMP mice, nontransgenic TRAMP littermates (n = 12 per group) were fed the AIN-76A diet with or without 450 ppm OSU-A9M from 18 through 24 weeks of age. Heparinized blood collected by intracardiac puncture at necropsy (n = 5 per group) was submitted to The Ohio State University Veterinary Clinical Laboratory Services for evaluation of serum chemistry (complete panel) and cell blood counts. Daily food consumption of mice receiving each diet was calculated as the g of food eaten per mouse per day. Body weights were measured once weekly in all studies except for the dose-ranging and OSU-A9 PC-3 xenograft studies in which mice were weighed twice weekly. All animal procedures were performed in accordance with protocols approved by the Institutional Animal Care and Use Committee of The Ohio State University.

**Histopathology and immunohistochemistry.** The entire carcass of each animal in all studies was evaluated for gross lesions and preserved in 10% formalin at necropsy.

PC-3 and TRAMP-C2 tumors were fixed overnight then processed into paraffin blocks by routine procedures. An extended set of tissues from animals in the OSU-A9 dose-ranging study was evaluated microscopically by a board-certified veterinary anatomic pathologist (A.S.) in accordance with Society of Toxicologic Pathology-proposed guidelines for repeat-dosing toxicity studies (Bregman et al., 2003), with the exception of spinal cord and female reproductive organs. Immunohistochemical detection of Ki67 and cleaved caspase-3 was performed on four  $\mu\text{M}$ -thick, paraffin-embedded PC-3 xenograft and TRAMP-C2 tumor sections by the manufacturers' recommendations.

**Statistical analysis.** A Student's *t*-test was used to determine if certain responses (immunohistochemistry results, subcutaneous tumor volumes and weights, diet consumption, hematologic parameters, and body and organ weights) were influenced by drug treatment.

## RESULTS

**OSU-A9 is well tolerated administered orally and does not induce the hepatic biotransformation enzymatic system.** In light of our plans to evaluate the ability of OSU-A9 to prevent prostate cancer long-term in transgenic mice, a dose-ranging study was carried out to identify appropriate doses of the drug that would not compromise body weight upon repeat oral exposure. Male C57BL/6 mice dosed by once daily gavage with vehicle alone or OSU-A9 at 10, 25, 50, 100, or 200 mg/kg permitted the evaluation of general toxicity in an immunocompetent system. Fig. 4.1 shows that none of these doses of OSU-A9 compromised body weight. The weights of 12 organs measured in select

groups were unchanged by drug treatment (Table 4.1), and no lesions were detected upon the histopathologic examination of all major organ systems. Considering that the parental compound indole-3-carbinol has been reported to cause centrilobular hepatocellular hypertrophy in association with the induction of Phase II drug-handling enzymes (Crowell et al., 2006), the normal morphology and weight of the OSU-A9-treated livers (Fig. 4.2) are especially noteworthy.

**Oral OSU-A9 achieves significant suppression of PC-3 xenograft and TRAMP-C2 tumor growth in association with decreased proliferation and increased apoptosis.** Having found an absence of dose-limiting toxicity in the dose-ranging study, we extended the use of OSU-A9 gavaged at 25, 50, and 100 mg/kg/day in a PC-3 xenograft tumor model to evaluate efficacy. Compared to vehicle-treated controls, the volume of subcutaneous PC-3 tumors was suppressed by 49% ( $P < 0.05$ ), 54% ( $P < 0.01$ ), and 55% ( $P < 0.01$ ), respectively, after 7 weeks of treatment at these doses (Fig. 4.3A). This effect on tumor growth was similarly reflected in the 42.9%, 42.3%, and 42.1% suppressions of the weights of the tumors dissected at necropsy ( $1.1 \pm 0.8$  g in controls vs.  $0.6 \pm 0.2$  g,  $0.6 \pm 0.1$  g, and  $0.6 \pm 0.1$  g at 25, 50, and 100 mg/kg, respectively; means  $\pm$  SEM). As expected from the dose-ranging study, treatment with these doses of OSU-A9 did not compromise body weight (Fig. 4.3B). Livers of all mice were weighed and examined microscopically to evaluate for cytochrome P450 induction in this longer treatment period. The drug treatment had no effect on the absolute or relative weights of the livers [ $1.1 \pm 0.2$  g ( $4.1 \pm 0.3\%$ ) in controls vs.  $1.3 \pm 0.2$  g ( $4.3 \pm 0.4\%$ ),  $1.1 \pm 0.1$  g ( $4.1 \pm 0.2\%$ ), and  $1.1 \pm 0.1$  g ( $4.1 \pm 0.2\%$ ) at 25, 50, and 100 mg/kg, respectively; liver

weight percent of body weight in parenthesis, means  $\pm$  SD, n = 8] and liver microscopic morphology was unchanged.

Next, to add predictive value to the drug's potency in the TRAMP model, and to measure drug efficacy in an immunocompetent system, a syngeneic model (C57BL/6 mice bearing subcutaneous TRAMP-C2 tumors) was similarly treated by once daily gavage. Compared to vehicle-treated control mice, OSU-A9 suppressed TRAMP-C2 tumor growth and increased the tumor-defined lifespan of the model by 48.1% ( $P < 0.01$ ), 48.2% ( $P < 0.01$ ), and 50.0% ( $P < 0.05$ ) at 25, 50, and 100 mg/kg/day (Fig. 4.4).

Since decreased cellular proliferation and increased apoptosis were found to be part of OSU-A9's broad spectrum of activity against prostate cancer (Weng et al., 2007), we measured hallmark indicators of these processes to correlate drug activity with tumor growth suppression. Specifically, immunohistochemistry performed on the PC-3 and TRAMP-C2 tumors showed decreased Ki67 and increased cleaved caspase-3 positivity in the drug-treated mice compared to controls (Fig. 4.5).

**Fluorinated OSU-A9 more potently suppresses PC-3 tumor growth but is less effective in the TRAMP-C2 model than OSU-A9.** Although OSU-A9 achieved significant tumor growth suppression in the PC-3 and TRAMP-C2 models, the suppressive effect was mild and without a dose-response relationship. Therefore, as part of a continued lead optimization effort, we repeated the two efficacy studies with a slightly modified (fluorinated) derivative of OSU-A9, OSU-A9F. We determined the *in vitro* potency with this agent against the viability of PC-3 and TRAMP-C2 cells to be similar to that of OSU-A9 (Fig. 6), which warranted its parallel investigation *in vivo*.

Following 44 days of treatment, OSU-A9F suppressed the volume of subcutaneous PC-3 tumors by 52.0% ( $P < 0.05$ ), 67.6% ( $P < 0.01$ ), and 60.7% ( $P < 0.01$ ) at 25, 50, and 100 mg/kg, respectively (Fig. 4.7A). As with OSU-A9, the body weights of OSU-A9F-treated mice were not affected. OSU-A9F was less potent than OSU-A9 in the suppression of tumor growth in the TRAMP-C2 syngeneic model, increasing the tumor-defined lifespan of mice treated with 25, 50, and 100 mg/kg by 15.0% ( $P = 0.3$ ), 32.5% ( $P < 0.05$ ), and 43.2% ( $P < 0.05$ ), respectively (Fig. 4.7B).

**Methylated OSU-A9 exhibits a therapeutic advantage in potency.** A methylated derivative of OSU-A9, OSU-A9M, exhibited greater potency than OSU-A9 and OSU-A9F against the viability of PC-3 and TRAMP-C2 cells *in vitro* (Fig. 4.6). Accordingly, as for OSU-A9F, the two prostate tumor model studies were repeated using OSU-A9M at 25, 50, and 100 mg/kg/day. After 7 weeks of treatment by gavage, OSU-A9M suppressed the volume of PC-3 tumor growth by 44.0%, 67.6%, and 71.0% (all  $P < 0.05$ ) at these doses (Fig. 4.8A). The tumor-defined lifespan of mice bearing subcutaneous TRAMP-C2 tumors was increased by 41.6%, 61.1%, and 67.2% (all  $P < 0.01$ ) at these doses compared to vehicle-treated controls (Fig. 4.8B).

Given the increased potency of OSU-A9M compared to the other lead derivatives, an experimental diet was formulated for the administration of this agent to TRAMP mice. Specifically, an AIN-76A rodent diet containing 450 ppm OSU-A9M was made to deliver approximately 50 mg/kg of drug per day to each mouse estimated by food consumption and body weight measurements. Because of assumed pharmacokinetic differences between gavage and diet-administered compound, a diet treatment group was

included in the efficacy studies to validate this method of drug delivery prior to use in the TRAMP model. Dietary OSU-A9M suppressed the growth of PC-3 xenograft tumors by 59.6% ( $P < 0.05$ ) and increased the lifespan of the TRAMP-C2 tumor model by 77.2% ( $P < 0.01$ ) compared to control mice fed an isocaloric diet lacking the drug (Fig. 4.8). The body weights of mice receiving the experimental diet were unchanged compared to controls.

**OSU-A9M administered at 450 ppm in the diet is well tolerated and without toxicity.** Given the promising effects of OSU-A9M against prostate cancer *in vitro* and *in vivo*, and the feasibility of administering the drug via diet, we selected this compound as our lead indole-3-carbinol derivative for use in the TRAMP model. In a final pilot study to confirm the safety of diet-administered OSU-A9 for use in this system, we administered the experimental diet to nontransgenic TRAMP littermates for 6 weeks and evaluated toxicologic endpoints while also estimating the drug dose that would be consumed by TRAMP mice.

Complete cell blood counts and serum chemistry profiles of mice fed the OSU-A9M diet shows that none of the measured parameters are affected by drug treatment (Table 4.2). Further supporting a lack of toxicity with the experimental diet is a preservation of body weight (Fig. 4.9) and liver weight of mice sacrificed at the conclusion of the 6-week treatment period [ $1.3 \pm 0.1$  g ( $3.9 \pm 0.5\%$ ) in drug-treated mice vs.  $1.5 \pm 0.3$  g ( $4.3 \pm 0.7\%$ ) in controls; liver percent body weight in parentheses following absolute weight, means  $\pm$  SD,  $n = 7$ ,  $P = 0.1$  and  $0.5$  for absolute and relative values]. There was no significant difference in the amount of control or experimental diet consumed by the mice

[ $2.4 \pm 0.3$  g in drug-treated mice vs.  $2.5 \pm 0.1$  g in controls ( $P = 0.5$ )]. Throughout the treatment period, the drug-treated mice consumed  $34.1 \pm 4.6$  mg OSU-A9M per kg body weight per day, calculated as g diet consumed per day/ g body weight x 450 (overall mean  $\pm$  SD of weekly means).

## DISCUSSION

Tumorigenesis is a multifactorial process involving genetic, epigenetic, and cellular changes that result in unbalanced proliferation, differentiation, and death of cells. Mechanistically, the ability of indole-3-carbinol to concomitantly target clinically relevant cellular abnormalities provides the basis for (i) its clinical investigation in prostate cancer, and (ii) our structural optimization efforts that have culminated in the OSU-A9 series of compounds. In the present study, we demonstrate the safety and tumor-suppressive efficacy of orally-administered OSU-A9 while also identifying an optimized agent (OSU-A9M) exhibiting increased anti-tumor potency, and flexibility in its delivery method *in vivo*.

We previously reported that OSU-A9 administered intraperitoneally at 10 and 25 mg/kg/day was without toxicity in nude mice with the exception of intra-abdominal fibrous adhesions that formed subsequent to repeated drug exposure (Weng et al., 2007). Since oral administration was the preferred route of drug delivery for our continued preclinical work, a dose-ranging study was performed and showed that OSU-A9, within our selected dose range, is without a dose-associated compromise of body weight or general health of mice. This lack of an observable effect up to 200 mg/kg/day is an

improvement over indole-3-carbinol, which has been shown to cause toxic responses at this approximate dose (Crowell et al., 2006). While we presume that some type of toxicity would eventually occur with escalating doses, the lack of any adverse effect at the therapeutic doses used here is not typical of novel pleiotropic anticancer agents in our experience. This observation predicts a high therapeutic index that would be advantageous in the clinical use of this series of compounds. Not surprisingly, OSU-A9 has been shown to be less toxic to normal human prostate epithelial cells relative to cancer cells *in vitro* (Weng et al., 2007).

The lack of changes typical of drug-handling enzyme induction in the liver by OSU-A9 is noteworthy. As a cancer preventive agent, the safe use of the parental compound has been controversial (Stoner et al., 2002), in part due to Phase II enzyme induction in the liver (Yoshida et al., 2004). Hepatic cytochrome P450 induction by indole-3-carbinol, for example, has been associated with modulated estrogen metabolism and the development of endometrial adenocarcinoma in rats (Yoshida et al., 2004). Our work shows that OSU-A9 retains the anticancer properties of indole-3-carbinol but with improved potency and metabolic properties and without this potential clinical obstacle.

To shed light onto the tumor-suppressive ability of orally-administered OSU-A9 and its slightly modified derivatives with relevance to both the TRAMP model and humans, the 3 compounds were tested in parallel in tumor models involving human PC-3 and murine TRAMP-C2 prostate cancer cell lines. Correlating with increased potency against the viability of these cell lines *in vitro*, OSU-A9M demonstrated a more potent suppression of tumor growth in both models in the absence of toxicity. The exact reason

for the increased potency of OSU-A9M over OSU-A9 and the fluorinated derivative is uncertain, but, given its improvement both *in vitro* and *in vivo*, is presumably not solely attributable to enhanced pharmacokinetic features of the drug. Importantly, we show here that dietary administration of OSU-A9M achieves similar efficacy and safety as gavage administration of the agent, which suggests a desirable pharmacokinetic feature and flexibility in its delivery method.

In summary, by optimizing the structure of indole-3-carbinol, we have developed more clinically relevant compounds which retain the broad-spectrum of anticancer activity with higher *in vivo* efficacy, improved safety, and enhanced metabolic stability. In light of the molecular heterogeneity of prostate cancer, these pleiotropic antitumor agents are hypothesized to optimize therapeutic outcomes, either as monotherapies or in combination with other agents. OSU-A9M has emerged as the lead compound from our series of studies completed in *in vitro* and *in vivo* models involving cell lines derived from both human and murine prostate cancer. Having confirmed the safety and efficacy of dietary OSU-A9M, our ongoing work is to evaluate this experimental diet in the TRAMP model for the drug's molecular and morphologic effects on the development of prostatic intraepithelial neoplasia and carcinoma, as we have done previously with other agents (Sargeant et al., 2007, Sargeant et al., 2008). Results of these studies will provide greater insight into the compound's clinical value in prostate cancer therapy and prevention.

## LIST OF REFERENCES

- Crowell JA, Page JG, Levine BS, Tomlinson MJ, and Hebert CD. Indole-3-carbinol, but not its major digestive product 3,3'-diindolylmethane, induces reversible hepatocyte hypertrophy and cytochrome P450. *Toxicol Appl Pharmacol* 2006;211:115-123.
- Bradlow HL. Review. Indole-3-carbinol as a chemopreventive agent in breast and prostate cancer. *In Vivo* 2008;22:441-5.
- Bradlow HL, Michnovicz J, Telang NT, et al. Effects of dietary indole-3-carbinol on estradiol metabolism and spontaneous mammary tumors in mice. *Carcinogenesis* 1991;12:1571-4
- Bregman CL, Adler RR, Morton DG, et al. Recommended tissue list for histopathologic examination in repeat-dose toxicity and carcinogenicity studies: a proposal of the Society of Toxicologic Pathology (STP). *Toxicol Pathol* 2003;31:252-3.
- Chinni S, Li Y, Upadhyay S, Koppolu P, and Sarkar F. Indole-3-carbinol (I3C) induced cell growth inhibition, G1 cell cycle arrest and apoptosis in prostate cancer cells. *Oncogene* 2001;20:2927-36.
- He YH, Friesen MD, Ruch RJ, et al. Indole-3-carbinol as a chemopreventive agent in 2-amino-1-methyl-6-phenyl-imidazol [4,5-*b*] pyridine (PhIP) carcinogenesis: inhibition of PhIP-DNA adduct formation, acceleration of PhIP metabolism, and induction of cytochrome P450 in female F344 rats. *Food Chem Toxicol* 2000;38:15-23.
- Kojima T, Tanaka T, Mori H. Chemoprevention of spontaneous endometrial cancer in female Donryu rats by dietary indole-3-carbinol. *Cancer Res* 1994;54:1446-9.
- Kulp SK, Chen CS, Wang D, Chen CY, and Chen CS. Antitumor effects of a novel phenylbutyrate-based histone deacetylase inhibitor, (*S*)-HDAC-42, in prostate cancer. *Clin Cancer Res* 2006;12:5199-5206.
- Nachshon-Kedmi M, Fares F, and Yannai S. Therapeutic activity of 3,3'-diindolylmethane on prostate cancer in an in vivo model. *The Prostate* 2004;61:153-160.
- Sargeant AM, Klein RD, Rengel RC, et al. Chemopreventive and bioenergetic signaling effects of PDK1/Akt pathway inhibition in a transgenic mouse model of prostate cancer. *Toxicol Pathol* 2007;35:549-61.
- Sargeant AM, Rengel RC, Kulp SK, Klein RD, Clinton SK, Wang YC, and Chen CS. OSU-HDAC42, a histone deacetylase inhibitor, blocks prostate tumor progression in the transgenic adenocarcinoma of the mouse prostate model. *Cancer Res*

- 2008;68:3999-4009.
- Shirai T. Significance of chemoprevention for prostate cancer development: Experimental *in vivo* approaches to chemoprevention. *Pathol Int* 2008;58:1-16.
- Society AC. Cancer facts and figures 2007. Available at <http://www.cancer.org/>. 2008;10.
- Souli E, Machluf M, Morgenstern A, Sabo E, and Yannai S. Indole-3-carbinol (I3C) exhibits inhibitory and preventive effects on prostate tumors in mice. *Food Chem Toxicol* 2008;46:863-870.
- Stoner G, Casto B, Ralston S, Roebuck B, Periera C, and Bailey G. Development of a multi-organ rat model for evaluating chemopreventive agents: efficacy of indole-3-carbinol. *Carcinogenesis* 2002;23:265-72.
- Weng JR, Tsai CH, Kulp S, Wang D, Lin CH, Yang HC, Ma Y, Sargeant A, Chiu CF, Tsai MH, and Chen CS. A potent indole-3-carbinol-derived antitumor agent with pleiotropic effects on multiple signaling pathways in prostate cancer cells. *Cancer Res* 2007;67:7815-24.
- Yoshida M, Katashima S, Ando J, Tanaka T, Uematsu F, Nakae D, and Mackawa A, Dietary indole-3-carbinol promotes endometrial adenocarcinoma development in rats initiated with *N*-ethyl-*N'*-nitro-*N*-nitrosoguanidine, with induction of cytochrome P450s in the liver and consequent modulation of estrogen metabolism. *Carcinogenesis* 2004;25:2257-2264.

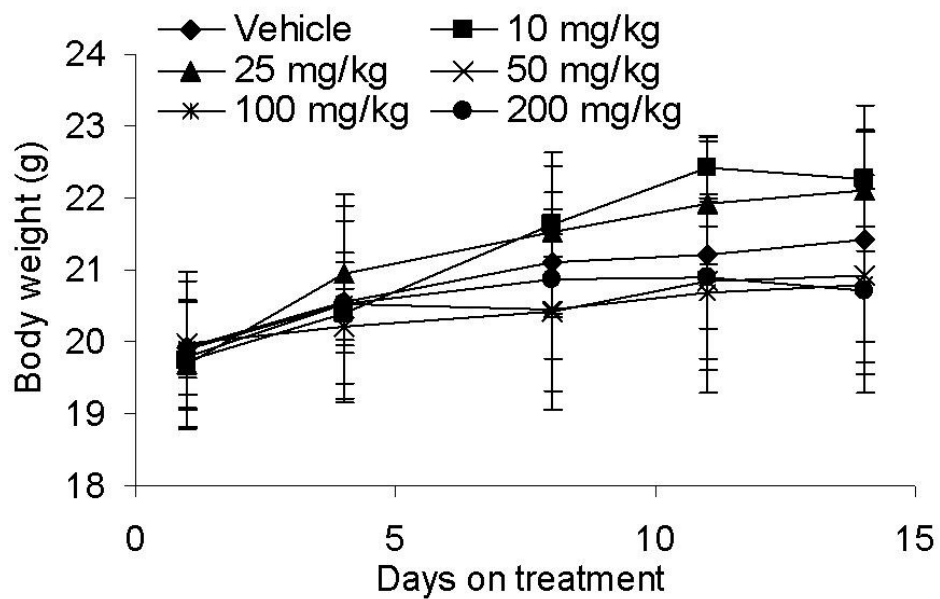


Figure 4.1: A dose-ranging study shows that OSU-A9 does not compromise body weight when administered up to 200 mg/kg for 14 days by once daily gavage. Data points represent means  $\pm$  SE of body weights measured twice weekly.

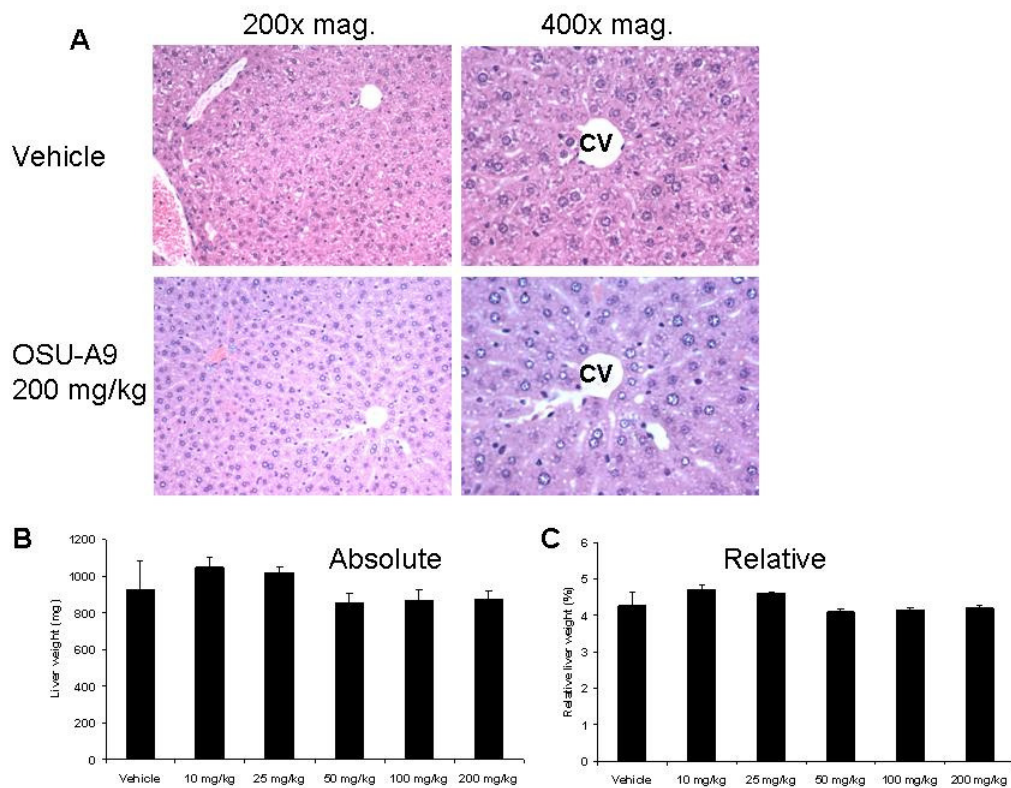


Figure 4.2: OSU-A9 does not affect liver weight or morphology after repeat oral dosing. C57BL/6 mice were treated for 14 days by once daily gavage in a dose-ranging study ranging from 10 to 200 mg/kg. There is no evidence of zone 3 hepatocellular hypertrophy by H&E staining of the liver (A), nor is there an effect on the absolute (B) or relative (C) weights of the drug-treated livers compared to vehicle-treated controls. Data points represent means  $\pm$  SD.

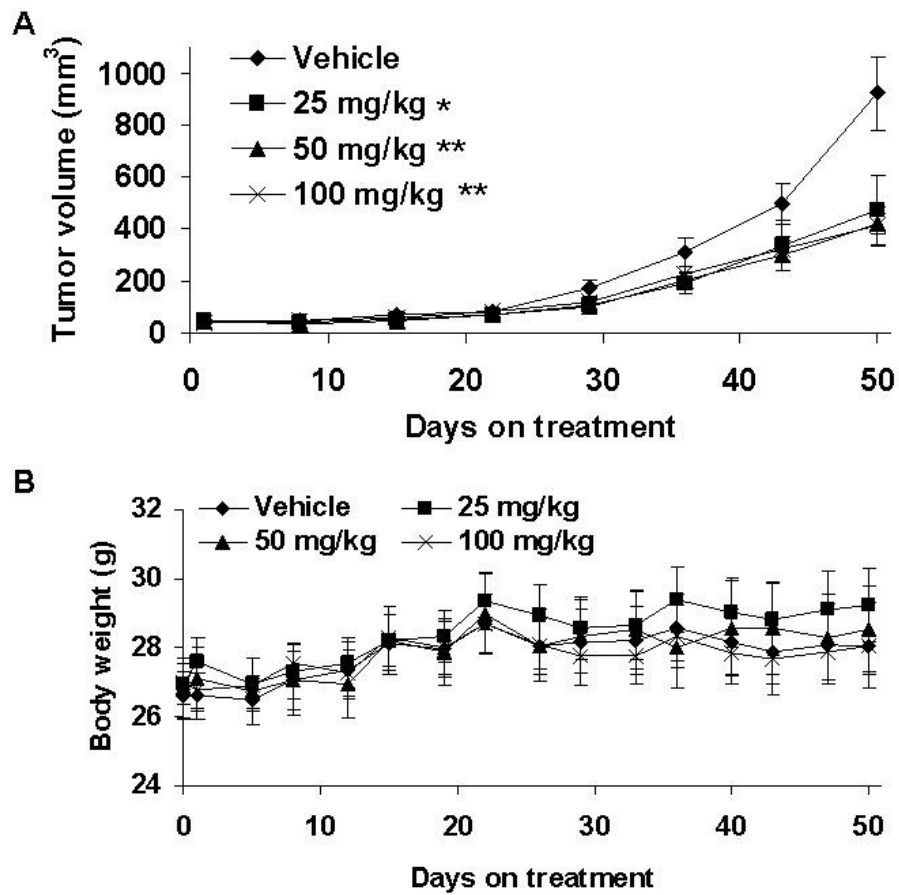


Figure 4.3: OSU-A9 administered by gavage at 25, 50, and 100 mg/kg/day achieved statistically significant suppressions of PC-3 tumor growth compared to vehicle alone. Tumor volumes in *A* show that a dose-response relationship is lacking beyond 25 mg/kg. Statistical analysis was performed on the final tumor volumes. Body weights (*B*) of mice measured twice weekly were not affected by drug treatment at these doses. Data points represent means  $\pm$  SE. \*  $P < 0.05$ , \*\*  $P < 0.01$ .

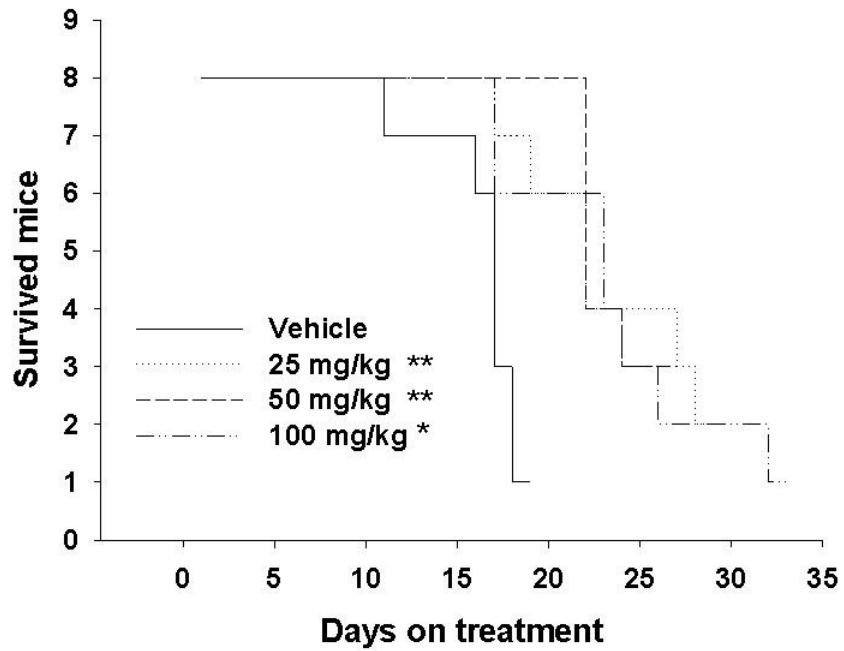


Figure 4.4: OSU-A9 prolongs the tumor-defined lifespan of a syngeneic mouse model of prostate cancer (C57BL/6 mice bearing subcutaneous TRAMP-C2 tumors). Days on treatment indicates the number of days that mice received drug treatment until tumors reached an approximate volume of 2,000 mm<sup>3</sup>. \* P < 0.05, \*\* P < 0.01.

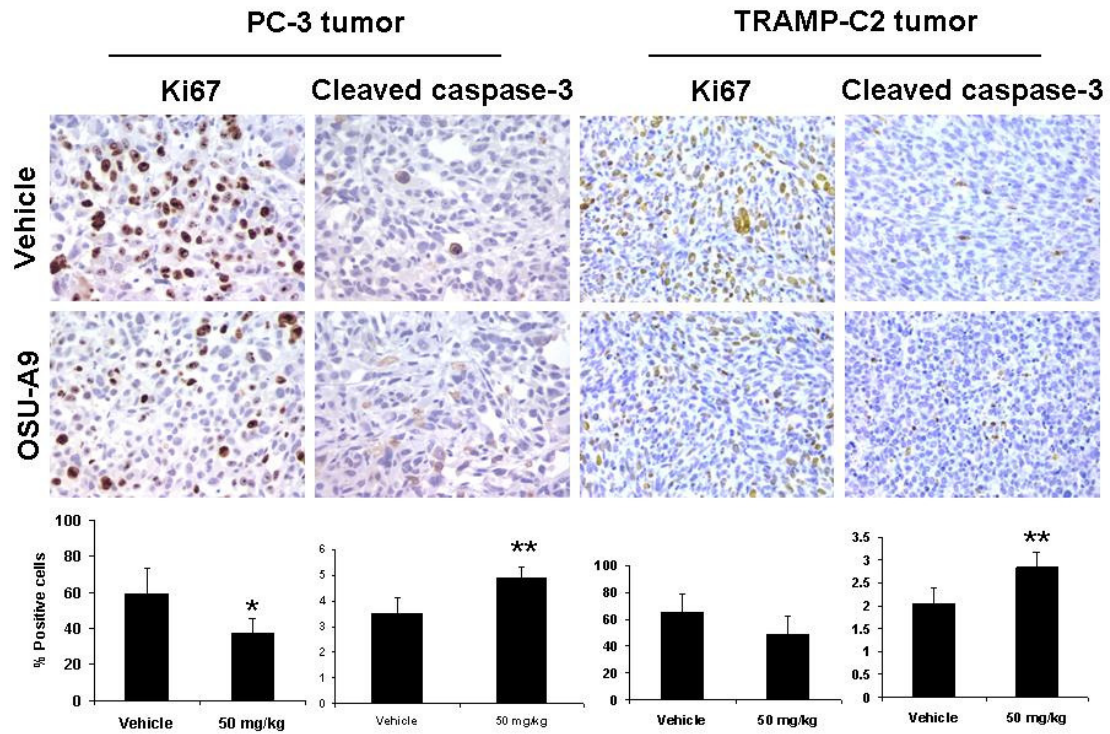


Figure 4.5: The suppression of PC-3 and TRAMP-C2 tumor growth by OSU-A9 is associated with decreased proliferation and increased apoptosis, indicated by Ki67 and cleaved caspase-3 immunostaining, respectively, of the tumors. Bar graphs indicate the percentage of positive-staining tumor cells counted in 5 randomly chosen 400x fields. \* P < 0.05, \*\* P < 0.01.

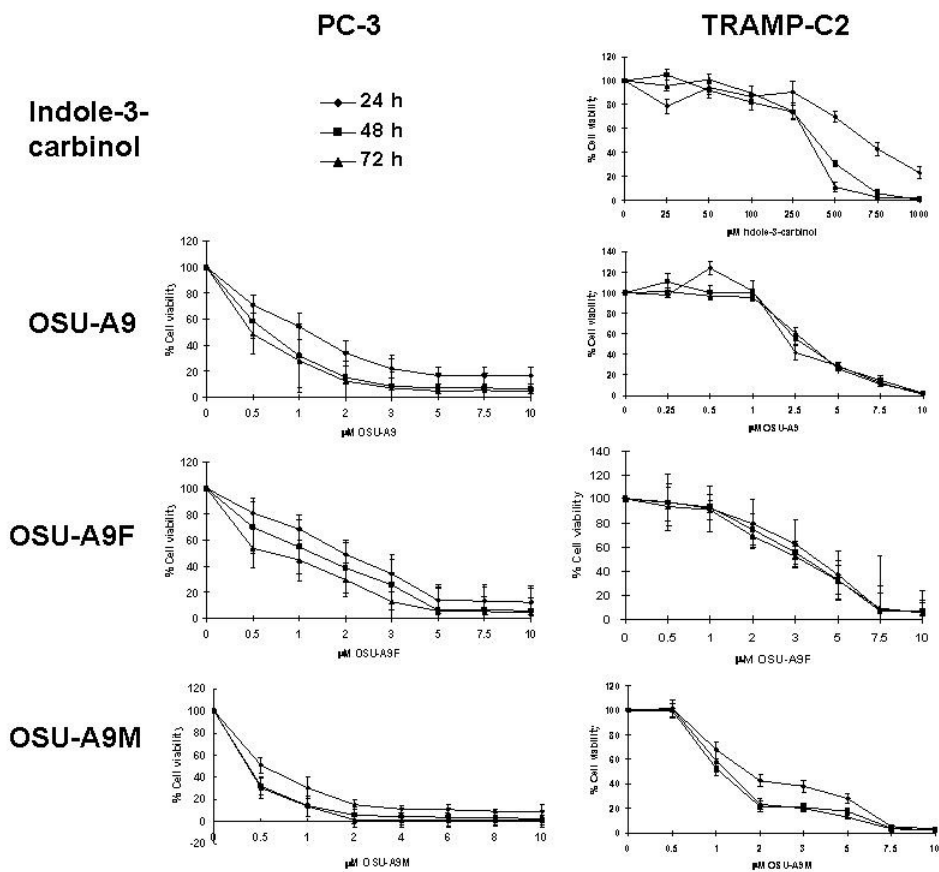


Figure 4.6. Dose and time-course effects of OSU-A9, OSU-A9F, and OSU-A9M vs. indole-3-carbinol on the viability of human PC-3 and murine TRAMP-C2 prostate cancer cells. MTT assay. Data points represent means  $\pm$  SD, n = 6-12.

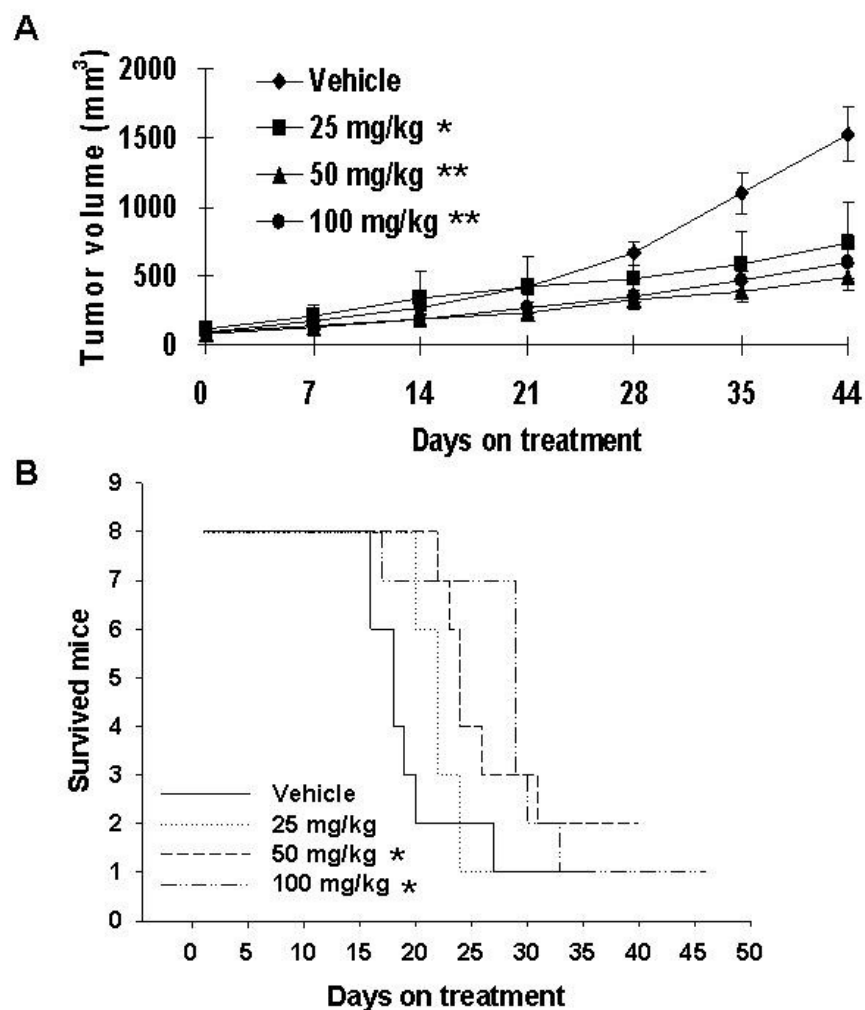


Figure 4.7: Fluorinated OSU-A9 (OSU-A9F) suppresses the growth of PC-3 xenograft tumors (A) and prolongs the tumor-defined lifespan of the TRAMP-C2 syngeneic mouse model (B). Mice received treatment by daily oral gavage for 6 weeks in A. Statistical analysis was performed on the final tumor volume. Data points represent means  $\pm$  SE. Days on treatment in B indicates the number of days that mice received drug treatment until tumors reached an approximate volume of 2,000 mm<sup>3</sup>. \* P < 0.05, \*\* P < 0.01.

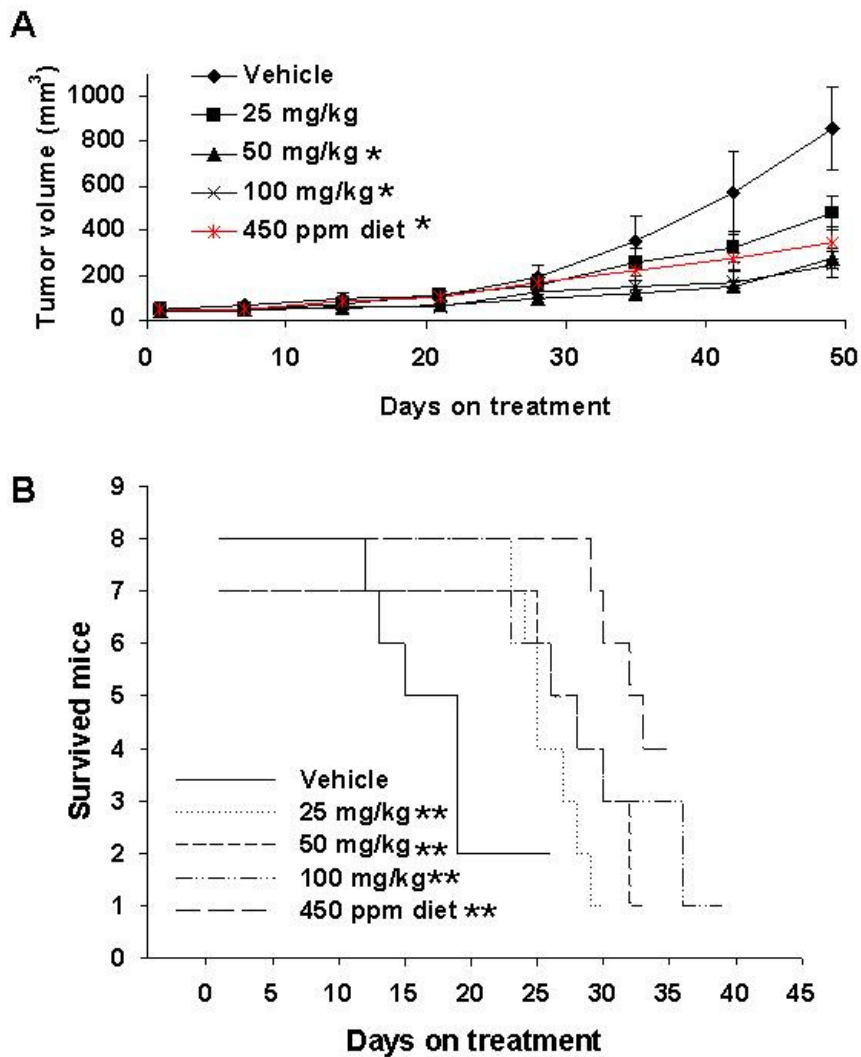


Figure 4.8: Methyated OSU-A9 (OSU-A9M) suppresses the growth of PC-3 xenograft tumors and prolongs the tumor-defined lifespan of the TRAMP-C2 syngeneic mouse model. Mice received treatment by daily oral gavage or a diet containing 450 ppm as indicated for 7 weeks in *A*. Statistical analysis was performed on the final tumor volume. Data points represent means  $\pm$  SE. Days on treatment in *B* indicates the number of days that mice received drug treatment until tumors reached an approximate volume of 2,000 mm<sup>3</sup>. \*  $P < 0.05$ , \*\*  $P < 0.01$ .

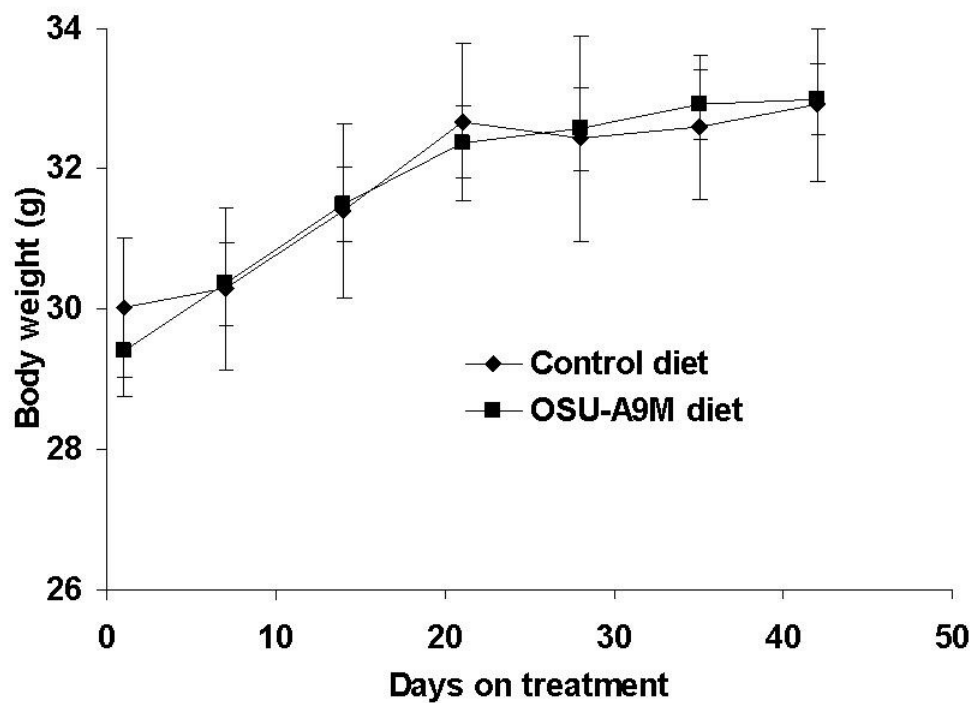


Figure 4.9: OSU-A9M administered at 450 ppm in the diet is well tolerated by the TRAMP model. Nontransgenic male TRAMP littermates (C57BL/6xFVB) were fed an AIN-76A diet with or without 450 ppm OSU-A9M from 18 to 24 weeks of age. Data points represent means  $\pm$  SE of body weights measured once weekly.

Organ	Vehicle control	50 mg/kg	200 mg/kg
Adrenal glands (mg)	4.1 ± 0.4 (0.0 ± 0.0)	4.2 ± 0.4 (0.0 ± 0.0)	3.4 ± 1.2 (0.0 ± 0.0)
Brain (mg)	437.6 ± 20.3 (2.1 ± 0.2)	449.5 ± 14.6 (2.2 ± 0.1)	433.6 ± 4.1 (2.1 ± 0.1)
Epididymides (mg)	53.0 ± 15.2 (0.2 ± 0.0)	47.9 ± 5.9 (0.2 ± 0.0)	48.4 ± 5.5 (0.2 ± 0.0)
Epididymal fat pad (mg)	275.0 ± 105.9 (1.3 ± 0.5)	328.9 ± 87.2 (1.6 ± 0.3)	264.7 ± 84.8 (1.3 ± 0.4)
Heart (mg)	111.1 ± 16.7 (0.5 ± 0.1)	112.9 ± 10.5 (0.5 ± 0.0)	114.7 ± 5.4 (0.5 ± 0.0)
Kidneys (mg)	289.1 ± 28.0 (1.3 ± 0.1)	267.7 ± 40.8 (1.3 ± 0.1)	257.0 ± 23.2 (1.2 ± 0.0)
Liver (mg)	928.6 ± 272.9 (4.3 ± 0.6)	855.5 ± 79.0 (4.1 ± 0.1)	870.4 ± 78.1 (4.2 ± 0.1)
Pituitary gland (mg)	1.2 ± 0.2 (0.0 ± 0.0)	1.6 ± 0.3 (0.0 ± 0.0)	1.7 ± 0.4 (0.0 ± 0.0)
Spleen (mg)	54.1 ± 6.4 (0.2 ± 0.0)	44.9 ± 5.1 (0.2 ± 0.0)	47.9 ± 4.3 (0.2 ± 0.0)
Testes (mg)	145.7 ± 6.6 (0.7 ± 0.1)	143.5 ± 14.8 (0.7 ± 0.1)	131.8 ± 2.3 (0.6 ± 0.0)
Thymus (mg)	46.8 ± 18.4 (0.2 ± 0.1)	45.9 ± 7.5 (0.2 ± 0.0)	47.6 ± 11.3 (0.2 ± 0.0)
Urogenital tract (mg)	176.7 ± 13.0 (0.8 ± 0.1)	188.8 ± 42.4 (0.9 ± 0.1)	180.5 ± 6.8 (0.9 ± 0.0)

<sup>a</sup>values represent means ± SD (n = 3); relative values are indicated in parentheses after the absolute weights and represent percentages calculated as organ weight/body weight x 100; paired organs were weighed together and evaluations were performed in accordance with guidelines proposed by Sellers RS, Morton D, Michael B, Roome N, Johnson JK, Yano BL, Perry R, Schafer K. Society of Toxicologic Pathology position paper: organ weight recommendations for toxicology studies. *Toxicol Pathol.* 2007;35(5):751-5.

Table 4.1: Absolute and relative organ weight values<sup>a</sup> of C57BL/6 mice treated for 14 days with OSU-A9 by once daily gavage.

<b>Hematology</b>	Control diet	OSU-A9M 450 ppm
PCV (%)	47.0 ± 2.4	44.4 ± 1.1
RBC (x 10 <sup>6</sup> /μl)	10.9 ± 0.5	10.3 ± 0.3
Nucleated cells (x 10 <sup>3</sup> /μl)	9.8 ± 3.2	11.4 ± 3.7
Segmented neutrophils (x 10 <sup>3</sup> /μl)	1.2 ± 0.3	1.3 ± 0.5
Lymphocytes (x 10 <sup>3</sup> /μl)	8.2 ± 2.8	9.8 ± 3.1
Platelets (x 10 <sup>3</sup> /μl)	101.5 ± 53.8	327.2 ± 310.0
<b>Serum Chemistry</b>		
BUN (mg/dl)	24.0 ± 3.0	23.6 ± 2.9
Creatinine (mg/dl)	0.1 ± 0.0	0.1 ± 0.0
Phosphorus (mg/dl)	7.0 ± 0.6	6.5 ± 0.5
Calcium (mg/dl)	10.8 ± 0.4	10.7 ± 0.2
Potassium (mEq/L)	7.3 ± 0.7	6.9 ± 0.4
ALT (iu/L)	28.8 ± 12.1	25.8 ± 8.0
AST (iu/L)	74.6 ± 25.1	69.6 ± 27.2
ALP (iu/L)	69.0 ± 8.4	70.0 ± 14.6
CK (iu/L)	173.6 ± 153.4	222.2 ± 144.5
Cholesterol (mg/dl)	212.0 ± 33.0	193.4 ± 28.1
Total Bilirubin (mg/dl)	0.2 ± 0.0	0.2 ± 0.0
Total Protein (g/dl)	6.2 ± 0.5	5.8 ± 0.3
Albumin (g/dl)	3.9 ± 0.2	3.6 ± 0.2
Globulin (g/dl)	2.3 ± 0.3	2.2 ± 0.1
Glucose (mg/dl)	251.2 ± 46.4	301.8 ± 53.6

<sup>a</sup>values represent means ± SD (n = 5)

<sup>b</sup>C57BL/6xFVB

PCV, packed cell volume; RBC, red blood cells; BUN, blood urea nitrogen; ALT, alanine aminotransferase; AST, aspartate aminotransferase; ALP, alkaline phosphatase; CK, creatine kinase

Table 4.2: Hematology and serum chemistry values<sup>a</sup> of nontransgenic male littermates<sup>b</sup> of TRAMP mice fed an AIN-76A rodent diet with or without 450 ppm OSU-A9M from 18 to 24 weeks of age.

## BIBLIOGRAPHY

- Abate-Shen, C. and Shen, M. M. (2002). Mouse models of prostate carcinogenesis. *Trends Genet* 18(5), S1-5.
- Almenara, J., Rosato, R., and Grant, S., Synergistic induction of mitochondrial damage and apoptosis in human leukemia cells by flavopiridol and the histone deacetylase inhibitor suberoylanilide hydroxamic acid (saha), *Leukemia* 16 (7), 1331-43, 2002.
- Arce, C., Perez-Plasencia, C., Gonzalez-Fierro, A. et al., A proof-of-principle study of epigenetic therapy added to neoadjuvant doxorubicin cyclophosphamide for locally advanced breast cancer, *PLoS ONE* 1, e98, 2006.
- Atadja, P., Hsu, M., Kwon, P. et al., Molecular and cellular basis for the anti-proliferative effects of the hdac inhibitor laq824, *Novartis Found Symp* 259, 249-66; discussion 266-8, 285-8, 2004.
- Bali, P., Pranpat, M., Swaby, R. et al., Activity of suberoylanilide hydroxamic acid against human breast cancer cells with amplification of her-2, *Clin Cancer Res* 11 (17), 6382-9, 2005.
- Barnes, P. J., Reduced histone deacetylase in copd: Clinical implications, *Chest* 129 (1), 151-5, 2006.
- Bhalla, K. N., Epigenetic and chromatin modifiers as targeted therapy of hematologic malignancies, *J Clin Oncol* 23 (17), 3971-93, 2005.
- Bodine S. C., Stitt, T. N., Gonzalez, M., Kline, W. O., Stover, G. L., Bauerlein, R., Zlotchenko, E., Scrimgeour, A., Lawrence, J. C., Glass, D. J., and Yancopoulos, G. D. (2001). Akt/mTOR pathway is a crucial regulator of skeletal muscle hypertrophy and can prevent atrophy *in vivo*. *Nat Cell Biol* 3, 1014-1019.
- Bolden, J. E., Peart, M. J., and Johnstone, R. W., Anticancer activities of histone deacetylase inhibitors, *Nat Rev Drug Discov* 5 (9), 769-84, 2006.

Bolon, B. (2004). Genetically engineered animals in drug discovery and development: a maturing resource for toxicologic research. *Basic Clin Pharmacol Toxicol* 95(4), 154-61.

Bonaldi, T., Talamo, F., Scaffidi, P. et al., Monocytic cells hyperacetylate chromatin protein hmgb1 to redirect it towards secretion, *Embo J* 22 (20), 5551-60, 2003.

Boone L, Meyer D, Cusick P, et al. Selection and interpretation of clinical pathology indicators of hepatic injury in preclinical studies. *Vet Clin Pathol* 2005;34:182-8.

Bouras, T., Fu, M., Sauve, A. A. et al., Sirt1 deacetylation and repression of p300 involves lysine residues 1020/1024 within the cell cycle regulatory domain 1, *J Biol Chem* 280 (11), 10264-76, 2005.

Bradbury, C. A., Khanim, F. L., Hayden, R. et al., Histone deacetylases in acute myeloid leukaemia show a distinctive pattern of expression that changes selectively in response to deacetylase inhibitors, *Leukemia* 19 (10), 1751-9, 2005.

Bradlow HL. Review. Indole-3-carbinol as a chemopreventive agent in breast and prostate cancer. *In Vivo* 2008;22:441-5.

Bradlow HL, Michnovicz J, Telang NT, et al. Effects of dietary indole-3-carbinol on estradiol metabolism and spontaneous mammary tumors in mice. *Carcinogenesis* 1991;12:1571-4.

Bregman CL, Adler RR, Morton DG, et al. Recommended tissue list for histopathologic examination in repeat-dose toxicity and carcinogenicity studies: a proposal of the Society of Toxicologic Pathology (STP). *Toxicol Pathol* 2003;31:252-3.

Brehm, A., Miska, E. A., McCance, D. J. et al., Retinoblastoma protein recruits histone deacetylase to repress transcription, *Nature* 391 (6667), 597-601, 1998.

Brush, M. H., Guardiola, A., Connor, J. H. et al., Deactylase inhibitors disrupt cellular complexes containing protein phosphatases and deacetylases, *J Biol Chem* 279 (9), 7685-91, 2004.

Cameron, E. E., Bachman, K. E., Myohanen, S. et al., Synergy of demethylation and histone deacetylase inhibition in the re-expression of genes silenced in cancer, *Nat Genet* 21 (1), 103-7, 1999.

Camphausen, K., Scott, T., Sproull, M. et al., Enhancement of xenograft tumor radiosensitivity by the histone deacetylase inhibitor ms-275 and correlation with histone hyperacetylation, *Clin Cancer Res* 10 (18 Pt 1), 6066-71, 2004.

Canettieri, G., Morantte, I., Guzman, E. et al., Attenuation of a phosphorylation-

dependent activator by an hdac-pp1 complex, *Nat Struct Biol* 10 (3), 175-81, 2003.

Catley, L., Weisberg, E., Kiziltepe, T. et al., Aggresome induction by proteasome inhibitor bortezomib and alpha-tubulin hyperacetylation by tubulin deacetylase (tdac) inhibitor lbh589 are synergistic in myeloma cells, *Blood* 108 (10), 3441-9, 2006.

Chen, C. S., Wang, Y. C., Yang, H. C. et al., Histone deacetylase inhibitors sensitize prostate cancer cells to agents that produce DNA double-strand breaks by targeting ku70 acetylation, *Cancer Res* 67 (11), 5318-27, 2007.

Chen, C. S., Weng, S. C., Tseng, P. H. et al., Histone acetylation-independent effect of histone deacetylase inhibitors on akt through the reshuffling of protein phosphatase 1 complexes, *J Biol Chem* 280 (46), 38879-87, 2005.

Chen, L. F. and Greene, W. C., Shaping the nuclear action of nf-kappab, *Nat Rev Mol Cell Biol* 5 (5), 392-401, 2004.

Chen, L., Meng, S., Wang, H. et al., Chemical ablation of androgen receptor in prostate cancer cells by the histone deacetylase inhibitor laq824, *Mol Cancer Ther* 4 (9), 1311-9, 2005.

Chinni S, Li Y, Upadhyay S, Koppolu P, and Sarkar F. Indole-3-carbinol (I3C) induced cell growth inhibition, G1 cell cycle arrest and apoptosis in prostate cancer cells. *Oncogene* 2001;20:2927-36.

Cho, H. H., Park, H. T., Kim, Y. J. et al., Induction of osteogenic differentiation of human mesenchymal stem cells by histone deacetylase inhibitors, *J Cell Biochem* 96 (3), 533-42, 2005.

Clark LC and Marshall JR Randomized, controlled chemoprevention trials in populations at very high risk for prostate cancer: Elevated prostate-specific antigen and high-grade prostatic intraepithelial neoplasia. *Urology* 2001;57:185-7.

Cohen, H. Y., Lavu, S., Bitterman, K. J. et al., Acetylation of the c terminus of ku70 by cbp and pcaf controls bax-mediated apoptosis, *Mol Cell* 13 (5), 627-38, 2004.

Cohen, H. Y., Miller, C., Bitterman, K. J. et al., Calorie restriction promotes mammalian cell survival by inducing the sirt1 deacetylase, *Science* 305 (5682), 390-2, 2004.

Crawford ED Epidemiology of prostate cancer. *Urology* 2003;62:3-12.

Cross, D. A., Alessi, D. R., Cohen, P., Andjelkovich, M., Hemmings, B. A. (1995). Inhibition of glycogen synthase kinase-3 by insulin mediated by protein kinase B. *Nature* 378(6559): 785-9.

Crowell JA, Page JG, Levine BS, Tomlinson MJ, and Hebert CD. Indole-3-carbinol, but not its major digestive product 3,3'-diindolylmethane, induces reversible hepatocyte hypertrophy and cytochrome P450. *Toxicol Appl Pharmacol* 2006;211:115-123.

Darnell, J. E., Jr., Stats and gene regulation, *Science* 277 (5332), 1630-5, 1997.

Dashwood, R. H., Myzak, M. C., and Ho, E., Dietary hdac inhibitors: Time to rethink weak ligands in cancer chemoprevention?, *Carcinogenesis* 27 (2), 344-9, 2006.

Dehmel, F., Ciossek, T., Maier, T. et al., Trithiocarbonates-exploration of a new head group for hdac inhibitors, *Bioorg Med Chem Lett* 17 (17), 4746-52, 2007.

Deng, G., Bell, I., Crawley, S. et al., Braf mutation is frequently present in sporadic colorectal cancer with methylated hmlh1, but not in hereditary nonpolyposis colorectal cancer, *Clin Cancer Res* 10 (1 Pt 1), 191-5, 2004.

Draeger, A., Monastyrskaya, K., Mohaupt, M., Hoppeler, H., Savolainen, H., Allemann, C., Babiychuk, E. B. (2006). Statin therapy induces ultrastructural damage in skeletal muscle in patients without myalgia. *J Pathol* 210(1), 94-102.

Drummond, D. C., Noble, C. O., Kirpotin, D. B. et al., Clinical development of histone deacetylase inhibitors as anticancer agents, *Annu Rev Pharmacol Toxicol* 45, 495-528, 2005.

Drysdale, M. J., Brough, P. A., Massey, A. et al., Targeting hsp90 for the treatment of cancer, *Curr Opin Drug Discov Devel* 9 (4), 483-95, 2006.

Duan, J., Friedman, J., Nottingham, L. et al., Nuclear factor-kappab p65 small interfering rna or proteasome inhibitor bortezomib sensitizes head and neck squamous cell carcinomas to classic histone deacetylase inhibitors and novel histone deacetylase inhibitor pxd101, *Mol Cancer Ther* 6 (1), 37-50, 2007.

Edwards, J., Krishna, N. S., Witton, C. J., and Bartlett, J. M. (2003). Gene amplifications associated with the development of hormone-resistant prostate cancer. *Clin Cancer Res* 9(14), 5271-81.

Eikel, D., Hoffmann, K., Zoll, K. et al., S-2-pentyl-4-pentynoic hydroxamic acid and its metabolite s-2-pentyl-4-pentynoic acid in the nmri-exencephaly-mouse model: Pharmacokinetic profiles, teratogenic effects, and histone deacetylase inhibition abilities of further valproic acid hydroxamates and amides, *Drug Metab Dispos* 34 (4), 612-20, 2006.

Elstrom, R. L., Bauer, D. E., Buzzai, M., Karnauskas, R., Harris, M. H., Plas, D. R.,

Zhuang, H., Cinalli, R. M., Alavi, A., Rudin, C. M., and Thompson, C. B. (2004). Akt stimulates aerobic glycolysis in cancer cells. *Cancer Res* 64(11), 3892-9.

Esteller, M. and Herman, J. G., Cancer as an epigenetic disease: DNA methylation and chromatin alterations in human tumours, *J Pathol* 196 (1), 1-7, 2002.

Farwell, D. G., Shera, K. A., Koop, J. I. et al., Genetic and epigenetic changes in human epithelial cells immortalized by telomerase, *Am J Pathol* 156 (5), 1537-47, 2000.

Feng, W., Lu, Z., Luo, R. Z. et al., Multiple histone deacetylases repress tumor suppressor gene arhi in breast cancer, *Int J Cancer* 120 (8), 1664-8, 2007.

Fenic I, Sonnack V, Failing K, et al. In vivo effects of histone-deacetylase inhibitor trichostatin-A on murine spermatogenesis. *J Androl* 2004;25:811-8.

Fischle, W., Dequiedt, F., Fillion, M. et al., Human hdac7 histone deacetylase activity is associated with hdac3 in vivo, *J Biol Chem* 276 (38), 35826-35, 2001.

Food and Drug Administration. Celebrex label (2005): <http://www.fda.gov/cder/foi/label/2005/020998s018,019lbl.pdf>

Fu, M., Liu, M., Sauve, A. A. et al., Hormonal control of androgen receptor function through sirt1, *Mol Cell Biol* 26 (21), 8122-35, 2006.

Fu, M., Rao, M., Wang, C. et al., Acetylation of androgen receptor enhances coactivator binding and promotes prostate cancer cell growth, *Mol Cell Biol* 23 (23), 8563-75, 2003.

Fuino, L., Bali, P., Wittmann, S. et al., Histone deacetylase inhibitor laq824 down-regulates her-2 and sensitizes human breast cancer cells to trastuzumab, taxotere, gemcitabine, and epothilone b, *Mol Cancer Ther* 2 (10), 971-84, 2003.

Furumai, R., Komatsu, Y., Nishino, N. et al., Potent histone deacetylase inhibitors built from trichostatin a and cyclic tetrapeptide antibiotics including trapoxin, *Proc Natl Acad Sci U S A* 98 (1), 87-92, 2001.

Furumai, R., Matsuyama, A., Kobashi, N. et al., Fk228 (depsipeptide) as a natural produg that inhibits class i histone deacetylases, *Cancer Res* 62 (17), 4916-21, 2002.

Garber K HDAC inhibitors overcome first hurdle. *Nat Biotechnol* 2007;25:17-9.

Garcia-Manero, G., Kantarjian, H. M., Sanchez-Gonzalez, B. et al., Phase 1/2 study of the combination of 5-aza-2'-deoxycytidine with valproic acid in patients with leukemia, *Blood* 108 (10), 3271-9, 2006.

- Gaughan, L., Logan, I. R., Cook, S. et al., Tip60 and histone deacetylase 1 regulate androgen receptor activity through changes to the acetylation status of the receptor, *J Biol Chem* 277 (29), 25904-13, 2002.
- Gaughan, L., Logan, I. R., Neal, D. E. et al., Regulation of androgen receptor and histone deacetylase 1 by mdm2-mediated ubiquitylation, *Nucleic Acids Res* 33 (1), 13-26, 2005.
- Gayther, S. A., Batley, S. J., Linger, L. et al., Mutations truncating the ep300 acetylase in human cancers, *Nat Genet* 24 (3), 300-3, 2000.
- George, P., Bali, P., Annavarapu, S. et al., Combination of the histone deacetylase inhibitor lbh589 and the hsp90 inhibitor 17-aag is highly active against human cml-bc cells and aml cells with activating mutation of flt-3, *Blood* 105 (4), 1768-76, 2005.
- Ghadially, F. N. (1982). Endoplasmic reticulum. In *Ultrastructural Pathology of the Cell and Matrix*, 2<sup>nd</sup> ed., pp. 370, 838. William Clowes (Beccles) Limited, Beccles and London, Great Britain.
- Giles, F., Fischer, T., Cortes, J. et al., A phase i study of intravenous lbh589, a novel cinnamic hydroxamic acid analogue histone deacetylase inhibitor, in patients with refractory hematologic malignancies, *Clin Cancer Res* 12 (15), 4628-35, 2006.
- Giles, R. H., Peters, D. J., and Breuning, M. H., Conjunction dysfunction: Cbp/p300 in human disease, *Trends Genet* 14 (5), 178-83, 1998.
- Glaser, K. B., Li, J., Staver, M. J. et al., Role of class i and class ii histone deacetylases in carcinoma cells using sirna, *Biochem Biophys Res Commun* 310 (2), 529-36, 2003.
- Glaser, K. B., Staver, M. J., Waring, J. F. et al., Gene expression profiling of multiple histone deacetylase (hdac) inhibitors: Defining a common gene set produced by hdac inhibition in t24 and mda carcinoma cell lines, *Mol Cancer Ther* 2 (2), 151-63, 2003.
- Gore, S. D., Baylin, S., Sugar, E. et al., Combined DNA methyltransferase and histone deacetylase inhibition in the treatment of myeloid neoplasms, *Cancer Res* 66 (12), 6361-9, 2006.
- Greaves, P. (2000). Digestive System 2. In *Histopathology of Preclinical Toxicity Studies. Interpretation and Relevance in Drug Safety Evaluation*, 2<sup>nd</sup> ed., p. 435-52. Elsevier.
- Greenberg, N. M., DeMayo, F., Finegold, M. J., Medina, D., Tilley, W. D., Aspinall, J. O., Cunha, G. R., Donjacour, A. A., Matusik, R. J., and Rosen, J. M. (1995). Prostate cancer in a transgenic mouse. *Proc Natl Acad Sci U S A* 92(8), 3439-43.

Greenberg NM, DeMayo FJ, Sheppard PC, et al. The rat probasin gene promoter directs hormonally and developmentally regulated expression of a heterologous gene specifically to the prostate in transgenic mice. *Mol Endocrinol* 1994;8:230-9.

Greenberg, V. L., Williams, J. M., Cogswell, J. P. et al., Histone deacetylase inhibitors promote apoptosis and differential cell cycle arrest in anaplastic thyroid cancer cells, *Thyroid* 11 (4), 315-25, 2001.

Greene, W. C. and Chen, L. F., Regulation of nf-kappab action by reversible acetylation, *Novartis Found Symp* 259, 208-17; discussion 218-25, 2004.

Gregorette, I. V., Lee, Y. M., and Goodson, H. V., Molecular evolution of the histone deacetylase family: Functional implications of phylogenetic analysis, *J Mol Biol* 338 (1), 17-31, 2004.

Gu, W., Luo, J., Brooks, C. L. et al., Dynamics of the p53 acetylation pathway, *Novartis Found Symp* 259, 197-205; discussion 205-7, 223-5, 2004.

Gu, W. and Roeder, R. G., Activation of p53 sequence-specific DNA binding by acetylation of the p53 c-terminal domain, *Cell* 90 (4), 595-606, 1997.

Guo, F., Sigua, C., Tao, J. et al., Cotreatment with histone deacetylase inhibitor laq824 enhances apo-2l/tumor necrosis factor-related apoptosis inducing ligand-induced death inducing signaling complex activity and apoptosis of human acute leukemia cells, *Cancer Res* 64 (7), 2580-9, 2004.

Gupta, S. (2004). Prostate cancer chemoprevention: models, limitations and potential (Review). *Int J Oncol* 25(4), 1133-48.

Gupta, S., Hastak, K., Ahmad, N., Lewin, J. S., and Mukhtar, H. (2001). Inhibition of prostate carcinogenesis in TRAMP mice by oral infusion of green tea polyphenols. *Proc Natl Acad Sci U S A* 98(18), 10350-5.

Haggarty, S. J., Koeller, K. M., Wong, J. C. et al., Domain-selective small-molecule inhibitor of histone deacetylase 6 (hdac6)-mediated tubulin deacetylation, *Proc Natl Acad Sci U S A* 100 (8), 4389-94, 2003.

Hague, A., Manning, A. M., Hanlon, K. A. et al., Sodium butyrate induces apoptosis in human colonic tumour cell lines in a p53-independent pathway: Implications for the possible role of dietary fibre in the prevention of large-bowel cancer, *Int J Cancer* 55 (3), 498-505, 1993.

Han, J. W., Ahn, S. H., Park, S. H. et al., Apicidin, a histone deacetylase inhibitor, inhibits proliferation of tumor cells via induction of p21waf1/cip1 and gelsolin, *Cancer*

*Res* 60 (21), 6068-74, 2000.

Hazzouri M, Pivot-Pajot C, Faure AK, et al. Regulated hyperacetylation of core histones during mouse spermatogenesis: involvement of histone deacetylases. *Eur J Cell Biol* 2000;79:950-60.

He YH, Friesen MD, Ruch RJ, et al. Indole-3-carbinol as a chemopreventive agent in 2-amino-1-methyl-6-phenyl-imidazol [4,5-*b*] pyridine (PhIP) carcinogenesis: inhibition of PhIP-DNA adduct formation, acceleration of PhIP metabolism, and induction of cytochrome P450 in female F344 rats. *Food Chem Toxicol* 2000;38:15-23.

Hennessy, B. T., Smith, D. L., Ram, P. T. et al., Exploiting the pi3k/akt pathway for cancer drug discovery, *Nat Rev Drug Discov* 4 (12), 988-1004, 2005.

Hoshikawa, Y., Kwon, H. J., Yoshida, M. et al., Trichostatin a induces morphological changes and gelsolin expression by inhibiting histone deacetylase in human carcinoma cell lines, *Exp Cell Res* 214 (1), 189-97, 1994.

Hsu, A. L., Ching, T. T., Wang, D. S., Song, X., Rangnekar, V. M., and Chen, C. S. (2000). The cyclooxygenase-2 inhibitor celecoxib induces apoptosis by blocking Akt activation in human prostate cancer cells independently of Bcl-2. *J Biol Chem* 275(15), 11397-403.

Hu, E., Dul, E., Sung, C. M. et al., Identification of novel isoform-selective inhibitors within class i histone deacetylases, *J Pharmacol Exp Ther* 307 (2), 720-8, 2003.

Hubbert, C., Guardiola, A., Shao, R. et al., Hdac6 is a microtubule-associated deacetylase, *Nature* 417 (6887), 455-8, 2002.

Huss WJ, Lai L, Barrios RJ, et al. Retinoic acid slows progression and promotes apoptosis of spontaneous prostate cancer. *Prostate* 2004;61:142-52.

Ihle, N. T., Paine-Murrieta, G., Berggren, M. I., Baker, A., Tate, W. R., Wipf, P., Abraham, R. T., Kirkpatrick, D. L., and Powis, G. (2005). The phosphatidylinositol-3-kinase inhibitor PX-866 overcomes resistance to the epidermal growth factor receptor inhibitor gefitinib in A-549 human non-small cell lung cancer xenografts. *Mol Cancer Ther* 4(9), 1349-57.

Inoue, S., Mai, A., Dyer, M. J. et al., Inhibition of histone deacetylase class i but not class ii is critical for the sensitization of leukemic cells to tumor necrosis factor-related apoptosis-inducing ligand-induced apoptosis, *Cancer Res* 66 (13), 6785-92, 2006.

Ito, A., Kawaguchi, Y., CH, L. et al., Mdm2-hdac1-mediated deacetylation of p53 is required for its degradation., *Embo J* 21, 6236-6245, 2002.

Ito A, Lai CH, Zhao X et al., P300/cbp-mediated p53 acetylation is commonly induced by p53-activating agents and is inhibited by mdm2, *Embo J* 20, 1331-1340, 2001.

Jemal A, Siegel R, Ward E, et al. Cancer statistics, 2007. *CA Cancer J Clin* 2007;57:43-66.

Johnson, A. J., Smith, L. L., Zhu, J., Heerema, N. A., Jefferson, S., Mone, A., Grever, M., Chen, C. S., and Byrd, J. C. (2005). A novel celecoxib derivative, OSU03012, induces cytotoxicity in primary CLL cells and transformed B-cell lymphoma cell line via a caspase- and Bcl-2-independent mechanism. *Blood* 105(6), 2504-9.

Johnstone, R. W. and Licht, J. D., Histone deacetylase inhibitors in cancer therapy: Is transcription the primary target?, *Cancer Cell* 4 (1), 13-8, 2003.

Juan, L. J., Shia, W. J., Chen, M. H. et al., Histone deacetylases specifically down-regulate p53-dependent gene activation, *J Biol Chem* 275 (27), 20436-43, 2000.

Kaplan-Lefko PJ, Chen TM, Ittmann MM, et al. Pathobiology of autochthonous prostate cancer in a pre-clinical transgenic mouse model. *Prostate* 2003;55:219-37.

Karagiannis, T. C. and El-Osta, A., Will broad-spectrum histone deacetylase inhibitors be superseded by more specific compounds? *Leukemia* 21 (1), 61-5, 2007.

Kawano, T., Horiguchi-Yamada, J., Iwase, S. et al., Depsipeptide enhances imatinib mesylate-induced apoptosis of bcr-abl-positive cells and ectopic expression of cyclin d1, c-myc or active mek abrogates this effect, *Anticancer Res* 24 (5A), 2705-12, 2004.

Kelly, W. K., O'Connor, O. A., Krug, L. M. et al., Phase i study of an oral histone deacetylase inhibitor, suberoylanilide hydroxamic acid, in patients with advanced cancer, *J Clin Oncol* 23 (17), 3923-31, 2005.

Kelly, W. K., Richon, V. M., O'Connor, O. et al., Phase i clinical trial of histone deacetylase inhibitor: Suberoylanilide hydroxamic acid administered intravenously, *Clin Cancer Res* 9 (10 Pt 1), 3578-88, 2003.

Kim, E. H., Kim, H. S., Kim, S. U. et al., Sodium butyrate sensitizes human glioma cells to trail-mediated apoptosis through inhibition of cdc2 and the subsequent downregulation of survivin and xiap, *Oncogene* 24 (46), 6877-89, 2005.

Kim, J. S., Jeung, H. K., Cheong, J. W. et al., Apicidin potentiates the imatinib-induced apoptosis of bcr-abl-positive human leukaemia cells by enhancing the activation of mitochondria-dependent caspase cascades, *Br J Haematol* 124 (2), 166-78, 2004.

- Kim, J. S., Lee, S., Lee, T. et al., Transcriptional activation of p21(waf1/cip1) by apicidin, a novel histone deacetylase inhibitor, *Biochem Biophys Res Commun* 281 (4), 866-71, 2001.
- Kim, M. S., Baek, J. H., Chakravarty, D. et al., Sensitization to uv-induced apoptosis by the histone deacetylase inhibitor trichostatin a (tsa), *Exp Cell Res* 306 (1), 94-102, 2005.
- Kim, M. S., Blake, M., Baek, J. H. et al., Inhibition of histone deacetylase increases cytotoxicity to anticancer drugs targeting DNA, *Cancer Res* 63 (21), 7291-300, 2003.
- Kim, M. S., Kwon, H. J., Lee, Y. M. et al., Histone deacetylases induce angiogenesis by negative regulation of tumor suppressor genes, *Nat Med* 7 (4), 437-43, 2001.
- Klein RD The use of genetically engineered mouse models of prostate cancer for nutrition and cancer chemoprevention research. *Mutat Res* 2005;576:111-9.
- Knight, Z. A., Gonzalez, B., Feldman, M. E., Zunder, E. R., Goldenberg, D. D., Williams, O., Loewith, R., Stokoe, D., Balla, A., Toth, B., Balla, T., Weiss, W. A., Williams, R. L., and Shokat, K. M. (2006). A pharmacological map of the PI3-K family defines a role for p110alpha in insulin signaling. *Cell* 125(4), 733-47.
- Kojima T, Tanaka T, Mori H. Chemoprevention of spontaneous endometrial cancer in female Donryu rats by dietary indole-3-carbinol. *Cancer Res* 1994;54:1446-9.
- Komander, D., Kular, G. S., Bain, J., Elliott, M., Alessi, D. R., and Van Aalten, D. M. (2003). Structural basis for UCN-01 (7-hydroxystaurosporine) specificity and PDK1 (3-phosphoinositide-dependent protein kinase-1) inhibition. *Biochem J* 375(Pt 2), 255-62.
- Kondapaka, S. B., Zarnowski, M., Yver, D. R., Sausville, E. A., and Cushman, S. W. (2004). 7-hydroxystaurosporine (UCN-01) inhibition of Akt Thr308 but not Ser473 phosphorylation: a basis for decreased insulin-stimulated glucose transport. *Clin Cancer Res* 10(21), 7192-8.
- Kouzarides, T., Acetylation: A regulatory modification to rival phosphorylation?, *Embo J* 19 (6), 1176-9, 2000.
- Kovacs, J. J., Cohen, T. J., and Yao, T. P., Chaperoning steroid hormone signaling via reversible acetylation, *Nucl Recept Signal* 3, e004, 2005.
- Kovacs, J. J., Murphy, P. J., Gaillard, S. et al., Hdac6 regulates hsp90 acetylation and chaperone-dependent activation of glucocorticoid receptor, *Mol Cell* 18 (5), 601-7, 2005.
- Kramer, O. H., Baus, D., Knauer, S. K. et al., Acetylation of stat1 modulates nf-kappab activity, *Genes Dev* 20 (4), 473-85, 2006.

Krusche, C. A., Wulfig, P., Kersting, C. et al., Histone deacetylase-1 and -3 protein expression in human breast cancer: A tissue microarray analysis, *Breast Cancer Res Treat* 90 (1), 15-23, 2005.

Kucab, J. E., Lee, C., Chen, C. S., Zhu, J., Gilks, C. B., Cheang, M., Huntsman, D., Yorlida, E., Emerman, J., Pollak, M., and Dunn, S. E. (2005). Celecoxib analogues disrupt Akt signaling, which is commonly activated in primary breast tumours. *Breast Cancer Res* 7(5), R796-807.

Kulp, S. K., Chen, C. S., Wang, D. S. et al., Antitumor effects of a novel phenylbutyrate-based histone deacetylase inhibitor, (s)-hdac-42, in prostate cancer, *Clin Cancer Res* 12 (17), 5199-206, 2006.

Kulp, S. K., Yang, Y. T., Hung, C. C., Chen, K. F., Lai, J. P., Tseng, P. H., Fowble, J. W., Ward, P. J., and Chen, C. S. (2004). 3-phosphoinositide-dependent protein kinase-1/Akt signaling represents a major cyclooxygenase-2-independent target for celecoxib in prostate cancer cells. *Cancer Res* 64(4), 1444-51.

Kwon, S. H., Ahn, S. H., Kim, Y. K. et al., Apicidin, a histone deacetylase inhibitor, induces apoptosis and fas/fas ligand expression in human acute promyelocytic leukemia cells, *J Biol Chem* 277 (3), 2073-80, 2002.

Langley, E., Pearson, M., Faretta, M. et al., Human sir2 deacetylates p53 and antagonizes pml/p53-induced cellular senescence, *Embo J* 21 (10), 2383-96, 2002.

Lawlor, M. A., Mora, A., Ashby, P. R., Williams, M. R., Murray-Tait, V., Malone, L., Prescott, A. R., Lucocq, J. M., and Alessi, D. R. (2002). Essential role of PDK1 in regulating cell size and development in mice. *Embo J* 21(14), 3728-38.

Leininger, J. R. (1999). Skeletal muscle. In Pathology of the Mouse (R. R. Maronpot, G. A. Boorman, B. W. Gaul, eds.) 1<sup>st</sup> ed, p. 637. Cache River Press, Vienna, IL.  
Levine, A. J., P53, the cellular gatekeeper for growth and division, *Cell* 88 (3), 323-31, 1997.

Li, L., Ittmann, M. M., Ayala, G., Tsai, M. J., Amato, R. J., Wheeler, T. M., Miles, B. J., Kadmon, D. and Thompson, T. C. (2005). The emerging role of the PI3-K-Akt pathway in prostate cancer progression. *Prostate Cancer Prostatic Dis* 8(2), 108-18.

Liao, Y., Grobholz, R., Abel, U., Trojan, L., Michel, M. S., Angel, P., and Mayer, D. (2003). Increase of AKT/PKB expression correlates with Gleason pattern in human prostate cancer. *Int J Cancer* 107(4), 676-80.

Lin, H. Y., Chen, C. S., Lin, S. P. et al., Targeting histone deacetylase in cancer therapy,

*Med Res Rev* 26 (4), 397-413, 2006.

Loprevite, M., Tiseo, M., Grossi, F. et al., In vitro study of ci-994, a histone deacetylase inhibitor, in non-small cell lung cancer cell lines, *Oncol Res* 15 (1), 39-48, 2005.

Lu Q, Wang DS, Chen CS, et al. Structure-based optimization of phenylbutyrate-derived histone deacetylase inhibitors. *J Med Chem* 2005;48:5530-5.

Lu Q, Yang YT, Chen CS, et al. Zn<sup>2+</sup>-chelating motif-tethered short-chain fatty acids as a novel class of histone deacetylase inhibitors. *J Med Chem* 2004;47:467-74.

Lu YS, Kashida Y, Kulp SK, et al. Efficacy of a novel histone deacetylase inhibitor in murine models of hepatocellular carcinoma. *Hepatology* 2007; 46:1119-30.

Luo, J., Nikolaev, A. Y., Imai, S. et al., Negative control of p53 by sir2alpha promotes cell survival under stress, *Cell* 107 (2), 137-48, 2001.

Luo, J., Su, F., Chen, D. et al., Deacetylation of p53 modulates its effect on cell growth and apoptosis, *Nature* 408 (6810), 377-81, 2000.

Magnaghi-Jaulin, L., Groisman, R., Naguibneva, I. et al., Retinoblastoma protein represses transcription by recruiting a histone deacetylase, *Nature* 391 (6667), 601-5, 1998.

Maiso, P., Carvajal-Vergara, X., Ocio, E. M. et al., The histone deacetylase inhibitor lbh589 is a potent antimyeloma agent that overcomes drug resistance, *Cancer Res* 66 (11), 5781-9, 2006.

Marks, P. A. and Breslow, R., Dimethyl sulfoxide to vorinostat: Development of this histone deacetylase inhibitor as an anticancer drug, *Nat Biotechnol* 25 (1), 84-90, 2007.

Marks PA and Dokmanovic M Histone deacetylase inhibitors: discovery and development as anticancer agents. *Expert Opin Investig Drugs* 2005;14:1497-511.

Marks PA, Richon VM, and Rifkind RA Cell cycle regulatory proteins are targets for induced differentiation of transformed cells: Molecular and clinical studies employing hybrid polar compounds. *Int J Hematol* 1996;63:1-17.

Matsuyama, A., Shimazu, T., Sumida, Y. et al., In vivo destabilization of dynamic microtubules by hdac6-mediated deacetylation, *Embo J* 21 (24), 6820-31, 2002.

McCabe, M. T., Low, J. A., Daignault, S., Imperiale, M. J., Wojno, K. J., Day, M. L. (2006). Inhibition of DNA methyltransferase activity prevents tumorigenesis in a mouse model of prostate cancer. *Cancer Res* 66(1), 385-92.

McCubrey, J. A., LaHair, M. M., Franklin, R. A. (2006). OSU-03012 in the treatment of glioblastoma. *Mol Pharmacol* 70(2), 437-39.

McDonald, M. M., and Hamilton, B. F. (1990). Skeletal muscle. In Pathology of the Fischer Rat (G. A. Boorman, S. L. Eustis, M. R. Elwell, C. A. Montgomery, W. F. MacKenzie, eds.) p. 202. Academic Press, Inc., San Diego, CA.

Menegola, E., Di Renzo, F., Broccia, M. L. et al., Inhibition of histone deacetylase activity on specific embryonic tissues as a new mechanism for teratogenicity, *Birth Defects Res B Dev Reprod Toxicol* 74 (5), 392-8, 2005.

Mimeault, M. and Batra, S. K. (2006). Recent advances on multiple tumorigenic cascades involved in prostatic cancer progression and targeting therapies. *Carcinogenesis* 27(1), 1-22.

Minucci, S. and Pelicci, P. G., Histone deacetylase inhibitors and the promise of epigenetic (and more) treatments for cancer, *Nat Rev Cancer* 6 (1), 38-51, 2006.

Molife, R., Fong, P., Scurr, M. et al., Hdac inhibitors and cardiac safety, *Clin Cancer Res* 13 (3), 1068; author reply 1068-9, 2007.

Mora, A., K. Sakamoto, McManus, E. J., and Alessi, D. R. (2005). Role of the PDK1-PKB-GSK3 pathway in regulating glycogen synthase and glucose uptake in the heart. *FEBS Lett* 579(17), 3632-8.

Nachshon-Kedmi M, Fares F, and Yannai S. Therapeutic activity of 3,3'-diindolylmethane on prostate cancer in an in vivo model. *The Prostate* 2004;61:153-160.

Narayanan, B. A., Narayanan, N. K., Pittman, B., and Reddy, B. S. (2004). Regression of mouse prostatic intraepithelial neoplasia by nonsteroidal anti-inflammatory drugs in the transgenic adenocarcinoma mouse prostate model. *Clin Cancer Res* 10(22), 7727-37.

Nemunaitis, J. J., Orr, D., Eager, R. et al., Phase i study of oral ci-994 in combination with gemcitabine in treatment of patients with advanced cancer, *Cancer J* 9 (1), 58-66, 2003.

Nielsen., J. N., Derave, W., Kristiansen, S., Ralston, E., Ploug, T., and Richter, E. A., (2001). Glycogen synthase localization and activity in rat skeletal muscle is strongly dependent on glycogen content. *J Physiol* (531), 757-769.

Nimmanapalli, R., Fuino, L., Bali, P. et al., Histone deacetylase inhibitor laq824 both lowers expression and promotes proteasomal degradation of bcr-abl and induces apoptosis of imatinib mesylate-sensitive or -refractory chronic myelogenous leukemia-

blast crisis cells, *Cancer Res* 63 (16), 5126-35, 2003.

Nimmanapalli, R., Fuino, L., Stobaugh, C. et al., Cotreatment with the histone deacetylase inhibitor suberoylanilide hydroxamic acid (saha) enhances imatinib-induced apoptosis of bcr-abl-positive human acute leukemia cells, *Blood* 101 (8), 3236-9, 2003.

Nome, R. V., Bratland, A., Harman, G. et al., Cell cycle checkpoint signaling involved in histone deacetylase inhibition and radiation-induced cell death, *Mol Cancer Ther* 4 (8), 1231-8, 2005.

O'Connor, O. A., Heaney, M. L., Schwartz, L. et al., Clinical experience with intravenous and oral formulations of the novel histone deacetylase inhibitor suberoylanilide hydroxamic acid in patients with advanced hematologic malignancies, *J Clin Oncol* 24 (1), 166-73, 2006.

Orho, M., Bosshard, N. U., Buist, N. R., Gitzelmann, R., Aynsley-Green, A., Blumel, P., Gannon, M. C., Nuttall, F. Q., Groop, L. C. (1998). Mutations in the liver glycogen synthase gene in children with hypoglycemia due to glycogen storage disease type 0. *J Clin Invest* 102(3), 507-15.

Osada, H., Tatematsu, Y., Saito, H. et al., Reduced expression of class ii histone deacetylase genes is associated with poor prognosis in lung cancer patients, *Int J Cancer* 112 (1), 26-32, 2004.

O'Shea, J. J., Kanno, Y., Chen, X. et al., Cell signaling. Stat acetylation--a key facet of cytokine signaling?, *Science* 307 (5707), 217-8, 2005.

Palazzo, A., Ackerman, B., and Gundersen, G. G., Cell biology: Tubulin acetylation and cell motility, *Nature* 421 (6920), 230, 2003.

Peart, M. J., Smyth, G. K., van Laar, R. K. et al., Identification and functional significance of genes regulated by structurally different histone deacetylase inhibitors, *Proc Natl Acad Sci U S A* 102 (10), 3697-702, 2005.

Pederson, B. A., Schroeder, J. M., Parker, G. E., Smith, M. W., Depaoli-Roach, A. A., and Roach, P. J. (2005). Glucose metabolism in mice lacking muscle glycogen synthase. *Diabetes* 54(12), 3466-73.

Piekarz, R. L., Frye, A. R., Wright, J. J. et al., Cardiac studies in patients treated with depsipeptide, fk228, in a phase ii trial for t-cell lymphoma, *Clin Cancer Res* 12 (12), 3762-73, 2006.

Plas, D. R. and Thompson, C. B. (2005). Akt-dependent transformation: there is more to growth than just surviving. *Oncogene* 24(50), 7435-42.

Plumb, J. A., Finn, P. W., Williams, R. J. et al., Pharmacodynamic response and inhibition of growth of human tumor xenografts by the novel histone deacetylase inhibitor pxd101, *Mol Cancer Ther* 2 (8), 721-8, 2003.

Plyte, S. E., Hughes, K., Nikolakaki, E., Pulverer, B. J., and Woodgett, J. R. (1992). Glycogen synthase kinase-3: functions in oncogenesis and development. *Biochem Biophys Acta* 1114(2-3), 147-62.

Qian, D. Z., Kato, Y., Shabbeer, S. et al., Targeting tumor angiogenesis with histone deacetylase inhibitors: The hydroxamic acid derivative lbh589, *Clin Cancer Res* 12 (2), 634-42, 2006.

Qian DZ, Wei YF, Wang X, et al. Antitumor activity of the histone deacetylase inhibitor MS-275 in prostate cancer models. *Prostate* 2007;67:1182-93.

Qian, X., LaRochelle, W. J., Ara, G. et al., Activity of pxd101, a histone deacetylase inhibitor, in preclinical ovarian cancer studies, *Mol Cancer Ther* 5 (8), 2086-95, 2006.

Qiu, L., Burgess, A., Fairlie, D. P. et al., Histone deacetylase inhibitors trigger a g2 checkpoint in normal cells that is defective in tumor cells, *Mol Biol Cell* 11 (6), 2069-83, 2000.

Quivy, V. and Van Lint, C., Regulation at multiple levels of nf-kappab-mediated transactivation by protein acetylation, *Biochem Pharmacol* 68 (6), 1221-9, 2004.

Raghow, S., Hooshdaran, M.Z., Katiyar, S., Steiner, M.S. (2002). Toremifene prevents prostate cancer in the transgenic adenocarcinoma of mouse prostate model. *Cancer Res* 62(5), 1370-6.

Raghow, S., Kuliyevev, E., Steakley, M., Greenberg, N., and Steiner, M. S. (2000). Efficacious chemoprevention of primary prostate cancer by flutamide in an autochthonous transgenic model. *Cancer Res* 60(15), 4093-7.

Rahmani, M., Reese, E., Dai, Y. et al., Coadministration of histone deacetylase inhibitors and perifosine synergistically induces apoptosis in human leukemia cells through akt and erk1/2 inactivation and the generation of ceramide and reactive oxygen species, *Cancer Res* 65 (6), 2422-32, 2005.

Rahmani, M., Yu, C., Dai, Y. et al., Coadministration of the heat shock protein 90 antagonist 17-allylamino-17-demethoxygeldanamycin with suberoylanilide hydroxamic acid or sodium butyrate synergistically induces apoptosis in human leukemia cells, *Cancer Res* 63 (23), 8420-7, 2003.

Rahmani, M., Yu, C., Reese, E. et al., Inhibition of pi-3 kinase sensitizes human leukemic cells to histone deacetylase inhibitor-mediated apoptosis through p44/42 map kinase inactivation and abrogation of p21(cip1/waf1) induction rather than akt inhibition, *Oncogene* 22 (40), 6231-42, 2003.

Ren, C., Zhang, L., Freitas, M. A. et al., Peptide mass mapping of acetylated isoforms of histone h4 from mouse lymphosarcoma cells treated with histone deacetylase (hdacs) inhibitors, *J Am Soc Mass Spectrom* 16 (10), 1641-53, 2005.

Richards, D. A., Boehm, K. A., Waterhouse, D. M. et al., Gemcitabine plus ci-994 offers no advantage over gemcitabine alone in the treatment of patients with advanced pancreatic cancer: Results of a phase ii randomized, double-blind, placebo-controlled, multicenter study, *Ann Oncol* 17 (7), 1096-102, 2006.

Rommel, C., Bodine, S. C., Clarke, B. A., Rossman, R., Nunez, L., Stitt, T. N., Yancopoulos, G. D., and Glass, D. J. (2001). Mediation of IGF-1-induced skeletal myotube hypertrophy by PI(3)K/Akt/mTOR and PI(3)K/Akt/GSK3 pathways. *Nat Cell Biol* 3(11): 1009-13.

Rosato, R. R., Almenara, J. A., Dai, Y. et al., Simultaneous activation of the intrinsic and extrinsic pathways by histone deacetylase (hdac) inhibitors and tumor necrosis factor-related apoptosis-inducing ligand (trail) synergistically induces mitochondrial damage and apoptosis in human leukemia cells, *Mol Cancer Ther* 2 (12), 1273-84, 2003.

Rosato, R. R., Almenara, J. A., Yu, C. et al., Evidence of a functional role for p21waf1/cip1 down-regulation in synergistic antileukemic interactions between the histone deacetylase inhibitor sodium butyrate and flavopiridol, *Mol Pharmacol* 65 (3), 571-81, 2004.

Rosato RR, Maggio SC, Almenara JA, et al. The histone deacetylase inhibitor LAQ824 induces human leukemia cell death through a process involving XIAP down-regulation, oxidative injury, and the acid sphingomyelinase-dependent generation of ceramide. *Mol Pharmacol* 2006;69:216-25.

Roy, S., Packman, K., Jeffrey, R. et al., Histone deacetylase inhibitors differentially stabilize acetylated p53 and induce cell cycle arrest or apoptosis in prostate cancer cells, *Cell Death Differ* 12 (5), 482-91, 2005.

Roy, S. and Tenniswood, M., Site-specific acetylation of p53 directs selective transcription complex assembly, *J Biol Chem* 282 (7), 4765-71, 2007.

Rubin, E. H., Agrawal, N. G., Friedman, E. J. et al., A study to determine the effects of food and multiple dosing on the pharmacokinetics of vorinostat given orally to patients with advanced cancer, *Clin Cancer Res* 12 (23), 7039-45, 2006.

Saji, S., Kawakami, M., Hayashi, S. et al., Significance of hdac6 regulation via estrogen signaling for cell motility and prognosis in estrogen receptor-positive breast cancer, *Oncogene* 24 (28), 4531-9, 2005.

Sakr WA and Partin AW Histological markers of risk and the role of high-grade prostatic intraepithelial neoplasia. *Urology* 2001;57:115-20.

Sander M, Trump BF, and Harris CC The Twenty-First Aspen Cancer Conference: Mechanisms of Toxicity, Carcinogenesis, Cancer Prevention, and Cancer Therapy, 2006. *Mol Carcinog* 2007;46:415-35.

Sandor, V., Bakke, S., Robey, R. W. et al., Phase i trial of the histone deacetylase inhibitor, depsipeptide (fr901228, nsc 630176), in patients with refractory neoplasms, *Clin Cancer Res* 8 (3), 718-28, 2002.

Sargeant AM, Klein RD, Rengel RC, et al. Chemopreventive and bioenergetic signaling effects of PDK1/Akt pathway inhibition in a transgenic mouse model of prostate cancer. *Toxicol Pathol* 2007;35:549-61.

Sargeant AM, Rengel RC, Kulp SK, Klein RD, Clinton SK, Wang YC, and Chen CS. OSU-HDAC42, a histone deacetylase inhibitor, blocks prostate tumor progression in the transgenic adenocarcinoma of the mouse prostate model. *Cancer Res* 2008;68:3999-4009.

Sasakawa, Y., Naoe, Y., Inoue, T. et al., Effects of fk228, a novel histone deacetylase inhibitor, on tumor growth and expression of p21 and c-myc genes in vivo, *Cancer Lett* 195 (2), 161-8, 2003.

Seigneurin-Berny D, Verdell A, Curtet S, et al. Identification of components of the murine histone deacetylase 6 complex: link between acetylation and ubiquitination signaling pathways. *Mol Cell Biol* 2001;21:8035-44.

Shah, M. H., Binkley, P., Chan, K. et al., Cardiotoxicity of histone deacetylase inhibitor depsipeptide in patients with metastatic neuroendocrine tumors, *Clin Cancer Res* 12 (13), 3997-4003, 2006.

Shappell SB, Thomas GV, Roberts RL, et al. Prostate pathology of genetically engineered mice: definitions and classification. The consensus report from the Bar Harbor meeting of the Mouse Models of Human Cancer Consortium Prostate Pathology Committee. *Cancer Res* 2004;64:2270-305.

Sheldon CA, Williams RD, and Fraley EE Incidental carcinoma of the prostate: a review of the literature and critical reappraisal of classification. *J Urol* 1980;124:626-31.

- Shirai T. Significance of chemoprevention for prostate cancer development: Experimental *in vivo* approaches to chemoprevention. *Pathol Int* 2008;58:1-16.
- Simonini, M. V., Camargo, L. M., Dong, E. et al., The benzamide ms-275 is a potent, long-lasting brain region-selective inhibitor of histone deacetylases, *Proc Natl Acad Sci U S A* 103 (5), 1587-92, 2006.
- Society AC. Cancer facts and figures 2007. Available at <http://www.cancer.org/>. 2008;10.
- Souli E, Machluf M, Morgenstern A, Sabo E, and Yannai S. Indole-3-carbinol (I3C) exhibits inhibitory and preventive effects on prostate tumors in mice. *Food Chem Toxicol* 2008;46:863-870.
- Stephen, J. K., Vaught, L. E., Chen, K. M. et al., Epigenetic events underlie the pathogenesis of sinonasal papillomas, *Mod Pathol* 20 (10), 1019-27, 2007.
- Stoner G, Casto B, Ralston S, Roebuck B, Periera C, and Bailey G. Development of a multi-organ rat model for evaluating chemopreventive agents: efficacy of indole-3-carbinol. *Carcinogenesis* 2002;23:265-72.
- Subramanian, C., Opihari, A. W., Jr., Bian, X. et al., Ku70 acetylation mediates neuroblastoma cell death induced by histone deacetylase inhibitors, *Proc Natl Acad Sci U S A* 102 (13), 4842-7, 2005.
- Subramanian, C., Opihari, A. W., Jr., Castle, V. P. et al., Histone deacetylase inhibition induces apoptosis in neuroblastoma, *Cell Cycle* 4 (12), 1741-3, 2005.
- Suckow, M. A., Danneman, P., Brayton, C. (2001). Important biological features. In *The Laboratory Mouse*, p. 12. CRC Press LLC, Boca Raton, Florida.
- Suttie, A. W., Dinse, G. E., Nyska, A., Moser, G. J., Goldsworthy, T. L., and Maronpot, R. R. (2005). An investigation of the effects of late-onset dietary restriction on prostate cancer development in the TRAMP mouse. *Toxicol Pathol* 33(3), 386-397.
- Suttie, A., Nyska, A., Haseman, J. K., Moser, G. J., Hackett, T. R., and Goldsworthy, T. L. (2003). A grading scheme for the assessment of proliferative lesions of the mouse prostate in the TRAMP model. *Toxicol Pathol* 31(1), 31-8.
- Tang, Y., Luo, J., Zhang, W. et al., Tip60-dependent acetylation of p53 modulates the decision between cell-cycle arrest and apoptosis, *Mol Cell* 24 (6), 827-39, 2006.
- Tani Y, Suttie A, Flake GP, et al. Epithelial-stromal tumor of the seminal vesicles in the transgenic adenocarcinoma mouse prostate model. *Vet Pathol* 2005;42:306-14.

- Thevenet, L., Mejean, C., Moniot, B. et al., Regulation of human sry subcellular distribution by its acetylation/deacetylation, *Embo J* 23 (16), 3336-45, 2004.
- Thompson, C. B. (2005). Metabolic regulation of cancer cell survival. In Mechanisms of toxicity, carcinogenesis, cancer prevention and cancer therapy. The Twentieth Aspen Cancer Conference. Session 8. Apoptosis. *Toxicol Pathol* 33(7), 829-31.
- Thompson IM, Lucia MS, Redman MW, et al. Finasteride decreases the risk of prostatic intraepithelial neoplasia. *J Urol* 2007;178:107-9; discussion 10.
- Tomita, Y., Morooka, T., Hoshida, Y., Zhang, B., Qiu, Y., Nakamichi, I., Hamada, K., Ueda, T., Naka, N., Kudawara, I., Aozasa, K. (2006). Prognostic significance of activated AKT expression in soft-tissue sarcoma. *Clin Cancer Res* 12, 3070-3077.
- Tran, A. D., Marmo, T. P., Salam, A. A. et al., Hdac6 deacetylation of tubulin modulates dynamics of cellular adhesions, *J Cell Sci* 120 (Pt 8), 1469-79, 2007.
- Tseng, P. H., Lin, H. P., Zhu, J., Chen, K. F., Hade, E. M., Young, D. C., Byrd, J. C., Grever, M., Johnson, K., Druker, B. J., Chen, C. S. (2005). Synergistic interactions between imatinib mesylate and the novel phosphoinositide-dependent kinase-1 inhibitor OSU-03012 in overcoming imatinib mesylate resistance. *Blood* 105, 4021-27.
- Tseng, P. H., Weng, S. C., Wang, Y. C., Weng, J. R., Chen, C. S., Brueggemeier, R. W., Shapiro, C. L., Chen, C. Y., Dunn, S. E., Pollak, M., Chen, C.S. (2006). Overcoming trastuzumab resistance in HER2-overexpressing breast cancer cells by using a novel celecoxib-derived PDK-1 inhibitor. *Mol Pharmacol* 70(5), 1534-41.
- Ungerstedt, J. S., Sowa, Y., Xu, W. S. et al., Role of thioredoxin in the response of normal and transformed cells to histone deacetylase inhibitors, *Proc Natl Acad Sci U S A* 102 (3), 673-8, 2005.
- Van Lint, C., Emiliani, S., and Verdin, E., The expression of a small fraction of cellular genes is changed in response to histone hyperacetylation, *Gene Expr* 5 (4-5), 245-53, 1996.
- Vannini, A., Volpari, C., Filocamo, G. et al., Crystal structure of a eukaryotic zinc-dependent histone deacetylase, human hdac8, complexed with a hydroxamic acid inhibitor, *Proc Natl Acad Sci U S A* 101 (42), 15064-9, 2004.
- Vaziri, H., Dessain, S. K., Ng Eaton, E. et al., Hsir2(sirt1) functions as an nad-dependent p53 deacetylase, *Cell* 107 (2), 149-59, 2001.
- Vogelstein, B., Lane, D., and Levine, A. J., Surfing the p53 network, *Nature* 408 (6810), 307-10, 2000.

Wang, R., Cherukuri, P., and Luo, J., Activation of stat3 sequence-specific DNA binding and transcription by p300/creb-binding protein-mediated acetylation, *J Biol Chem* 280 (12), 11528-34, 2005.

Wang, X. Q., Alfaro, M. L., Evans, G. F. et al., Histone deacetylase inhibition results in decreased macrophage cd9 expression, *Biochem Biophys Res Commun* 294 (3), 660-6, 2002.

Warrener, R., Beamish, H., Burgess, A. et al., Tumor cell-selective cytotoxicity by targeting cell cycle checkpoints, *Faseb J* 17 (11), 1550-2, 2003.

Watanabe, T., Manabe, S., Ohashi, Y., Okamiya, H., Onodera, H., and Mitsumori, K. (1998). Comparison of the induction profile of hepatic drug-metabolizing enzymes between piperonyl butoxide and phenobarbital in rats. *J Toxicol Pathol* 11, 1-10.

Wechter, W. J., Leipold, D. D., Murray, E. D., Jr., Quiggle, D., McCracken, J. D., Barrios, R. S., and Greenberg, N. M. (2000). E-7869 (R-flurbiprofen) inhibits progression of prostate cancer in the TRAMP mouse. *Cancer Res* 60(8), 2203-8.

Weng JR, Tsai CH, Kulp S, Wang D, Lin CH, Yang HC, Ma Y, Sargeant A, Chiu CF, Tsai MH, and Chen CS. A potent indole-3-carbinol-derived antitumor agent with pleiotropic effects on multiple signaling pathways in prostate cancer cells. *Cancer Res* 2007;67:7815-24.

Westwood, F. R., Bigley, A., Randall, K., Marsden, A. M., and Scott, R. C. (2005). Statin-induced muscle necrosis in the rat: distribution, development, and fibre selectivity." *Toxicol Pathol* 33(2), 246-57.

Whitesell, L. and Lindquist, S. L., Hsp90 and the chaperoning of cancer, *Nat Rev Cancer* 5 (10), 761-72, 2005.

Wilson, A. J., Byun, D. S., Popova, N. et al., Histone deacetylase 3 (hdac3) and other class i hdacs regulate colon cell maturation and p21 expression and are deregulated in human colon cancer, *J Biol Chem* 281 (19), 13548-58, 2006.

Xie, Z., Yuan, H., Yin, Y., Zeng, X., Bai, R., and Glazer, R. I. (2006). 3-phosphoinositide-dependent protein kinase-1 (PDK1) promotes invasion and activation of matrix metalloproteinases. *BMC Cancer* 6, 77.

Xu W, Ngo L, Perez G, et al. Intrinsic apoptotic and thioredoxin pathways in human prostate cancer cell response to histone deacetylase inhibitor. *Proc Natl Acad Sci U S A* 2006;103:15540-5.

- Yamamoto, H., Fujimoto, J., Okamoto, E. et al., Suppression of growth of hepatocellular carcinoma by sodium butyrate in vitro and in vivo, *Int J Cancer* 76 (6), 897-902, 1998.
- Yang, L., Dan, H. C., Sun, M., Liu, Q., Sun, X. M., Feldman, R. I., Hamilton, A. D., Polokoff, M., Nicosia, S. V., Herlyn, M., Sebt, S. M., and Cheng, J. Q. (2004). Akt/protein kinase B signaling inhibitor-2, a selective small molecule inhibitor of Akt signaling with antitumor activity in cancer cells overexpressing Akt. *Cancer Res* 64(13), 4394-9.
- Yang, W. M., Tsai, S. C., Wen, Y. D. et al., Functional domains of histone deacetylase-3, *J Biol Chem* 277 (11), 9447-54, 2002.
- Yang, Y., Hou, H., Haller, E. M. et al., Suppression of foxo1 activity by fhl2 through sirt1-mediated deacetylation, *Embo J* 24 (5), 1021-32, 2005.
- Yeung, F., Hoberg, J. E., Ramsey, C. S. et al., Modulation of nf-kappab-dependent transcription and cell survival by the sirt1 deacetylase, *Embo J* 23 (12), 2369-80, 2004.
- Yoshida M, Katashima S, Ando J, Tanaka T, Uematsu F, Nakae D, and Mackawa A, Dietary indole-3-carbinol promotes endometrial adenocarcinoma development in rats initiated with *N*-ethyl-*N'*-nitro-*N*-nitrosoguanidine, with induction of cytochrome P450s in the liver and consequent modulation of estrogen metabolism. *Carcinogenesis* 2004;25:2257-2264.
- Yoshida, M., Matsuyama, A., Komatsu, Y. et al., From discovery to the coming generation of histone deacetylase inhibitors, *Curr Med Chem* 10 (22), 2351-8, 2003.
- Yu, C., Dasmahapatra, G., Dent, P. et al., Synergistic interactions between mek1/2 and histone deacetylase inhibitors in bcr/abl+ human leukemia cells, *Leukemia* 19 (9), 1579-89, 2005.
- Yu, C., Rahmani, M., Almenara, J. et al., Histone deacetylase inhibitors promote sti571-mediated apoptosis in sti571-sensitive and -resistant bcr/abl+ human myeloid leukemia cells, *Cancer Res* 63 (9), 2118-26, 2003.
- Yu, J., Angelin-Duclos, C., Greenwood, J. et al., Transcriptional repression by blimp-1 (prdi-bf1) involves recruitment of histone deacetylase, *Mol Cell Biol* 20 (7), 2592-603, 2000.
- Yu, X., Guo, Z. S., Marcu, M. G. et al., Modulation of p53, erbb1, erbb2, and raf-1 expression in lung cancer cells by depsipeptide fr901228, *J Natl Cancer Inst* 94 (7), 504-13, 2002.
- Yuan, Z. L., Guan, Y. J., Chatterjee, D. et al., Stat3 dimerization regulated by reversible

acetylation of a single lysine residue, *Science* 307 (5707), 269-73, 2005.

Zhang, L., Su, X., Liu, S. et al., Histone h4 n-terminal acetylation in kasumi-1 cells treated with decapeptide determined by acetic acid-urea polyacrylamide gel electrophoresis, amino acid coded mass tagging, and mass spectrometry, *J Proteome Res* 6 (1), 81-8, 2007.

Zhang, Y., Jung, M., and Dritschilo, A., Enhancement of radiation sensitivity of human squamous carcinoma cells by histone deacetylase inhibitors, *Radiat Res* 161 (6), 667-74, 2004.

Zhang, Y., Li, N., Caron, C. et al., Hdac-6 interacts with and deacetylates tubulin and microtubules in vivo, *Embo J* 22 (5), 1168-79, 2003.

Zhang, Z., Yamashita, H., Toyama, T. et al., Quantitation of hdac1 mRNA expression in invasive carcinoma of the breast\*, *Breast Cancer Res Treat* 94 (1), 11-6, 2005.

Zhu, J., Huang, J. W., Tseng, P. H., Yang, Y. T., Fowble, J., Shiau, C.W., Shaw, Y. J., Kulp, S. K., and Chen, C.S. (2004). From the cyclooxygenase-2 inhibitor celecoxib to a novel class of 3-phosphoinositide-dependent protein kinase-1 inhibitors. *Cancer Res* 64(12), 4309-18.

Zhu, P., Martin, E., Mengwasser, J. et al., Induction of hdac2 expression upon loss of apc in colorectal tumorigenesis, *Cancer Cell* 5 (5), 455-63, 2004.

Zhu, W. G. and Otterson, G. A., The interaction of histone deacetylase inhibitors and DNA methyltransferase inhibitors in the treatment of human cancer cells, *Curr Med Chem Anticancer Agents* 3 (3), 187-99, 2003.